IGNITION AND COMBUSTION IN A LAMINAR MIXING ZONE

Thesis by

Thomas Charles Adamson Jr.

In Partial Fulfillment of the Requirements

For the Degree of

Doctor of Philosophy

California Institute of Technology

Pasadena, California

1954

ACKNOWLEDGMENTS

I wish to thank Dr. Frank E. Marble most sincerely for his constant help and encouragement. Dr. H. S. Tsien's suggestions and criticisms were very much appreciated. I should like to express my thanks to the Guggenheim Jet Propulsion Center for the opportunity to continue graduate study provided by the Jet Propulsion Fellowships. The completion of this work was made possible by the Jet Propulsion Laboratory through the use of its facilities and the help of its personnel. Day by day discussions with Dr. F. H. Wright and Mr. E. E. Zukoski were very useful in interpreting some of the results. I am most grateful to Mrs. Mabel Swafford and Miss Janet Chandler for their excellent work in preparing the manuscript.

ABSTRACT

The equations describing combustion in a flow field are modified for use in laminar flows where the so called boundary layer approximations may be employed. These equations are transformed into a corresponding incompressible flow with the Howarth transformation.

As an example of the use of boundary layer concepts this analysis considers the ignition and combustion in the laminar mixing zone between two parallel moving gas streams. One stream consists of a cool combustible mixture, the second is hot combustion products. The two streams come into contact at a given point and a laminar mixing process follows in which the velocity distribution is modified by viscosity, and the temperature and composition distributions by conduction, diffusion and chemical reaction. The decomposition of the combustible stream is assumed to follow first-order reaction kinetics with temperature dependence according to the Arrhenius law. For a given initial velocity, composition, and temperature distribution, the questions to be answered are: (1) Does the combustible material ignite and (2) How far downstream of the initial contact point does the flame appear and what is the detailed process of development?

Since the hot stream is of infinite extent it is found that ignition always takes place at some point of the stream. However when the temperature of the hot stream drops below a certain value, the distance required for ignition increases so enormously that it essentially does not occur in a physical apparatus of finite dimension. The complete development of the laminar flame front is computed using an approximation similar to the von Kármán integral technique in boundary layer theory.

TABLE OF CONTENTS

LIST OF SYMBOLS

$\underline{(\ )}$ => Vector quantity

$\overline{(\ )}$ => Mean value

A Activation energy, cal/mole/°K.

$\underline{c}_i^*$ Actual velocity of molecule of i^{th} kind, cm/sec.

$\underline{c}_o$ Mass average velocity of gas mixture at any point,

$$\underline{c}_o = \sum_i \rho_i \overline{\underline{c}}_i^*$$

$\underline{C}_i$ Peculiar velocity of molecule of i^{th} kind.

$$\underline{C}_i = \underline{c}_i^* - \underline{c}_o$$

$\overline{\underline{C}}_i$ Diffusion velocity of molecule of i^{th} kind, referred to $\underline{c}_o$.

$$\overline{\underline{C}}_i = \overline{\underline{c}_i^* - \underline{c}_o} = \overline{\underline{c}}_i^* - \underline{c}_o$$

and

$$\sum_i \rho_i \overline{\underline{C}}_i = \sum_i \rho_i \overline{\underline{c}}_i^* - \sum_i \rho_i \underline{c}_o = 0$$

c_{p_i} Specific heat at constant pressure of i^{th} species, cal/gm/°K.

$\overline{c}_p$ Average specific heat at constant pressure.

$$\overline{c}_p = \frac{1}{\rho} \sum_i \rho_i c_{p_i}$$

D_{ij} Multi component diffusion coefficient, $\frac{cm^2}{sec}$.

$\mathcal{D}_{ij}$ Binary diffusion coefficient, $\frac{cm^2}{sec}$.

D_i^T Multi component thermal diffusion coefficient, $\frac{cm^2}{sec}$.

f Dimensionless stream function.

$\hat{h}_i$ Enthalpy per gram of i^{th} species, $\frac{cal}{gm}$.

$\hat{h}$ Enthalpy per gram of mixture,

$$\hat{h} = \frac{1}{\rho} \sum_i \rho_i \hat{h}_i$$

k Boltzman's Constant.

K_i Rate at which molecules of i^{th} species are formed per unit volume, due to chemical reaction, molecules/cc/sec.

ℓ Characteristic chemical length, cm.

L Characteristic length in flow direction, cm.

m_i Mass of molecules of i^{th} kind, $\frac{\text{gms}}{\text{molecules}}$.

M_i Molecular weight of i^{th} species, $\frac{\text{gms}}{\text{mole}}$.

$\overline{M}$ Average molecular weight of mixture,

$$\overline{M} = \sum_i N_i M_i$$

n_i Number density of i^{th} species, number/cc.

n Number density of mixture. $n = \sum_i n_i$

m_i Molar density of i^{th} species, moles/cc.

m Molar density of mixture, $m = \sum_i m_i$.

N_i Mole fraction of i^{th} species, $N_i = \frac{m_i}{m} = \frac{n_i}{n}$.

P Hydrostatic pressure of gas at any point, $\frac{\text{gm}}{\text{cm}^2}$.

$\underline{\underline{P}}$ Pressure tensor.

P_r Prandtl number, $c_p \mu / \lambda$.

$\underline{q}$ Heat flux vector, cal/cm^2/sec.

R Universal gas constant, cal/mole/°K.

S_c Schmidt number, $\mu / \rho \mathcal{D}_{ij}$.

T Local stream temperature, °K.

$\hat{u}_i$ Thermodynamic internal energy per gram of i^{th} species, cal/gm.

$\hat{u}$ Thermodynamic internal energy of mixture,

$$\hat{u} = \frac{1}{\rho} \sum \rho_i \hat{u}_i$$

u_o Local axial stream velocity in compressible flow, cm/sec.

LIST OF SYMBOLS (Continued)

u Local axial stream velocity in corresponding incompressible flow.

u_i Local axial diffusion velocity of i^{th} species.

U Dimensionless axial stream velocity, $\frac{u}{u_I}$.

v_o Local transverse stream velocity, in compressible flow, cm/sec.

v Local transverse stream velocity in corresponding incompressible flow.

v_i Local diffusion velocity of i^{th} species.

V Dimensionless transverse stream velocity, $\frac{v}{u_I}$.

$\underline{X}_i$ Force on i^{th} molecule due to external field, $\frac{\text{dyne}}{\text{molecule}}$.

x Axial distance coordinate, cm.

y Transverse distance coordinate, cm.

β Boundary of thermal zone, cm.

Δ Boundary of diffusion zone, cm.

δ Boundary of velocity boundary layer, cm.

η Dimensionless coordinate, $y\sqrt{\frac{u_I}{\nu x}}$.

ϑ Dimensionless temperature, $\frac{T}{T_I}$.

ϑ_a Dimensionless activation energy, $\frac{A}{RT_I}$.

ϑ_f Dimensionless adiabatic flame temperature, $\frac{T_f}{T_I}$.

K_i Dimensionless mass concentration of i^{th} species, $\frac{\rho_i}{\rho}$.

Λ Velocity ratio, $\frac{u_x}{u_I}$.

λ Coefficient of thermal conductivity, cal/cm/sec/°K.

μ Dynamic viscosity, gm/cm/sec.

ν Kinematic viscosity, $\frac{\mu}{\rho}$, cm^2/sec.

ξ Dimensionless coordinate, $\frac{x}{\ell}$.

LIST OF SYMBOLS (Concluded)

ρ_i Density of i^{th} species, $n_i m_i$, gms/cc.

ρ Density of mixture, $\rho = \sum_i \rho_i$.

τ Characteristic time of the chemical reaction, sec.

I. INTRODUCTION

The study of combustion in a laminar flow field presents many complex problems. A complete description of the various mechanisms involved requires knowledge from the fields of gas and chemical kinetics, and at the present time, a complete formulation seems too complicated to solve except in the case of the simplest first order reactions in one dimensional flow. However, even this case is complex,[1] unless one makes simplifying approximations.[2, 3, 4]

In order to achieve any solution of this problem, then, one must resort to formulating simplified concepts of the mechanisms involved, and hence one is restricted to solving specialized problems covered by the range of validity of the approximations chosen. A crude approximation[5, 6] that has been rather intensively studied is that in which the flame is considered to be an infinitesimally thin discontinuity in the flow. The flow problem is formulated similarly to the shock wave problem, in this case, and gives some idea of the effect of a flame front on a given flow.

However, many problems exist in which the physical situation can be approximated by neither a plane one dimensional flame nor a discontinuity in the flow. For example, the thermal quenching of a gaseous mixture[7] near a cool wall and the thermal ignition near a heated wall essentially involve both two dimensional fields and a knowledge of the structure of the flame. Also, combustion processes in free jets and combustion under conditions of mixing between two gaseous streams require

considerations beyond the one dimensional or discontinuity type theories. In many situations which arise in thermal jet propulsion systems, a relatively cool stream of fuel is ignited by mixing and contact with a hot stream of gas. This process occurs near the injector of a rocket nozzle, in the flow in and through turbojet combustion cans, and plays a definite and vital role in the stabilization of flames behind bluff body flame holders.

In each of the problems mentioned as examples of the process of ignition and combustion through mixing, the flow has the physical property that for large stream velocities, the variations of temperature, composition, and velocity, are much larger in the direction normal to the main stream than they are in the direction of the main stream. In fluid mechanics, problems exhibiting this characteristic are treated by the so-called boundary layer approximations which simplify the description of the problem by deleting certain variations in the direction of flow in comparison with those normal to the flow. Hence, an extension of this idea to cover flows with combustion allows treatment of this entire class of problems, either by analytic, or by simple numerical methods.

The present treatment, then, is concerned with this class of problems, and in particular with that problem of ignition and development of a flame front in the laminar mixing region between parallel streams of combustible gas and hot products of combustion. The general conservation equations are first rewritten in terms of variables more familiar to the aerodynamicist so that the boundary layer approximations may be applied more easily. Next, the resulting relations are modified, with the use of several approximations, to the usual boundary layer equations with the

addition of terms due to combustion, and added conservation equations for the chemical species.

After discussing the physical and chemical relations which apply to the problem and simplifying the equations through extension of the boundary layer concept, the initial portion of the mixing zone with two components is investigated where the heat evolved through chemical reaction is yet small and the problem is solved through a perturbation to the solution for mixing without combustion. Then using the integral technique introduced by von Kármán into the study of the boundary layer, the development of combustion is traced from initial mixing through development of the flame front. The equations for a ternary system with the concentration of two of the components small compared to the third are developed, and a perturbation solution is obtained for the same mixing problem.

II. CONSERVATION EQUATIONS FOR COMBUSTION IN FLOWING GASEOUS SYSTEMS.

The equations necessary to describe the flow field of a multi-component gas mixture, either with, or without chemical reaction, have been stated in detail by Hirschfelder, Curtis, Bird, and Spatz[8] through a generalization of the work of Chapman and Cowling.[9] The general conservation relations were obtained from the Boltzman equation, and, by the usual method of perturbing the velocity distribution function slightly from a Maxwellian distribution, the non-equilibrium calculations of the transport properties were carried out. In generalizing the work of Chapman and Cowling to a multi-component gas system, Hirschfelder et al used a slightly different method of solving the integral equations for the perturbation function. Instead of expanding the unknown functions in an infinite series of Sonine polynomials, as done by Chapman and Cowling, Hirschfelder and his group considered a finite series of Sonine polynomials and employed a variational procedure to find the coefficients of the expansion. Thus, while the two methods of solution are equivalent, the form and in some cases the definition of the transport properties vary. (i.e.: D_{ij}, the multicomponent diffusion coefficient, reduces to $\mathcal{D}_{ij}$ the binary coefficient, but D_i^T, the multi-component thermal diffusion coefficient does not reduce to Chapman and Cowling's definition for the binary case.) Another point of variance arises in the definition of the diffusion velocity. While Chapman and Cowling define $(\bar{C}_2 - \bar{C}_1)$ as the diffusion velocity for a binary mixture, Hirschfelder defines $\bar{C}_i$ as the diffusion velocity of the i^{th} component. In order to avoid

confusion, the Hirschfelder definitions will be used throughout this paper.

The conservation equations modified for the presence of chemical reactions and polyatomic molecules are employed. The coefficients of diffusion and viscosity are not changed by considering molecules with internal degrees of freedom, but the heat flux vector $\underline{q}$, and the coefficient of thermal conductivity, λ , are affected. The best approximation to λ at the present time involves the Eucken correction.

Following the notation of Hirschfelder, the conservation equations are written in the following form:

Conservation of mass

The continuity equation for each species is,

$$\frac{\partial n_i}{\partial t} + \nabla \cdot n_i (\underline{c}_0 + \overline{\underline{C}}_i) = K_i \tag{1}$$

If this equation is multiplied by m_i and summed over i, the total continuity equation is obtained. Thus,

$$\frac{\partial \rho}{\partial t} + \nabla \cdot \rho \underline{c}_0 = 0 \tag{2}$$

since $\sum_i n_i m_i = \rho$, by definition, and $\sum_i m_i K_i = 0$ and $\sum_i n_i m_i \overline{\underline{C}}_i = 0$ from mass conservation considerations.

Conservation of momentum

Summation of the separate momentum equations for each species gives the overall momentum equation.

$$\frac{\partial \underline{c}_0}{\partial t} + \underline{c}_0 \cdot \nabla \underline{c}_0 = \frac{1}{\rho} \nabla \cdot \underline{\underline{P}} + \frac{1}{\rho} \sum_i n_i \underline{X}_i \tag{3}$$

Conservation of Energy

Again, summation of the separate energy equations for each species gives the energy equation for the mixture,

$$\frac{d\hat{u}}{dt} + \underline{c}_0 \cdot \nabla \hat{u} = -\frac{1}{\rho} \nabla \cdot \underline{q} - \left[\underline{\underline{P}} : \nabla \underline{c}_0 + \sum_i n_i \bar{\underline{c}}_i \cdot \underline{X}_i \right] \frac{1}{\rho} \tag{4}$$

where

$$\underline{q} = -\lambda \nabla T + \sum_i \rho_i \bar{\underline{c}}_i \hat{h}_i + \frac{kT}{n} \sum_{i,j} \frac{n_j}{m_i} \frac{D_i^T}{\mathcal{D}_{ij}} (\bar{\underline{c}}_i - \bar{\underline{c}}_j) \tag{5}$$

is defined as the heat flux vector.

State

The equation of state for each species is that of a perfect gas,

$$P_i = n_i k T$$

so that the overall equation of state is:

$$P = nkT \tag{6}$$

Diffusion Velocities:

The diffusion velocity of each component is defined as

$$\bar{\underline{c}}_i = \bar{\underline{c}}_i (u_i, v_i) = \frac{n^2}{n_i \rho} \sum_{j \neq i} \left[m_j D_{ij} \underline{d}_j - \frac{1}{n_i m_i} D_i^T \nabla \ln T \right] \tag{7}$$

where

$$\underline{d}_j = \nabla \frac{n_j}{n} + \left(\frac{n_j}{n} - \frac{n_j m_j}{\rho} \right) \nabla \ln P - \frac{n_j m_j}{P \rho} \left(\rho \underline{X}_j \frac{1}{m_j} - \sum_\ell n_\ell \underline{X}_\ell \right) \tag{8}$$

Finally, one can write the identity

$$\sum_i K_i = \sum_i \frac{\rho_i}{\rho} = 1 \tag{9}$$

The species continuity equations (1), may be written in terms of the relative mass concentration K_i , after multiplication by m_i . Thus $m_i n_i = \rho \frac{\rho_i}{\rho} = \rho K_i$, and equation (1) becomes

$$\frac{\partial}{\partial t}(\rho K_i) + \nabla \cdot \rho K_i (\underline{C}_0 + \underline{\bar{C}}_i) = m_i \dot{K}_i$$

so that

$$\rho\left(\frac{\partial K_i}{\partial t} + \underline{C}_0 \cdot \nabla K_i\right) + K_i\left(\frac{\partial \rho}{\partial t} + \nabla \cdot \rho \underline{C}_0\right) + \nabla \cdot \rho K_i \underline{\bar{C}}_i = m_i \dot{K}_i$$

and employing equation (2), one obtains

$$\rho\left(\frac{\partial K_i}{\partial t} + \underline{C}_0 \cdot \nabla K_i\right) = -\nabla \cdot \rho K_i \underline{\bar{C}}_i + m_i \dot{K}_i \tag{10}$$

Also, the energy equation can be written in terms of the enthalpy, and finally, in terms of a mass average specific heat.

Since

$$\hat{h}_i = \hat{u}_i + \frac{kT}{m_i}$$

then

$$\hat{h} = \frac{1}{\rho}\sum_i \rho_i \hat{h}_i = \frac{1}{\rho}\left(\sum_i \rho_i \hat{u}_i + \sum_i n_i m_i \frac{kT}{m_i}\right)$$

$$= \hat{u} + \frac{1}{\rho} nkT$$

or

$$\hat{h} = \hat{u} + \frac{p}{\rho} \tag{11}$$

where the equation of state (6) has been used. With the aid of equation (11) and the definition of $\bar{C}_p = \sum \frac{\rho_i}{\rho} C_{p_i}$, the energy equation can be

transformed as follows: Taking the derivatives indicated,

$$\frac{\partial \hat{u}}{\partial t} + \underline{c}_0 \cdot \nabla \hat{u} = \frac{\partial \hat{h}}{\partial t} - \frac{1}{\rho}\frac{\partial P}{\partial t} + \frac{P}{\rho^2}\frac{\partial \rho}{\partial t} + \underline{c}_0 \cdot \nabla \hat{h} - \frac{\underline{c}_0}{\rho} \cdot \nabla P + \frac{P}{\rho^2}\underline{c}_0 \cdot \nabla \rho$$

and using equation (2), one obtains

$$\frac{\partial \hat{u}}{\partial t} + \underline{c}_0 \cdot \nabla \hat{u} = \frac{\partial \hat{h}}{\partial t} - \frac{1}{\rho}\frac{\partial P}{\partial t} + \underline{c}_0 \cdot \nabla \hat{h} - \frac{\underline{c}_0}{\rho} \cdot \nabla P - \frac{P}{\rho} \nabla \cdot \underline{c}_0 \tag{13}$$

Next, through substitution of $\hat{h} = \frac{1}{\rho}\sum_i n_i m_i \hat{h}_i$ and elimination of $\frac{\partial h_i}{\partial t}$ with equation (1), equation (13) becomes:

$$\frac{\partial \hat{u}}{\partial t} + \underline{c}_0 \cdot \nabla \hat{u} = \frac{1}{\rho}\left\{ \rho \bar{c}_p \frac{\partial T}{\partial t} - \frac{\partial P}{\partial t} + \rho \bar{c}_p \underline{c}_0 \cdot \nabla T - \right. \tag{14}$$

$$\left. - \nabla \cdot P \underline{c}_0 - \sum_i m_i \hat{h}_i \nabla \cdot n_i \bar{c}_i + \sum_i m_i \hat{h}_i K_i \right\}$$

where the general derivative

$$\frac{\partial \hat{h}_i}{\partial S} = \frac{\partial \hat{h}_i}{\partial T}\Big|_P \frac{\partial T}{\partial S} + \frac{\partial \hat{h}_i}{\partial P}\Big|_T \frac{\partial P}{\partial S}$$

$$= \frac{\partial \hat{h}_i}{\partial T}\Big|_P \frac{\partial T}{\partial S}$$

$$= c_{p_i} \frac{\partial T}{\partial S}$$

since each component is assumed to be a calorimetrically perfect gas.

Substitution of equation (14) into the general energy equation, gives

$$\rho \bar{C}_p \frac{\partial T}{\partial t} - \frac{\partial P}{\partial t} + \rho \bar{C}_p \underline{C}_o \cdot \nabla T - \nabla \cdot P \underline{C}_o - \sum_i m_i \hat{h}_i \nabla \cdot n_i \bar{\underline{C}}_i +$$

$$+ \sum_i m_i \hat{h}_i K_i = -\nabla \cdot \underline{q} - \underline{\underline{P}} : \nabla \underline{C}_o + \sum n_i \bar{\underline{C}}_i \cdot \underline{\underline{X}}_i$$

However,

$$\underline{\underline{P}} : \nabla \underline{C}_o = P \nabla \cdot \underline{C}_o - \Phi$$

where Φ contains the terms due to viscous dissipation. Also the terms $\sum_i m_i \hat{h}_i \nabla \cdot n_i \bar{\underline{C}}_i$ and the heat flux vector $\underline{q}$ may be combined to yield

$$-\nabla \cdot \underline{q} + \sum_i m_i \hat{h}_i \nabla \cdot n_i \bar{\underline{C}}_i = \nabla \cdot \lambda \nabla T - \nabla \cdot \sum_i m_i n_i \bar{\underline{C}}_i \hat{h}_i -$$

$$- \nabla \cdot \frac{kT}{n} \sum_{i,j} \frac{n_j}{m_i} \frac{D_i^T}{\mathcal{D}_{ij}} \left(\bar{\underline{C}}_i - \bar{\underline{C}}_j \right) + \sum_i m_i \hat{h}_i \nabla \cdot n_i \bar{\underline{C}}_i$$

$$= \nabla \cdot \lambda \nabla T - \sum_i m_i n_i \bar{\underline{C}}_i C_{p_i} \cdot \nabla T - \nabla \cdot \frac{kT}{n} \sum_{i,j} \frac{n_j}{m_i} \frac{D_i^T}{\mathcal{D}_{ij}} \left(\bar{\underline{C}}_i - \bar{\underline{C}}_j \right)$$

Finally, the energy equation may be written:

$$\rho \bar{C}_p \left\{ \frac{\partial T}{\partial t} + \underline{C}_o \cdot \nabla T \right\} - \left\{ \frac{\partial P}{\partial t} + \underline{C}_o \cdot \nabla P \right\} = \nabla \cdot \lambda \nabla T - \sum_i m_i n_i \bar{\underline{C}}_i C_{p_i} \cdot \nabla T -$$

$$- \nabla \cdot \frac{kT}{n} \sum_{i,j} \frac{n_j}{m_i} \frac{D_i^T}{\mathcal{D}_{ij}} \left(\bar{\underline{C}}_i - \bar{\underline{C}}_j \right) + \Phi -$$

$$- \sum_i m_i \hat{h}_i K_i + \sum_i n_i \bar{\underline{C}}_i \cdot \underline{\underline{X}}_i \qquad (15)$$

The equations necessary to describe the phenomena of combustion in a flow field, in terms of the familiar physical variables of density, relative mass concentration, velocity, pressure, and temperature, can be collected now. While both the species and the overall continuity equations are written, it is evident that since $K_i = \frac{\rho_i}{\rho}$, if one is considering a system of r components, only $r-1$ of the species equations and the overall continuity equation need be solved.

The necessary equations are as follows:

$$\frac{\partial \rho}{\partial t} + \nabla \cdot \rho \underline{c}_o = 0 \tag{2}$$

$$\rho \left\{ \frac{\partial K_i}{\partial t} + \underline{c}_o \cdot \nabla K_i \right\} = - \nabla \cdot \rho K_i \bar{C}_i + m_i \mathcal{H}_i \tag{10}$$

$$\rho \left\{ \frac{\partial \underline{c}_o}{\partial t} + \underline{c}_o \cdot \nabla \underline{c}_o \right\} = - \nabla \cdot \underline{\underline{P}} + \sum_i n_i \underline{X}_i \tag{3}$$

$$\bar{C}_p \rho \left\{ \frac{\partial T}{\partial t} + \underline{c}_o \cdot \nabla T \right\} - \left\{ \frac{\partial P}{\partial t} + \underline{c}_o \cdot \nabla P \right\} = \nabla \cdot \lambda \nabla T -$$

$$- \sum_i m_i \hat{h}_i \mathcal{H}_i + \Phi - \sum_i \rho_i c_{p_i} \bar{C}_i \cdot \nabla T -$$

$$- \nabla \cdot \frac{kT}{n} \sum_{i,j} \frac{n_i}{m_i \omega_{ij}} \frac{D_i^T}{} \left(\bar{C}_i - \bar{C}_j \right) + \sum_i n_i \bar{C}_i \cdot \underline{X}_i \tag{15}$$

$$P = n k T \tag{6}$$

$$\underline{C}_i = \frac{n^2}{n_i \rho} \sum_{j \neq i} m_j D_{ij} \underline{d}_j - \frac{1}{n_i m_i} D_i^T \nabla \ln T \tag{7}$$

where

$$\underline{d}_j = \nabla\left(\frac{n_j}{n}\right) + \left(\frac{n_j}{n} - \frac{n_j m_j}{\rho}\right) \nabla \ln p - \frac{n_j m_j}{p \rho}\left(\rho \underline{X}_j \frac{1}{m_j} - \sum_\ell n_\ell \underline{X}_\ell\right) \tag{8}$$

III. FORMULATION OF COMBUSTION PROBLEM

Consider two semi infinite gas streams flowing steadily parallel to the X_o axis. The upper stream consists of a cool combustible at temperature T_I, density ρ_I, and velocity u_I, while the lower stream consists of hot products of combustion at temperature T_{II}, density ρ_{II}, and velocity u_{II}. At $X_o = 0$, the two streams mix, and due to diffusion of species and thermal conduction, a reaction is initiated, releasing heat and forming products of combustion.

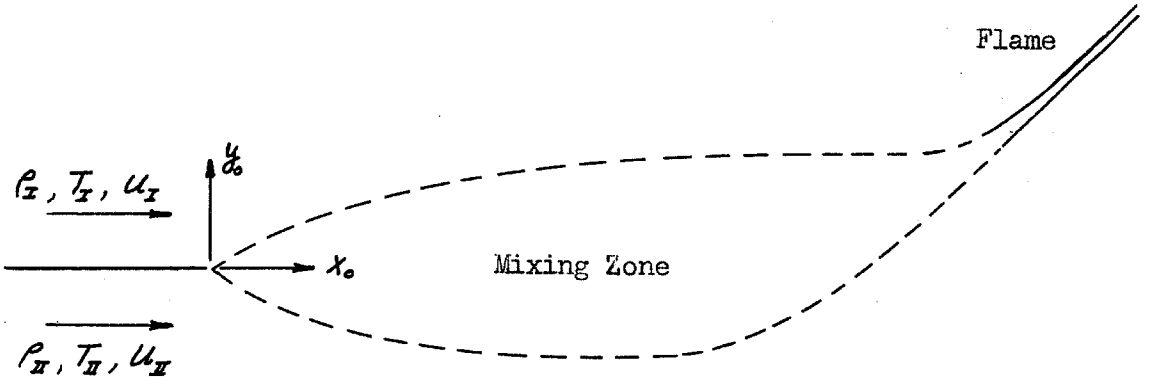

Throughout the mixing region, the reaction rate is increasing until at some distance downstream of the point $X_o = 0$, an equilibrium is reached where the reaction rate has reached its final constant value, and thus a flame has been established.

In establishing a model with which to study the mixing region with reaction, the following assumptions are made:

1) The flow is two-dimensional, steady flow, with no external forces.

2) The mixing region is a laminar mixing region in which the usual boundary layer assumptions hold.

3) The pressure variation in the direction of flow is negligible. This, coupled with the results of assumption (2), that the lateral pressure variation is negligible, implies that the pressure is constant throughout the mixing region.

4) The action rate is of first order occurring in a binary system so that the general chemical reaction is $[A] \rightarrow b[B]$, where $[A]$ and $[B]$ are the molar concentrations of the two components, and b is the number of moles of B formed by decomposition of one mole of A.

5) The specific heats at constant pressure of each of the two components are approximately equal and constant, defined by the ratio of the total heat release due to reaction, to the temperature rise. This assumption, then, considers the components to consist of gases with approximately the same heat capacity so that a change in concentration has a negligible effect on the heat capacity of a given mass of mixture.

6) The Prandtl number $\left(\frac{c_p \mu}{\lambda}\right)$ of the mixture is a constant.

7) The Schmidt number $\left(\frac{\mu}{\rho \mathcal{D}_{12}}\right)$ of the mixture is a constant.

8) The molecular weights of the two components are the same, equal to the average actual molecular weight. Since the pressure is assumed constant, this implies that $\rho \propto \frac{1}{T}$.

9) The transport properties of each of the components are equal and vary as though the molecules were Maxwellian (i.e.: The

molecules are assumed to be point centers of force repelling proportionately to $r^{-\nu}$, where r is the distance between molecules, and ν is the force index. For Maxwellian molecules, $\nu = 5$.) Thus $\mu \propto T^{s}$ where $s = \frac{1}{2} + \frac{2}{\nu - 1}$ so that $\mu \propto T$ and $\rho\mu$ is a constant.

10) The Eucken correction for the coefficient of thermal conduction holds for the mixture.

11) The diffusion coefficients do not vary appreciably with concentration, and the thermal diffusion is negligibly small.

12) The ratio of thermal to kinetic energy is so high as to make viscous dissipation negligible.

13) The Arrhenius rate law holds for the rate at which chemical reaction proceeds. Thus $K_i = \pm \frac{n_i}{\tau} e^{-A/RT}$, where τ is the characteristic time of reaction, A, the activation energy, R, the universal gas constant, and n_i, the number of molecules per unit volume. The plus sign refers to the products of reaction while the minus sign refers to the combustible. No backward reaction is considered.

Both parts of assumption (11) arise from the fact that, using Hirschfelder's[10] development, one considers only one term of the expansion for the first approximation to the non-equilibrium distribution function. The use of this one term gives good approximation to the transport coefficients; to this order of approximation, moreover, the diffusion coefficient is independent of the concentration and the thermal diffusion coefficient is identically zero. If two terms of the expansion are used, the dependence of $\mathcal{D}_{ij}$ on concentration, and D_i^T can be approximated.

That assumptions (5) through (10) are mutually consistent can be shown by the following analysis. By assumption (6) $\frac{c_p \mu}{\lambda}$ is constant and from (5), c_p is constant. Therefore, $\mu \propto \lambda$. However, by assumption (10), $\lambda = \left(c_{p_{mole}} + 1.25 R\right)\frac{\mu}{\bar{M}}$, where $\bar{M}$ is the molecular weight of mixture at any temperature and mixture. Therefore, if N_i and M_i are the i^{th} mole fraction and molecular weight respectively, $\bar{M} = \sum_i N_i M_i$. Now, by assumptions (5) and (8), $c_{p_{mole}}$ is constant and $\bar{M}$ is constant, so again $\mu \propto \lambda$.

Also, from assumption (7), $\mu/\rho \mathcal{D}_{12}$ is constant. Now, from assumptions (8) and (9), $\rho \propto \frac{1}{T}$ and $\mu \propto T^s$. Therefore $\frac{\mu}{\rho \mathcal{D}_{12}} \propto \frac{T^{s+1}}{\mathcal{D}_{12}}$ From gas kinetic theory, however, one can show that for molecules which behave as point centers of force, at constant pressure,(11) $\mathcal{D}_{12} \propto T^{s+1}$ so that $\frac{\mu}{\rho \mathcal{D}_{12}} \propto \frac{T^{s+1}}{T^{s+1}} = 1$, or $\frac{\mu}{\rho \mathcal{D}_{12}}$ is constant.

In reality, then, assumptions (6) and (7) are the motivation for assumptions (5), (8), (9) and (10). The motivation for assuming the molecules to be Maxwellian so that $s=1$, will become apparent in later transformations of the mixing region equations.

IV. CONSERVATION RELATIONS FOR COMBUSTION IN A LAMINAR MIXING REGION: BINARY SYSTEM

While the simplification to the general equations due to most of the assumptions are evident, the use of the boundary layer assumptions in a reacting gas flow should be clarified. With regard to the momentum equations, it can be seen that since there are no new terms due to reaction, the results of assuming that $P \neq P(x_0)$, $u_0 = O(1)$, $v_0 = O(\frac{\delta}{L})$, $\frac{\partial}{\partial x_0} = O(\frac{1}{L})$, $\frac{\partial}{\partial y_0} = O(\frac{1}{\delta})$, and $\frac{\delta}{L} = O(\frac{1}{\sqrt{R_e}})$ where δ is of the order of the thickness of the mixing region, L is the distance downstream, and R_e is the Reynolds number, are exactly those results obtained in boundary layer study. That is, the axial, or x_0, momentum equation is simplified, and the lateral, or y_0, momentum equation reduces to $\frac{\partial P}{\partial y_0} = O(\frac{\delta}{L})$ so that $P \simeq$ constant. This assumption then hinges on whether or not reaction affects the pressure in the mixing zone. Since the change in P through a fully developed laminar flame is usually negligible, the chemically induced change in P throughout the mixing region where the effects of reaction are even smaller, must be negligible.

In both the continuity and energy equations one makes the same type of order of magnitude comparison usually made in boundary layer theory, and finds that the resulting equations differ from the familiar equations of continuity and energy by reaction terms which are explicitly independent of the velocity or any derivatives. Thus, as far as the order of magnitude comparison is concerned, the combustion terms are not considered. However, by assuming that the changes in concentration, temperatures and velocity in the x_0 direction are negligible compared to those in the y_0 direction, one has tacitly assumed that the reaction

induced changes in these variables, follow this same pattern. Since a flame is usually much thinner than a mixing zone, this means that in order to keep these assumptions valid in the whole region, the flame must lie at a very small angle with respect to the x_o or flow axis. This implies that if u_n is the flame speed, $u_n/u_x << 1$ in order to validate the boundary layer assumptions through a fully developed flame. However, even if u_n/u_x is not small compared to unity the assumptions hold throughout most of the mixing region and break down only at the incipience of a stabilized flame, since the effects of reaction are very small initially but increase exponentially. Therefore, when these effects become large enough to affect the assumptions, their rate of growth is so large that the final equilibrium flame is reached very quickly. This will become apparent upon following the growth of the maximum temperature through the mixing region, a result which is given in the solutions obtained for the decomposition of azomethane. As will be seen in a later section, the only result of increasing the initial flow velocity to the point where $u_n/u_x << 1$ is to allow computation of a flame speed, and thickness, results which could be gained by much simpler analyses.

The application of the assumptions to the general equations results in a great simplification. Before the final equations are collected, the transport and reaction rate terms can be developed to their final form. After the boundary layer approximations have been employed, the transport terms become:

$$\nabla \cdot \underline{P} \simeq \frac{\partial}{\partial y_o}\left(\mu \frac{\partial u_o}{\partial y_o}\right) \qquad (16)$$

$$\nabla \cdot \rho K_i \bar{C}_i \simeq \frac{\partial}{\partial y_0} (\rho K_i v_i)$$

where (17)

$$v_i = \frac{n^2}{n_i \rho} \sum_{j \neq i} m_j D_{ij} \frac{\partial}{\partial y_0} \left(\frac{n_j}{n}\right)$$

since P is constant, and $\underline{X}_j = 0$, so that $\underline{d}_j$ reduces to $\nabla(\frac{n_j}{n})$, and,

$$\nabla \cdot \lambda \nabla T \simeq \frac{\partial}{\partial y_0} \left(\lambda \frac{\partial T}{\partial y_0}\right) \tag{18}$$

For a binary system, equation (17) becomes particularly simple, for in this case $D_{ij} = \mathcal{D}_{ij}$, the binary diffusion coefficient, and v_1 may be calculated as,

$$v_1 = \frac{n^2}{n_1 \rho} \left(m_2 \mathcal{D}_{12} \frac{\partial}{\partial y_0} \left(\frac{n_2}{n}\right)\right)$$

so that

$$\nabla \cdot \rho K_1 \bar{C}_1 \simeq \frac{\partial}{\partial y_0} \left(K_1 \frac{n^2}{n_1} m_2 \mathcal{D}_{12} \frac{\partial}{\partial y_0} \left(\frac{n_2}{n}\right)\right) \tag{19}$$

In order to transform this mass transport term into a function of K_1, the following identities may be employed;

$$\frac{n_1}{n} = \frac{n_1}{n_1 + n_2} = \frac{n_1 m_1}{n_1 m_1 + n_2 m_2 \frac{m_1}{m_2}}$$

$$= \frac{K_1}{K_1 \left(1 - \frac{m_1}{m_2}\right) + \frac{m_1}{m_2}}$$

since

$$K_1 + K_2 = 1$$

Also, since

$$\frac{n_2}{n} = 1 - \frac{n_1}{n}$$

then

$$\frac{\partial (n_2/n)}{\partial y_0} = - \frac{\partial (n_1/n)}{\partial y_0}$$

so that

$$\nabla \cdot \rho K_1 \bar{C}_1 \simeq - \frac{\partial}{\partial y_0} \left(\frac{1}{K_1} n_1 m_1 \mathcal{D}_{12} \frac{\partial K_1}{\partial y_0} \right)$$

$$= - \frac{\partial}{\partial y_0} \left(\rho \mathcal{D}_{12} \frac{\partial K_1}{\partial y_0} \right) \qquad (20)$$

$$= - \frac{\partial}{\partial y_0} \left(\frac{\mu}{S_c} \frac{\partial K_1}{\partial y_0} \right)$$

where

$$S_c = \frac{\mu}{\rho \mathcal{D}_{12}}$$

Since C_p is assumed constant, equation (18) becomes,

$$\nabla \cdot \lambda \nabla T \simeq C_p \frac{\partial}{\partial y_0} \left(\frac{\lambda}{C_p} \frac{\partial T}{\partial y_0} \right) = C_p \frac{\partial}{\partial y_0} \left(\frac{\mu}{P_r} \frac{\partial T}{\partial y_0} \right) \qquad (21)$$

where

$$P_r = \frac{C_p \mu}{\lambda}$$

The term which gives the energy addition due to diffusion in the energy equation reduces to zero with the assumption that $C_{p_1} = C_{p_2} = \bar{C}_p = C_p$. Thus,

$$\sum_i m_i n_i C_{p_i} \bar{C}_i \cdot \nabla T = C_p \sum_i m_i n_i \bar{C}_i \cdot \nabla T = 0$$

since $\sum_i m_i n_i \bar{C}_i = 0$ from continuity of mass.

Finally, $m_i \dot{K}_i$, the rate at which mass of the i^{th} kind is produced through reaction can be computed for component one, the combustible

$$m_1 K_1 = -m_1 n_1 \frac{1}{\tau} e^{-A/RT}$$

$$= -\rho K_1 \frac{1}{\tau} e^{-A/RT}$$

In terms of $m_1 K_1$, the heat addition due to combustion is

$$\sum_i m_i \hat{h}_i K_i = m_1 \hat{h}_1 K_1 + m_2 \hat{h}_2 K_2$$

$$= m_1 K_1 (\hat{h}_1 - \hat{h}_2) = m_1 K_1 \Delta H_{12}$$

where $m_1 K_1 = -m_2 K_2$, since the mass formed must equal the mass consumed. In this heat addition term, $\Delta H_{12} = \hat{h}_1 - \hat{h}_2$ is defined as the negative of enthalpy of reaction per gram of combustible. Although $\hat{h}_i$ is defined as $\hat{h}_i = \int_{298.16}^{T} C_{P_i}\, dT + \Delta H^\circ_{f_i}$ (where ΔH°_f is the heat of formation at 298.16° Kelvin so that $\Delta H_{12} = \int_{298.16}^{T} (C_{P_1} - C_{P_2})\, dT + (\Delta H^\circ_{f_1} - \Delta H^\circ_{f_2})$) and although the C_{P_i} are assumed as approximately constant and equal, in order to account somewhat for the fact that the C_{P_i} are slightly different and dependent on temperature, an average ΔH_{12} may be defined as

$$\overline{\Delta H_{12}} = \frac{\Delta H_{12}(T_I) + \Delta H_{12}(T_f)}{2} \qquad (22)$$

where T_I and T_f refer to initial temperature and adiabatic flame temperature respectively. Therefore, if C_{P_1} , and C_{P_2} are known analytically as functions of temperature, a better approximation than the net heat of formation at T = 298.16°K can be computed.

The application of all assumptions to the general equations, then, gives the following set of equations which hold in two-dimensional boundary layer or laminar mixing flows with reaction. Since a binary system is considered, one needs only the overall continuity and one separate species equation to completely specify the conservation of mass.

$$\frac{\partial}{\partial x_o}(\rho u_o) + \frac{\partial}{\partial y_o}(\rho v_o) = 0$$

$$\rho u_o \frac{\partial K_1}{\partial x_o} + \rho v_o \frac{\partial K_1}{\partial y_o} = \frac{\partial}{\partial y_o}\left(\frac{\mu}{S_c}\frac{\partial K_1}{\partial y_o}\right) - \rho K_{1,\perp} e^{-A/RT}$$

$$\rho u_o \frac{\partial u_o}{\partial x_o} + \rho v_o \frac{\partial u_o}{\partial y_o} = \frac{\partial}{\partial y_o}\left(\mu \frac{\partial u_o}{\partial y_o}\right) \qquad (23)$$

$$\rho u_o \frac{\partial T}{\partial x_o} + \rho v_o \frac{\partial T}{\partial y_o} = \frac{\partial}{\partial y_o}\left(\frac{\mu}{P_r}\frac{\partial T}{\partial y_o}\right) + \frac{\overline{\Delta H_{12}}}{C_p}\rho K_{1,\perp} e^{-A/RT}$$

$$P = \text{constant}$$

$$= nkT$$

$$= \rho \frac{R}{M} T$$

While the above equations are greatly simplified from the original relations, they still refer to a compressible flow regime, and thus are not easily solved. However, through the use of the so called Howarth[12] or Dorodnitzyn[13] transformation, a new vertical scale is introduced with which the equations are reduced to incompressible form: denote

$$y = \int_0^{y_o} \frac{\rho}{\rho_r}\, dy_o \qquad (24)$$

where ρ_I is the density of the combustible free stream. Thus introducing a new coordinate system X , Y , where $X = X_o$, one can write the variable transformation as follows;

$$\frac{\partial}{\partial x_o} = \frac{\partial}{\partial X} + \frac{\partial Y}{\partial x_o}\frac{\partial}{\partial Y}$$

and (25)

$$\frac{\partial}{\partial y_o} = \frac{\rho}{\rho_I}\frac{\partial}{\partial Y}$$

where

$$\frac{\partial Y}{\partial x_o} = \int_0^{y_o} \frac{\partial}{\partial x_o}\left(\frac{\rho}{\rho_I}\right) dy_o \tag{26}$$

Also, introducing the usual aerodynamic stream function, $\psi(x_o, y_o)$ defined such that

$$\rho u_o = \rho_I \frac{\partial \psi}{\partial y_o}$$

$$\rho v_o = -\rho_I \frac{\partial \psi}{\partial x_o} \tag{27}$$

one finds that

$$\rho u_o = \rho \frac{\partial \psi}{\partial Y}$$

and (28)

$$\rho v_o = -\rho_I \left(\frac{\partial \psi}{\partial X} + \frac{\partial \psi}{\partial Y}\frac{\partial Y}{\partial x_o}\right)$$

Finally, denoting by u , and v , the velocities in a corresponding incompressible flow, where now

$$u \equiv \frac{\partial \psi}{\partial Y}$$

$$v \equiv -\frac{\partial \psi}{\partial X}. \tag{29}$$

so that from equations (28),

$$u_o = u$$

$$v_o = -\frac{\rho_I}{\rho}\left(-v + u\int_o^{y_o}\frac{\partial}{\partial x_o}\left(\frac{\rho}{\rho_I}\right)dy_o\right) \tag{30}$$

one can see that

$$u_o\frac{\partial}{\partial x_o} + v_o\frac{\partial}{\partial y_o} = u\frac{\partial}{\partial x} + v\frac{\partial}{\partial y}$$

and

$$\frac{\partial}{\partial y_o}\left(\mu\frac{\partial}{\partial y_o}\right) = \frac{\rho}{\rho_I}\frac{\partial}{\partial y}\left(\frac{\rho\mu}{\rho_I}\frac{\partial}{\partial y}\right) = \rho\nu\frac{\partial^2}{\partial y^2} \tag{31}$$

since by assumption (9), $\rho\mu = \rho_I\mu_I$, and $\frac{\mu_I}{\rho_I} = \nu_I \equiv \nu$.

Applying these transformations, equations (30) and (31), to the equations (23), one obtains the corresponding set of equations in the corresponding incompressible flow

$$\frac{\partial u}{\partial x} + \frac{\partial v}{\partial y} = 0$$

$$u\frac{\partial K_1}{\partial x} + v\frac{\partial K_1}{\partial y} = \frac{\nu}{S_c}\frac{\partial^2 K_1}{\partial y^2} - K_1\frac{1}{\tau}e^{-A/RT}$$

$$u\frac{\partial u}{\partial x} + v\frac{\partial u}{\partial y} = \nu\frac{\partial^2 u}{\partial y^2} \tag{32}$$

$$u\frac{\partial T}{\partial x} + v\frac{\partial T}{\partial y} = \frac{\nu}{P_r}\frac{\partial^2 T}{\partial y^2} + \frac{\overline{\Delta H}_{12}}{c_p\tau}K_1 e^{-A/RT}$$

The simplification given by the use of the Howarth transformation coupled with the assumption $\rho\mu$ = constant is now immediately apparent. The momentum equation is now completely uncoupled from the energy and concentration relations and hence its solution demands only the consideration of a pure mixing problem such as that solved by Lock.(14) The effects of temperature, through density, are brought in only upon transforming the solution back to the compressible flow, and these effects serve only to change the vertical scale and leave the horizontal, or flow

direction scale, unchanged. Also, in the incompressible flow, the velocity need be considered only insofar as the region under consideration lies within the velocity mixing zone. After the flame propagates out of this zone, the velocity is constant, $u = u_I$.

It is convenient to consider the equations with dependent variables in dimensionless form. Since the flame finally propagates into the upper combustible stream, at which time a fully developed laminar flame is developed, the velocity u_I, and the flame velocity will determine the angle at which the flame lies with respect to the x axis. Hence u_I is used as the characteristic velocity. The characteristic temperature is chosen as T_I. κ is, of course, already dimensionless.

Denote:

$$
\begin{aligned}
U &= \frac{u}{u_I} & \Lambda &= \frac{u_{II}}{u_I} \\
V &= \frac{v}{u_I} & \vartheta_2 &= \frac{T_{II}}{T_I} \\
\vartheta &= \frac{T}{T_I} & \vartheta_f &= \frac{T_f}{T_I} \\
\vartheta_a &= \frac{A}{R T_I}
\end{aligned}
\tag{33}
$$

Since, through the assumptions on c_p, $\overline{\Delta H_{12}} = c_p (T_f - T_I)$, where T_f is the adiabatic flame temperature, equations (32) become:

$$
\begin{aligned}
&\frac{\partial U}{\partial x} + \frac{\partial V}{\partial y} = 0 \\
&U \frac{\partial \kappa_1}{\partial x} + V \frac{\partial \kappa_1}{\partial y} = \frac{\nu}{s_c u_I} \frac{\partial^2 \kappa_1}{\partial y^2} - \frac{\kappa_1}{\tau u_I} e^{-\vartheta_a/\vartheta} \\
&U \frac{\partial U}{\partial x} + V \frac{\partial U}{\partial y} = \frac{\nu}{u_I} \frac{\partial^2 U}{\partial y^2} \\
&U \frac{\partial \vartheta}{\partial x} + V \frac{\partial \vartheta}{\partial y} = \frac{\nu}{P_r u_I} \frac{\partial^2 \vartheta}{\partial y^2} + \frac{(\vartheta_f - 1)}{u_I \tau} \kappa_1 e^{-\vartheta_a/\vartheta}
\end{aligned}
\tag{34}
$$

The problem then consists of solving equations (34) with the boundary conditions:

$$K_1 = 1,\ \vartheta = 1,\ U = 1\ ; \quad \begin{cases} y > 0,\ x = 0 \\ y = +\infty,\ \text{all } x \end{cases}$$

$$K_1 = 0,\ \vartheta = \vartheta_2,\ U = \Lambda\ ; \quad \begin{cases} y < 0,\ x = 0 \\ y = -\infty,\ \text{all } x \end{cases}$$

$$\frac{\partial K_1}{\partial y} = \frac{\partial \vartheta}{\partial y} = \frac{\partial U}{\partial y} = 0\ ; \quad y = \pm\infty,\ \text{all } x$$

It should be noted that after the flame is fully developed and propagating in the constant velocity combustible stream, the previous equations reduce to those for a one-dimensional flame if these relations are written in terms of a length normal to the flame front. Thus, if the front is plane, and one defines S as a length normal to the front, φ the angle of the flame with respect to the X axis, and u_n the velocity normal to the front, then:

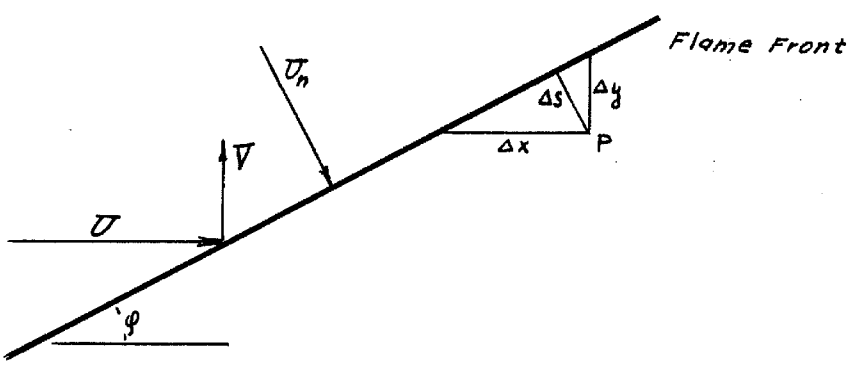

$$U_n = U \sin\varphi - V \cos\varphi = \sin\varphi - V \cos\varphi$$

since $u = u_I$ in the upper stream.

Also, starting at any point on the front along which physical variables are constant, and moving to some point P in the flame along a line $y =$ constant gives $\Delta S\big|_y = \sin\varphi\,\Delta x$. Likewise, starting somewhere on the flame front and moving to P along a line $x =$ constant gives $\Delta S\big|_x = -\cos\varphi\,\Delta y$. In terms of the changes of any of the physical variables with respect to x , y and S , these equalities imply that

$$\frac{\partial}{\partial x} = \sin\varphi\,\frac{\partial}{\partial S}$$

and

$$\frac{\partial}{\partial y} = -\cos\varphi\,\frac{\partial}{\partial S}$$

$$\frac{\partial^2}{\partial y^2} = \cos^2\varphi\,\frac{\partial^2}{\partial S^2}$$

Thus the concentration equation (33) for example, becomes:

$$(\sin\varphi - V\cos\varphi)\frac{\partial K_1}{\partial S} = \frac{\nu}{S_c u_I}\cos^2\varphi\frac{\partial^2 K_1}{\partial S^2} - \frac{K_1}{u_I \tau}\,e^{-\vartheta_a/\vartheta}$$

or since

$$V_n = \frac{u_n}{u_I} = \sin\varphi - V\cos\varphi \quad ,$$

$$V_n\frac{\partial K_1}{\partial S} = \frac{\nu}{S_c u_I}\cos^2\varphi\frac{\partial^2 K_1}{\partial S^2} - \frac{K_1}{\tau u_I}\,e^{-\vartheta_a/\vartheta} .$$

However, since the boundary layer assumptions are assumed to hold, the flame must lie at a small angle with respect to the flow axis so that $\cos^2\varphi \approx 1$.

Thus, the concentration and the energy equations may be written in terms of one independent variable as,

$$u_n\frac{dK_1}{dS} = \frac{\nu}{S_c}\frac{d^2K_1}{dS^2} - \frac{K_1}{\tau}\,e^{-\vartheta_a/\vartheta}$$

$$u_n\frac{d\vartheta}{dS} = \frac{\nu}{P_r}\frac{d^2\vartheta}{dS^2} + \frac{(\vartheta_f - 1)}{\tau}K_1\,e^{-\vartheta_a/\vartheta} \qquad (35)$$

which are recognized as those relations usually employed for one dimensional flame propagation at constant pressure, transformed into a corresponding incompressible flow.

V. INITIAL DEVELOPMENT OF THE COMBUSTION ZONE

In view of the fact that the lower, hot stream is in general at a temperature lower than the adiabatic flame temperature, the transport phenomena of diffusion and heat conduction must govern the ignition and initial reaction rate. Hence, there will be a region immediately after mixing begins where the effects of reaction are small and the concentration and temperature field differ only slightly from those of a classical mixing problem. Figure 1 represents the velocity and temperature profiles found in such a classical mixing problem. The initial profiles are smoothed by the action of viscosity in the case of velocity and by heat conduction in the case of temperature. Figure 2, then, exhibits the expected changes in the temperature distribution when reaction takes place. After proceeding a short distance downstream, the heat addition is still small, and the dotted line in the second profile illustrates the change in temperature. At some point downstream, of course, the local temperature exceeds the lower stream temperature so that a bulge forms, shown by the solid line in the third profile, and finally, after a laminar flame is developed, the local temperature is essentially at the adiabatic flame temperature. The steep gradients associated with the laminar flame are formed, as is shown by the dotted line in the third profile. For a short distance downstream, however, the variations due to combustion may be treated as a perturbation to the pure mixing problem.

Since in the pure mixing problem, it is possible to reduce the conservation equations to total differential equations through the

introduction of a variable

$$\eta = \left(\frac{u_I}{\nu x}\right)^{1/2} y \tag{36}$$

with the assumption that all dependent variables are functions only of η, this variable is used as one of the independent variables for the perturbation development. Thus, changing variables from x, y to s, η, one can write

$$\frac{\partial}{\partial x} = \frac{\partial s}{\partial x}\frac{\partial}{\partial s} + \frac{\partial \eta}{\partial x}\frac{\partial}{\partial \eta}$$

With a similar relation for $\frac{\partial}{\partial y}$. If now, $s = x$, one finds:

$$\frac{\partial}{\partial x} = \frac{\partial}{\partial x} - \frac{\eta}{2x}\frac{\partial}{\partial \eta}$$

$$\frac{\partial}{\partial y} = \left(\frac{u_I}{\nu x}\right)^{1/2}\frac{\partial}{\partial \eta} \tag{37}$$

$$\frac{\partial^2}{\partial y^2} = \frac{u_I}{\nu x}\frac{\partial^2}{\partial \eta^2}$$

Also choosing a stream function in the usual manner, gives

$$\psi = (\nu u_I x)^{1/2} f(\eta)$$

Then

$$u = \frac{\partial \psi}{\partial y} = u_I \frac{df}{d\eta} = u_I f'$$

and

$$v = -\frac{\partial \psi}{\partial x} = -\tfrac{1}{2}\left(\frac{\nu u_I}{x}\right)^{1/2}(f - \eta f')$$

so that the operator $u\frac{\partial}{\partial x} + v\frac{\partial}{\partial y}$ becomes $f'\frac{\partial}{\partial x} - \frac{f}{2x}\frac{\partial}{\partial \eta}$.

These relations plus the transformations (37), identically satisfy the overall continuity equation and transform the momentum, concentration, and energy equations (34) to;

$$f''' + \frac{f}{2} f'' = 0$$

$$\frac{1}{S_c} \frac{\partial^2 \kappa}{\partial \eta^2} + \frac{f}{2} \frac{\partial \kappa}{\partial \eta} - f' x \frac{\partial \kappa}{\partial x} = \frac{x}{u_I \tau} \kappa e^{-\vartheta_a/\vartheta} \qquad (38)$$

$$\frac{1}{P_r} \frac{\partial^2 \vartheta}{\partial \eta^2} + \frac{f}{2} \frac{\partial \vartheta}{\partial \eta} - f' x \frac{\partial \vartheta}{\partial x} = -(\vartheta_f - 1) \frac{x}{u_I \tau} \kappa e^{-\vartheta_a/\vartheta}$$

where the equations have been rearranged slightly, and the subscript on κ dropped. For the remainder of the text, then, κ will refer to the concentration of the combustible.

Now, if the reaction were taking place at a temperature τ, and a concentration κ, the rate at which fuel would be consumed would be $\frac{\kappa}{\tau} e^{-\vartheta_a/\vartheta}$. Since the Arrhenius factor has such a strong influence, the maximum rate takes place deep in the lower stream where the temperature is close to τ_{II}. It, of course, cannot equal τ_{II} exactly since $\tau = \tau_{II}$ at $\eta = -\infty$ where $\kappa = 0$. Thus, some measure of the concentration, κ, at the maximum reaction rate must be found so that the order of magnitude of the heat release may be calculated. If one considers the initial mixing to be practically that of a classical mixing problem, in which the variables are functions of η alone, it follows that the maximum reaction rate occurs when

$$\frac{d}{d\eta} \left(\frac{\kappa}{\tau} e^{-\vartheta_a/\vartheta} \right) = 0$$

Thus

$$\frac{1}{\tau} \frac{d\kappa}{d\eta} e^{-\vartheta_a/\vartheta} + \frac{\kappa}{\tau} \frac{\vartheta_a}{\vartheta^2} e^{-\vartheta_a/\vartheta} \frac{d\vartheta}{d\eta} = 0$$

and

$$\kappa = -\left(\frac{d\kappa}{d\eta}\Big/\frac{d\vartheta}{d\eta}\right)\frac{\vartheta^2}{\vartheta_a}$$

However, an approximate value for the term in parenthesis may be found by considering the case where the Schmidt number and Prandtl number are equal. Then, in the same η increment, κ goes from 1 to κ while ϑ goes from 1 to ϑ Hence

$$\frac{d\kappa}{d\eta}\Big/\frac{d\vartheta}{d\eta} \simeq \frac{1-\kappa}{1-\vartheta}$$

Finally, accounting for the fact that at the maximum reaction rate, $T \simeq T_{II}$, $\kappa \simeq 0$, one may calculate the order of κ at the maximum reaction rate as

$$\kappa_{max\ rate} \simeq -\left[\frac{1-\kappa}{1-\vartheta}\frac{\vartheta^2}{\vartheta_a}\right]_{\substack{\vartheta=\vartheta_2\\ \kappa=0}}$$

$$= \frac{1}{\vartheta_2-1}\frac{\vartheta_2^2}{\vartheta_a} \tag{39}$$

and the maximum reaction rate is then approximately

$$\frac{1}{\tau}\frac{\vartheta_2^2}{(\vartheta_2-1)\vartheta_a}\, e^{-\vartheta_a/\vartheta_2}$$

with the maximum heat release rate being proportional to this rate. Since the maximum rate occurs far down in the hot stream where $u \simeq u_{II}$ then the time taken to go a distance x downstream in this region will be of the order of $\frac{x}{u_{II}}$ where u_{II} is the initial velocity of the hot lower stream. Hence, the heat released in a distance x downstream will be proportional to

$$\frac{x}{u_\infty \tau (\theta_2-1)\theta_a} \frac{\theta_2^2}{} e^{-\theta_a/\theta_2}$$

From the foregoing computations, then, it seems logical to define a chemical characteristic length

$$\ell \equiv u_\infty \tau (\theta_2-1)\frac{\theta_a}{\theta_2^2} e^{\theta_a/\theta_2} \tag{40}$$

which can be used as a measure of the heat release in the initial mixing region. Define $\xi \equiv \frac{x}{\ell}$. Then the energy and concentration equations may be written in the dimensionless forms,

$$\begin{aligned}
&\frac{1}{S_c}\frac{\partial^2 K}{\partial \eta^2} + \frac{f}{2}\frac{\partial K}{\partial \eta} - f'\xi\frac{\partial K}{\partial \xi} = \Lambda(\theta_2-1)\frac{\theta_a}{\theta_2^2}\xi K e^{-\theta_a\left(\frac{1}{\theta}-\frac{1}{\theta_2}\right)} \\
&\frac{1}{P_r}\frac{\partial^2 \theta}{\partial \eta^2} + \frac{f}{2}\frac{\partial \theta}{\partial \eta} - f'\xi\frac{\partial \theta}{\partial \xi} = -\Lambda(\theta_2-1)(\theta_2-1)\frac{\theta_a}{\theta_2^2}\xi K e^{-\theta_a\left(\frac{1}{\theta}-\frac{1}{\theta_2}\right)}
\end{aligned} \tag{41}$$

Now, for $\xi = \frac{x}{\ell} << 1$ or, the distance downstream very small compared to the characteristic chemical length, the appropriate expressions for K and θ are

$$\begin{aligned}
K &= K^{(0)}(\eta) + \xi K^{(1)}(\eta) + \xi^2 K^{(2)}(\eta) + \cdots \\
\theta &= \theta^{(0)}(\eta) + \xi\,\theta^{(1)}(\eta) + \xi^2\theta^{(2)}(\eta) + \cdots
\end{aligned} \tag{42}$$

Substitution of the relations (42) into equations (41) gives then, the zero'th, first, second, etc. order equations according to a classical perturbation calculation. The zero'th order equations, of course, reduce to the pure mixing equations, since the x dependence becomes unnecessary. Hence, the zero'th order equations are,

$$\frac{1}{S_c}\frac{d^2K^{(0)}}{d\eta^2} + \frac{f}{2}\frac{dK^{(0)}}{d\eta} = 0$$

$$\frac{1}{P_r}\frac{d^2\theta^{(0)}}{d\eta^2} + \frac{f}{2}\frac{d\theta^{(0)}}{d\eta} = 0 \qquad (43)$$

while the first and second order are,

$$\frac{1}{S_c}\frac{d^2K^{(1)}}{d\eta^2} + \frac{f}{2}\frac{dK^{(1)}}{d\eta} - f'K^{(1)} = \Lambda(\theta_2-1)\frac{\theta_a}{\theta_2^2}K^{(0)}e^{-\theta_a\left(\frac{1}{\theta^{(0)}}-\frac{1}{\theta_2}\right)}$$

$$\frac{1}{P_r}\frac{d^2\theta^{(1)}}{d\eta^2} + \frac{f}{2}\frac{d\theta^{(1)}}{d\eta} - f'\theta^{(1)} = -\Lambda(\theta_f-1)(\theta_2-1)\frac{\theta_a}{\theta_2^2}K^{(0)}e^{-\theta_a\left(\frac{1}{\theta^{(0)}}-\frac{1}{\theta_2}\right)} \qquad (44)$$

and

$$\frac{1}{S_c}\frac{d^2K^{(2)}}{d\eta^2} + \frac{f}{2}\frac{dK^{(2)}}{d\eta} - 2f'K^{(2)} = \Lambda(\theta_2-1)\frac{\theta_a}{\theta_2^2}K^{(0)}e^{-\theta_a\left(\frac{1}{\theta^{(0)}}-\frac{1}{\theta_2}\right)} \times$$

$$\times\left\{\frac{K^{(1)}}{K^{(0)}} + \frac{\theta^{(1)}}{\theta^{(0)}}\frac{\theta_a}{\theta^{(0)}}\right\}$$

$$\frac{1}{P_r}\frac{d^2\theta^{(2)}}{d\eta^2} + \frac{f}{2}\frac{d\theta^{(2)}}{d\eta} - 2f'\theta^{(2)} = -\Lambda(\theta_f-1)(\theta_2-1)\frac{\theta_a}{\theta_2^2}K^{(0)}e^{-\theta_a\left(\frac{1}{\theta^{(0)}}-\frac{1}{\theta_2}\right)} \times \qquad (45)$$

$$\times\left\{\frac{K^{(1)}}{K^{(0)}} + \frac{\theta^{(1)}}{\theta^{(0)}}\frac{\theta_a}{\theta^{(0)}}\right\}$$

The boundary conditions on the zeroth order functions are now,

$$\left.\begin{aligned} &K^{(0)} = 1\ ,\quad \theta^{(0)} = 1 \\ &\frac{dK^{(0)}}{d\eta} = \frac{d\theta^{(0)}}{d\eta} = 0 \end{aligned}\right\}\ \eta = +\infty$$

$$\left.\begin{aligned} &K^{(0)} = 0\ ,\quad \theta^{(0)} = \theta_2 \\ &\frac{dK^{(0)}}{d\eta} = \frac{d\theta^{(0)}}{d\eta} = 0 \end{aligned}\right\}\ \eta = -\infty$$

while all perturbations and their derivatives vanish at $\eta = \pm\infty$. It should be noted that it is assumed that the reaction is nonexistent at $\eta = +\infty$, or in other words at $T = T_I$. Since the exponential variation of the rate with temperature does not predict this zero value, it must be assumed that although the combustible enters the mixing field with a temperature T_I , at which there would be a small rate, the effects are negligible so that there is effectively no reaction at temperature T_I . This cold boundary condition is discussed by von Kármán in reference 4.

It is evident that while the Blasius equation (38) and equations (43), (44), and (45) have been simplified to the extent that they are now total differential equations, it is not possible to find a general solution. However, it is sufficient to solve the special case of velocities equal $(\Lambda = 1)$ with an added calculation showing the results of changing the velocity ratio.

If, then, the velocities of the two streams are supposed equal, it is not necessary to consider the momentum equation since no shear field exists in the incompressible flow field. Moreover, the streamlines are lines $g =$ constant, so that $f = \eta$, where the zero streamline is supposed as the line $g = 0$, satisfies the conditions on f . The zero'th order equations are then very simple to integrate and give the following solutions:

$$\vartheta^{(0)} = \frac{\vartheta_2 + 1}{2} - \frac{\vartheta_2 - 1}{2}\, erf\left(\sqrt{\frac{P_r}{4}}\,\eta\right)$$

$$K^{(0)} = \frac{1}{2}\left(1 + erf\left(\sqrt{\frac{S_c}{4}}\,\eta\right)\right) \qquad (46)$$

where $erf(s) = \frac{2}{\sqrt{\pi}} \int_0^s e^{-t^2} dt$. These are well known solutions of the heat conduction and diffusion equations.

Considering, next, the first order energy equation, it is first, rewritten as

$$\frac{d^2\theta^{(1)}}{d\eta^2} + \frac{P_r}{2}\eta \frac{d\theta^{(1)}}{d\eta} - P_r \theta^{(1)} = -P_r(\theta_f - 1)(\theta_2 - 1)\frac{\partial \theta_2}{\partial \theta_2^2} \mathcal{R}(\eta) \tag{47}$$

where

$$\mathcal{R}(\eta) \equiv K^{(0)} e^{-\theta_2}\left(\frac{1}{\theta^{(0)}} - \frac{1}{\theta_2}\right) \tag{48}$$

The homogeneous equation has two linearly independent solutions[15] which may be written in the form:

$$\begin{aligned} \mathcal{H}_1(\eta) &= \sqrt{P_r}\,\eta\, e^{-\frac{P_r}{4}\eta^2} + 2\sqrt{\pi}\left(\frac{1}{2} + \frac{P_r}{4}\eta^2\right)\left(erf\left(\sqrt{\frac{P_r}{4}}\eta\right) - 1\right) \\ \mathcal{H}_2(\eta) &= \sqrt{P_r}\,\eta\, e^{-\frac{P_r}{4}\eta^2} + 2\sqrt{\pi}\left(\frac{1}{2} + \frac{P_r}{4}\eta^2\right)\left(erf\left(\sqrt{\frac{P_r}{4}}\eta\right) + 1\right) \end{aligned} \tag{49}$$

Also, defining a Green's function, $G(\eta, \bar{\eta}; P_r)$, such that

$$\theta^{(1)}(\eta) = P_r(\theta_f - 1)(\theta_2 - 1)\frac{\partial \theta_2}{\partial \theta_2^2}\int_{-\infty}^{\infty} G(\eta, \bar{\eta}; P_r)\mathcal{R}(\bar{\eta})\, d\bar{\eta}$$

and substituting into equation (47), one obtains,

$$\int_{-\infty}^{\infty}\left\{\frac{\partial^2 G}{\partial \eta^2} + \frac{\eta}{2}P_r\frac{\partial G}{\partial \eta} - P_r G\right\}\mathcal{R}(\bar{\eta})\, d\bar{\eta} = -\mathcal{R}(\eta)$$

so that

$$\frac{\partial^2 G}{\partial \eta^2} + \frac{P_r}{2}\eta\frac{\partial G}{\partial \eta} - P_r G = -\delta(\eta - \bar{\eta}) \tag{50}$$

where $\delta(\eta-\bar{\eta})$ is the usual delta function defined such that

$$\delta(\eta-\bar{\eta}) = 0 \;,\quad \eta \neq \bar{\eta}$$

$$= \infty \;,\quad \eta = \bar{\eta}$$

$$\int_{\bar{\eta}-\varepsilon}^{\bar{\eta}+\varepsilon} \delta(\eta-\bar{\eta})\,d\eta = 1 \quad (\varepsilon \text{ arbitrary})$$

Thus G must satisfy the boundary conditions on $\mathcal{G}^{(1)}$ in η and a jump condition in slope, for, integrating (50) between $\bar{\eta}-\varepsilon$ and $\bar{\eta}+\varepsilon$ where $\varepsilon << 1$,

$$\int_{\bar{\eta}-\varepsilon}^{\bar{\eta}+\varepsilon} \left\{ \frac{\partial^2 G}{\partial \eta^2} + \frac{\eta}{2} P_r \frac{\partial G}{\partial \eta} - P_r G \right\} d\eta = -\int_{\bar{\eta}-\varepsilon}^{\bar{\eta}+\varepsilon} \delta(\eta-\bar{\eta})\,d\eta$$

and thus:

$$\frac{\partial G}{\partial \eta}\Big|_{\bar{\eta}-\varepsilon}^{\bar{\eta}+\varepsilon} + \frac{P_r}{2}\eta G\Big|_{\bar{\eta}-\varepsilon}^{\bar{\eta}+\varepsilon} - \frac{3}{2}P_r \int_{\bar{\eta}-\varepsilon}^{\bar{\eta}+\varepsilon} G\,d\eta = -\int_{\bar{\eta}-\varepsilon}^{\bar{\eta}+\varepsilon} \delta(\eta-\bar{\eta})\,d\eta = -1$$

However, G and thus $\int G\,d\eta$ are by necessity continuous, so that as $\varepsilon \to 0$

$$\frac{\partial G}{\partial \eta}\Big|_{\bar{\eta}-\varepsilon}^{\bar{\eta}+\varepsilon} \longrightarrow -1$$

Thus if

$$G(\eta, \bar{\eta}; P_r) = G_1(\eta, \bar{\eta}; P_r) \;,\quad \eta > \bar{\eta}$$

$$= G_2(\eta, \bar{\eta}; P_r) \;,\quad \eta < \bar{\eta}$$

the jump condition becomes,

$$\frac{\partial G_1}{\partial \eta}\Big|_{\bar{\eta}} - \frac{\partial G_2}{\partial \eta}\Big|_{\bar{\eta}} = -1 \tag{51}$$

with

$$G_1\Big|_{\bar{\eta}} = G_2\Big|_{\bar{\eta}}$$

and the boundary conditions on G_1, and G_2 are now; $G_1 \to 0$ as $\eta \to +\infty$

and $G_2 \to 0$ as $\eta \to -\infty$.

Since for $\eta = \bar{\eta}$, equation (50) is homogeneous, one can separate variables. Farther, in view of the boundary conditions which G_1 , and G_2 must satisfy, these functions may be written as

$$G_1 = -k_1(\bar{\eta})\,\mathcal{H}_1(\eta)$$
$$G_2 = -k_2(\bar{\eta})\,\mathcal{H}_2(\eta) \qquad (52)$$

where the minus sign is used to account for the fact that $\mathcal{H}_1$ is always negative, $\mathcal{H}_2$, always positive. This then makes G inherently positive, as will be seen later.

The functions $k_1(\bar{\eta})$ and $k_2(\bar{\eta})$ must be evaluated by the jump condition and the continuity of G at $\bar{\eta}$.

Thus,

$$-k_1(\bar{\eta})\left.\frac{d\mathcal{H}_1}{d\eta}\right|_{\bar{\eta}} + k_2(\bar{\eta})\left.\frac{d\mathcal{H}_2}{d\eta}\right|_{\bar{\eta}} = -1$$

and (53)

$$k_1(\bar{\eta})\,\mathcal{H}_1(\bar{\eta}) = k_2(\bar{\eta})\,\mathcal{H}_2(\bar{\eta})$$

or writing $\left.\frac{d\mathcal{H}_1}{d\eta}\right|_{\bar{\eta}} = \frac{d\mathcal{H}_1}{d\bar{\eta}}$, etc.,

$$k_2(\bar{\eta}) = -\frac{1}{\mathcal{H}_2}\left\{\frac{1}{\mathcal{H}_2}\frac{d\mathcal{H}_2}{d\bar{\eta}} - \frac{1}{\mathcal{H}_1}\frac{d\mathcal{H}_1}{d\bar{\eta}}\right\}^{-1}$$

But

$$\frac{1}{\mathcal{H}_2}\frac{d\mathcal{H}_2}{d\bar{\eta}} - \frac{1}{\mathcal{H}_1}\frac{d\mathcal{H}_1}{d\bar{\eta}} = \frac{1}{\mathcal{H}_2}\left\{\frac{2}{\bar{\eta}}\mathcal{H}_2 - \frac{2\sqrt{\pi}}{\bar{\eta}}\left(\operatorname{erf}\left(\sqrt{\tfrac{R}{4}}\,\bar{\eta}\right)+1\right)\right\} -$$

$$-\frac{1}{\mathcal{H}_1}\left\{\frac{2}{\bar{\eta}}\mathcal{H}_1 - \frac{2\sqrt{\pi}}{\bar{\eta}}\left(\operatorname{erf}\left(\sqrt{\tfrac{R}{4}}\,\bar{\eta}\right)-1\right)\right\}$$

$$= \frac{2\sqrt{\pi}}{\bar{\eta}}\frac{1}{\mathcal{H}_1\mathcal{H}_2}\left\{\mathcal{H}_2\left(\operatorname{erf}\left(\sqrt{\tfrac{R}{4}}\,\bar{\eta}\right)-1\right) - \mathcal{H}_1\left(\operatorname{erf}\left(\sqrt{\tfrac{R}{4}}\,\bar{\eta}\right)+1\right)\right\}$$

$$= \frac{2\sqrt{\pi}}{\bar{\eta}} \frac{1}{\mathcal{K}_1 \mathcal{K}_2} \sqrt{P_r}\, \bar{\eta}\, e^{-\frac{P_r}{4}\bar{\eta}^2} \left\{ \left(\operatorname{erf}\left(\sqrt{\tfrac{P_r}{4}}\bar{\eta} \right) - 1 \right) - \left(\operatorname{erf}\left(\sqrt{\tfrac{P_r}{4}}\bar{\eta} \right) + 1 \right) \right\}$$

$$= \frac{4\sqrt{P_r \pi}\, e^{-\frac{P_r}{4}\bar{\eta}^2}}{\mathcal{K}_1 \mathcal{K}_2}$$

so that

$$k_2(\bar{\eta}) = \frac{\mathcal{K}_1(\bar{\eta})\, e^{\frac{P_r}{4}\bar{\eta}^2}}{4\sqrt{P_r \pi}}$$

and

$$k_1(\bar{\eta}) = \frac{\mathcal{K}_2(\bar{\eta})\, e^{\frac{P_r}{4}\bar{\eta}^2}}{4\sqrt{P_r \pi}} \qquad (54)$$

from equation (53).

The solution for $\mathcal{G}^{(1)}$ can be written now as;

$$\mathcal{G}^{(1)}(\eta) = P_r (\vartheta_1 - 1)(\vartheta_2 - 1) \frac{\partial \mathcal{G}}{\partial \vartheta_2^2} \int_{-\infty}^{\infty} G(\eta, \bar{\eta}; P_r)\, \mathcal{R}(\bar{\eta})\, d\bar{\eta}$$

$$= -\sqrt{\frac{P_r}{\pi}} \frac{(\vartheta_1 - 1)}{4} (\vartheta_2 - 1) \frac{\partial \mathcal{G}}{\partial \vartheta_2^2} \left\{ \mathcal{K}_1(\eta) \int_{-\infty}^{\eta} \mathcal{K}_2(\bar{\eta})\, e^{\frac{P_r}{4}\bar{\eta}^2}\, \mathcal{R}(\bar{\eta})\, d\bar{\eta} + \right.$$

$$\left. + \mathcal{K}_2(\eta) \int_{\eta}^{\infty} \mathcal{K}_1(\bar{\eta})\, e^{\frac{P_r}{4}\bar{\eta}^2}\, \mathcal{R}(\bar{\eta})\, d\bar{\eta} \right\} \qquad (55)$$

where since $\mathcal{H}_1(\eta)$ is always < 0, and $\mathcal{H}_2(\eta)$ always > 0, $G > 0$, and $\vartheta^{(0)} > 0$.

Likewise, the solution for $\kappa^{(1)}$ can be written immediately since the equation is similar to the equation just solved; hence

$$\kappa^{(1)}(\eta) = -S_c(\mathcal{H}_2 - 1)\frac{\mathcal{H}_1}{\mathcal{H}_2^2}\int_{-\infty}^{\infty} G(\eta, \bar{\eta}; S_c)\, R(\bar{\eta})\, d\bar{\eta} \qquad (56)$$

where, as indicated, the Schmidt number replaces the Prandtl number in the Green's function.

This form is very suitable for numerical calculation by Simpson's rule of numerical integration since the Green's function and the rest of the integrand are easily computed (Appendix C). Figure 3 shows the results of one such computation for the temperature profiles. In this figure $f = 0$ corresponds to the classical mixing problem solution, since in this case $\vartheta = \vartheta^{(0)}(\eta)$. The physical constants used are approximately those of the combustible azomethane,[16] which follows a first order rate law in its decomposition. Calculations for the physical parameters are given in Appendix B.

Figure 3 indicates that the maximum perturbation occurs well below the center line of the two streams, showing the preponderant effect of the Arrhenius factor in the reaction rate. It shows, also, that very early, a bulge is formed in the temperature profile, when the temperature exceeds T_{∞}, the lower stream temperature. This bulge grows and continues to rise toward the combustible stream, due to the effect of the concentration on the reaction rate; the maximum rate occurs not at the point of maximum temperature, but a little above it where the concentration of combustible is greater.

Since, according to the first perturbation, the temperature increases with X, and the bulge rises toward the combustible stream, the tendency is for the initial reaction to develop into a flame, with no retardation or blowoff possible. The principal question is then what length of time is taken, or more practically, how great a distance downstream is traversed before combustion is assured? The simplest significant length to calculate is that distance which is traversed downstream before a bulge in the temperature profile first occurs. This distance may be calculated, using only the zero'th and first order functions, since at the bulge in the temperature profile,

$$\frac{\partial \theta}{\partial \eta} \simeq \frac{d z^{(0)}}{d \eta} + \xi \frac{d z^{(1)}}{d \eta} = 0 \tag{57}$$

This expression can be solved for ξ as a function of η, giving the distance downstream to a bulge, for any given η. Since one wishes to find the minimum distance it is necessary to travel before a bulge occurs, one must calculate the minimum X with respect to η. This minimum X is defined as the detachment distance, and denoted by X_i, or in dimensionless notation, ξ_i. Likewise, the η at which this minimum occurs is denoted by η_i. Thus, to calculate η_i,

$$\left.\frac{d \xi}{d \eta}\right|_{\eta_i} = \frac{1}{\left(\frac{d z^{(0)}}{d \eta}\right)^2} \left(\frac{d^2 z^{(0)}}{d \eta^2} \frac{d z^{(1)}}{d \eta} - \frac{d^2 z^{(1)}}{d \eta^2} \frac{d z^{(0)}}{d \eta} \right) = 0$$

but, since $\frac{d z^{(1)}}{d \eta}$ is certainly finite over the entire region, the bracketed terms must disappear, and employing the equation for $z^{(0)}(\eta)$ (43), it is seen that

$$\frac{d\vartheta^{(o)}}{d\eta}\left[\frac{d^2\vartheta^{(1)}}{d\eta^2}+\frac{P_r}{2}f\frac{d\vartheta^{(1)}}{d\eta}\right]=0$$

However, since $\frac{d\vartheta^{(o)}}{d\eta}=0$ occurs only at $\eta=\pm\infty$ where $\frac{d\vartheta^{(1)}}{d\eta}=0$ and thus $\frac{\partial\vartheta}{\partial\eta}=0$ for all ξ, the interesting solution occurs when the bracketed terms disappear. Comparison of these terms with equation (44) gives a simple algebraic relation,

$$f'\vartheta^{(1)}=\Lambda(\vartheta_f-1)(\vartheta_b-1)\frac{\vartheta_b}{\vartheta_2^2}R \tag{58}$$

which has a solution η_i.

Finally, ξ_i is computed from equation (57)

$$\xi_i=-\left(\frac{d\vartheta^{(o)}}{d\eta}\Big/\frac{d\vartheta^{(1)}}{d\eta}\right)_{\eta_i} \tag{59}$$

While it is not possible to solve (58) and (59) exactly, due to the integral form of the solution for $\vartheta^{(1)}$, it is possible to calculate η_i and ξ_i if one makes use of the fact that the bulge in the temperature profile first occurs for $\eta<<0$. This can be seen in figure 3 where the first bulge shown occurs at $\eta\simeq-4$. This suggests using asymptotic forms to calculate the detachment distance, in view of the fact that, in figure 3, as ξ gets smaller, $|\eta|$ at the bulge becomes larger. Further, all the functions involved are composed of exponential and error functions which converge very rapidly.

The necessary functions are easily expanded for η large and negative to,

$$\mathcal{H}_1(\eta) \sim -2\sqrt{\pi}\left(1+\frac{P_r}{2}\eta^2\right) + \frac{8}{P_r^{3/2}}\frac{e^{-\frac{P_r}{4}\eta^2}}{\eta^3}\left(1-\frac{12}{P_r\eta^2}+\cdots\right)$$

$$\mathcal{H}_2(\eta) \sim -\frac{8}{P_r^{3/2}}\frac{e^{-\frac{P_r}{4}\eta^2}}{\eta^3}\left(1-\frac{12}{P_r\eta^2}+\cdots\right)$$

$$K^{(0)}(\eta) \sim -\frac{1}{\sqrt{\pi}}\frac{e^{-\frac{S_c}{4}\eta^2}}{\sqrt{S_c}\,\eta}\left(1-\frac{2}{S_c\eta^2}+\cdots\right)$$

$$\vartheta^{(0)}(\eta) \sim \vartheta_2 + \frac{\vartheta_2-1}{\sqrt{\pi P_r}}\frac{e^{-\frac{P_r}{4}\eta^2}}{\eta}\left(1-\frac{2}{P_r\eta^2}+\cdots\right) \qquad (60)$$

$$e^{-\vartheta_2\left(\frac{1}{\vartheta^{(0)}}-\frac{1}{\vartheta_2}\right)} \sim 1 + \frac{\vartheta_2}{\vartheta_2^2}\frac{(\vartheta_2-1)}{\sqrt{P_r\pi}}\frac{e^{-\frac{P_r}{4}\eta^2}}{\eta}\left(1-\frac{2}{P_r\eta^2}+\cdots\right)+\cdots$$

$$R(\eta) \sim -\frac{1}{\sqrt{\pi}}\frac{e^{-\frac{S_c}{4}\eta^2}}{\sqrt{S_c}\,\eta}\left(1-\frac{2}{S_c\eta^2}+\cdots\right) - \frac{1}{\pi}\frac{\vartheta_2}{\vartheta_2^2}\frac{(\vartheta_2-1)}{\sqrt{S_cP_r}}\frac{e^{-\frac{\eta^2}{4}(S_c+P_r)}}{\eta^2}+\cdots$$

$$\int_{-\infty}^{\eta}\mathcal{H}_2(\bar\eta)e^{\frac{P_r}{4}\bar\eta^2}R(\bar\eta)\,d\bar\eta \sim -\frac{16}{\sqrt{\pi}}\frac{e^{-\frac{S_c}{4}\eta^2}}{(S_cP_r)^{3/2}\eta^5}\left[1-12\left(\frac{1}{S_c}+\frac{1}{P_r}\right)\frac{1}{\eta^2}+\cdots\right]$$

$$\int_{\eta}^{\infty}\mathcal{H}_1(\bar\eta)e^{\frac{P_r}{4}\bar\eta^2}R(\bar\eta)\,d\bar\eta = -C + \frac{2P_r}{\sqrt{S_c}(S_c-P_r)}e^{-\frac{\eta^2}{4}(S_c-P_r)}\left(1+\frac{S_c-P_r}{P_rS_c}\frac{2}{\eta^2}+\cdots\right)$$

for $P_r \neq S_c$

$$= C(\eta_0) - \frac{2}{\sqrt{P_r}}\left(\frac{P_r\eta^2}{24}-\frac{2}{P_r\eta^2}\right)$$

for $P_r = S_c$

where

$$C = -\int_{-\infty}^{\infty} \mathcal{H}_1(\bar{\eta}) e^{\frac{P_r}{4}\bar{\eta}^2} R(\bar{\eta})\, d\bar{\eta}$$

and

$$C(\eta_0) = -\int_{\eta_0}^{\infty} \mathcal{H}_1(\bar{\eta}) e^{\frac{P_r}{4}\bar{\eta}^2} R(\bar{\eta})\, d\bar{\eta} + \frac{2}{\sqrt{P_r}}\left(\frac{P_r \eta_0^2}{4} - \frac{2}{P_r \eta_0^2}\right) \tag{61}$$

and the error function expansion

$$1 - \operatorname{erf} x \sim \frac{1}{\sqrt{\pi}} \frac{e^{-x^2}}{x}\left\{1 - \frac{1}{2x^2} + \frac{3}{(2x^2)^2} - \cdots\right\}$$

has been used. In order to calculate C, it was necessary only to use calculations of the integral made for the temperature profiles. (Appendix C) To calculate $C(\eta_0)$ it would be necessary to compute the whole integral for a few large and negative values of η until it was seen that the expansion gave the accuracy desired.

The use of these expansions (equations 60) then gives an asymptotic expansion for $\vartheta^{(1)}$;

$$\vartheta^{(1)}(\eta) \sim -\frac{2}{\sqrt{\pi}} \frac{(\vartheta_1 - 1)(\vartheta_2 - 1)}{P_r} \frac{\vartheta_2}{\vartheta_2'^2} \frac{1}{\eta^3} \left\{ \frac{4}{S_c^{3/2}} \left(1 + \frac{P_r}{2}\eta^2\right)\left(1 - 12\left(\frac{1}{S_c} + \frac{1}{P_r}\right)\frac{1}{\eta^2} + \cdots\right) \frac{e^{-\frac{S_c}{4}\eta^2}}{\eta^2} + \right.$$

$$\left. + e^{-\frac{P_r}{4}\eta^2}\left(1 - \frac{12}{P_r \eta^2} + \cdots\right)\left(C - \frac{2 P_r}{\sqrt{S_c}(S_c - P_r)} e^{-\frac{\eta^2}{4}(S_c - P_r)} + \cdots\right) \right\} \tag{62}$$

Finally, for this case of velocities equal, equation (58) reduces to

$$\vartheta^{(1)}(\eta_i) = (\vartheta_1 - 1)(\vartheta_2 - 1) \frac{\vartheta_2}{\vartheta_2'^2} R(\eta_i) \tag{63}$$

since $f' = \Lambda = 1$, so that substitution of the expansions for $\vartheta^{(1)}$, (62), and R, (60), into equation (63), gives

$$\frac{2\sqrt{S_c}}{P_r}\frac{1}{\eta_i^2}\left\{\frac{4}{S_c^{3/2}}\left(1+\frac{P_r}{2}\eta_i^2\right)\left(1-12\left(\frac{1}{S_c}+\frac{1}{P_r}\right)\frac{1}{\eta_i^2}+\cdots\right)\frac{1}{\eta_i^2}+\right.$$

$$\left.+e^{\frac{\eta_i^2(S_c-P_r)}{4}}\left(1-\frac{12}{P_r\eta_i^2}+\cdots\right)\left(C-\frac{2P_r e^{-\frac{\eta_i^2(S_c-P_r)}{4}}}{\sqrt{S_c}(S_c-P_r)}\right)\right\}=1-\frac{2}{S_c\eta_i^2}+\cdots \qquad (64)$$

a relation which may be solved by trial and error for η_i . It might be remarked that, using the physical constants for azomethane, as before, the value of η_i obtained was approximately 6, so that the asymptotic expansion was justified. (Appendix C)

In order to solve for f_i , then, $\frac{d\vartheta^{(1)}}{d\eta}$ must be calculated. From equation (55),

$$\frac{d\vartheta^{(1)}}{d\eta}=-\sqrt{\frac{P_r}{\pi}}\frac{(2\vartheta_1-1)(2\vartheta_2-1)}{4}\frac{\vartheta_a}{\vartheta_2^2}\left\{\frac{d\mathcal{H}_1}{d\eta}\int_{-\infty}^{\eta}\mathcal{H}_2(\bar\eta)e^{\frac{P_r}{4}\bar\eta^2}\mathcal{R}(\bar\eta)d\bar\eta+\right.$$

$$\left.+\frac{d\mathcal{H}_2}{d\eta}\int_{\eta}^{\infty}\mathcal{H}_1(\bar\eta)e^{\frac{P_r}{4}\bar\eta^2}\mathcal{R}(\bar\eta)d\bar\eta\right\} \qquad (65)$$

and, again, using the asymptotic expansions, (60) in the above relation, and calculating $\frac{d\vartheta^{(0)}}{d\eta}$ from equation (46), one can compute f_i from equation (59) as;

$$f_i=\frac{\sqrt{P_r}}{2}\frac{\vartheta_2^2}{\vartheta_a(\vartheta_1-1)}\eta_i^2\left\{\left(1-\frac{6}{P_r\eta_i^2}\right)\left(C-\frac{2P_r e^{-\frac{\eta_i^2(S_c-P_r)}{4}}}{\sqrt{S_c}(S_c-P_r)}\right)-\right.$$

$$\left.-\frac{8}{S_c^{3/2}}\frac{e^{-\frac{\eta_i^2(S_c-P_r)}{4}}}{\eta_i^2}\left(1-\frac{12}{\eta_i^2}\left(\frac{1}{S_c}+\frac{1}{P_r}\right)\right)\right\}^{-1} \quad \text{for } P_r\neq S_c \qquad (66)$$

In order to find the variation of the detachment distance with T_{II} , it is first necessary to find how η_i and f_i vary with T_{II} .

The variation in η_i due to changes in the lower stream temperature as well as the activation energy and the Schmidt and Prandtl numbers can be investigated, using equation (64). Changing the variable to $z = \sqrt{\frac{P_r}{4}}\,\eta$ and solving for $\overline{C}$, one obtains the following relation:

$$\overline{C} = \frac{e^{-z_i^2\left(\frac{S_c}{P_r}-1\right)}}{\sqrt{S_c/P_r}} \int \left[\frac{2}{\left(\frac{S_c}{P_r}-1\right)} + \frac{1}{\left(1-\frac{3}{z_i^2}\right)} \left[2z_i^2 - \frac{3}{\left(\frac{S_c}{P_r}\right)} + \frac{1}{\frac{S_c}{P_r} z_i^2} \left(\frac{6}{\left(\frac{S_c}{P_r}\right)} + 5 + 3\left(\frac{1}{\left(\frac{S_c}{P_r}\right)} + 1 \right) \frac{1}{z_i^2} \right) \right] \right] \qquad (64a)$$

where, also,

$$\overline{C} = \sqrt{P_r}\, C = -2 \int_{-\infty}^{\infty} \mathcal{H}_1(z)\, e^{z^2} K^{(0)}\left(\sqrt{\tfrac{S_c}{P_r}}\, z\right) e^{-\frac{\vartheta_a}{\vartheta_2}\left(\frac{\vartheta_2}{\vartheta^{(0)}}-1\right)} dz$$

Also, $\frac{\vartheta_2}{\vartheta^{(0)}} - 1$ may be written as

$$\frac{\vartheta_2}{\vartheta^{(0)}} - 1 = \left(1-\frac{1}{\vartheta_2}\right) \frac{\frac{1}{2}(1+\operatorname{erf} z)}{1-\left(1-\frac{1}{\vartheta_2}\right)(1+\operatorname{erf} z)}$$

but since the integrand reaches a maximum when $z << 0$, this expression may be approximated in the integral by $\frac{\vartheta_2}{\vartheta^{(0)}} - 1 \simeq \left(1-\frac{1}{\vartheta_2}\right)\left(\frac{1+\operatorname{erf} z}{2}\right)$ so that

$$\overline{C} \simeq -2 \int_{-\infty}^{\infty} \mathcal{H}_1(z)\, e^{z^2} K^{(0)}\left(\sqrt{\tfrac{S_c}{P_r}}\, z\right) e^{-\frac{\vartheta_a}{\vartheta_2}\left(1-\frac{1}{\vartheta_2}\right)\left(\frac{1+\operatorname{erf} z}{2}\right)} dz$$

Hence, the parameters in equation (64a) are $\frac{S_c}{P_r}$ and $\frac{\vartheta_a}{\vartheta_2}\left(1-\frac{1}{\vartheta_2}\right)$.

Calculations were made finding the values of $\sqrt{\frac{P_r}{4}}\,\eta_i$ for several values of the parameters. The resulting curves are presented in figure 4 and indicate that there is very little variation in η_i due to changes in activation energy or lower stream temperatures. Thus, since $\eta_i \sim y_i/\sqrt{x_i}$ and η_i is almost invariant with $\frac{\vartheta_a}{\vartheta_2}\left(1-\frac{1}{\vartheta_2}\right)$, y_i varies as $x_i^{1/2}$ or as $\left[(\vartheta_2-1)\, e^{\vartheta_a/\vartheta_2}\right]^{1/2}$. Therefore, as either A decreases or T_π increases y_i decreases, as one would expect from physical considerations.

Figure 4 also shows that as $\frac{S_c}{P_r}$ increases, or in other words, as the diffusion zone gets smaller relative to the thermal mixing zone, η_i decreases. Since the calculations for $\frac{S_c}{P_r} = 1.30$ gave values of z of about 2.4, it is evident that for larger values of $\frac{S_c}{P_r}$, more terms of the asymptotic expansion might have to be used to keep the same accuracy.

Next, equation (66) indicates that f_i is proportional to T_{II}^2 through $z\ell_2^2$. Finally, since $x_i = f_i \ell = f_i u_{II} \tau (z\ell_2 - 1) \frac{z\ell_2}{z\ell_2^2} e^{z\ell_2/\ell_2}$ then $x_i \sim (z\ell_2 - 1) e^{z\ell_2/\ell_2}$ so that x_i essentially depends exponentially on T_{II}. Figure 5 gives the variation of x_i with T_{II}, for the combustible azomethane, using the same values for the physical constants as used for the temperature profiles. It is seen from figure 4 that the value of x_i increases enormously as the hot stream temperature decreases. Therefore it is apparent that although this process of combustion in a laminar mixing region shows no distinct blowoff, the detachment distance becomes so great for low hot stream temperatures that it exceeds the physical dimensions of any apparatus. Thus, the limitation present in making it impossible to calculate any blowoff velocity seems to be the fact that streams of semi infinite extent were considered, rather than the streams of finite extent which would result from using any practical apparatus.

Using the results of the foregoing analysis, it is now possible to estimate the effects of a velocity difference between the two streams on the detachment distance. The Blasius function must be known, of course, to solve the equations even for x_i. However, since it is

now established that the first bulge in the temperature profile occurs at an $\eta << 0$, it is possible to estimate the Blasius function and its derivative using asymptotic representations.

According to Lock,[17] the Blasius function for a laminar mixing region may be represented in the following manner, for η large and negative, and $\Lambda \neq 0$;

$$f \sim \Lambda\eta + B + B_1 \frac{e^{-\bar{z}^2}}{\bar{z}^2}\left(1 - \frac{3}{2\bar{z}^2} + \frac{15}{4\bar{z}^4} + \cdots\right) - \frac{1}{8} B_1^2 \frac{e^{-2\bar{z}^2}}{\Lambda^{1/4}\bar{z}^5} + \cdots$$

$$f' \sim \Lambda + B_1 \Lambda^{1/4} \frac{e^{-\bar{z}^2}}{\bar{z}}\left(1 - \frac{1}{2\bar{z}^2} + \cdots\right) - \frac{B_1^2}{4}\frac{e^{-2\bar{z}^2}}{\bar{z}^4} + \cdots . \qquad (67)$$

where $\bar{z} = -\frac{1}{2}\Lambda^{1/4}\left(\eta + \frac{B}{\Lambda}\right)$ and B and B_1 are constants.

However, for η very large and negative f may be approximated by the first two linear terms, and f' by the constant Λ to very good accuracy. This was checked numerically, using the results of Lock's work for $\Lambda = 0.5$. That more terms would be superfluous in order to calculate f_i , can also be seen by noting that in the energy equation, f is multiplied by $\frac{d\theta^{(0)}}{d\eta}$, and f' by $\theta^{(0)}$, both of which are of order $e^{-\frac{\eta^2}{4}}$. Thus, including the third term in f or the second in f' would merely add terms of order $\left(e^{-\frac{\eta^2}{4}}\right)^2$. Since only terms of the first power of this exponential are retained, the added terms are unnecessary to this approximation.

The significance of the constant B must still be explained, since it is, in fact, the only difference between the value of f for velocities different and velocities equal. The stream function is never known uniquely, but only to within an arbitrary constant. This constant

is set by arbitrarily giving one streamline a numerical value. In the present case defining the dividing streamline as the zero'th streamline sets the constant for each velocity ratio. Also, far from the centerline, f must vary as η since there the stream is undisturbed. Hence, B is simply the difference between f and $\Lambda\eta$ for η large and negative.

$$\lim_{\eta \to -\infty} (f - \Lambda\eta) = B \tag{68}$$

From the above discussion, it is apparent that B not only depends on Λ, the velocity ratio, but also can be determined only by finding the complete solution to the momentum equation.

In order to compute f_i for different values of Λ, then, it is convenient to define a new variable

$$\eta^* = \Lambda^{1/2}\left(\eta + \frac{B}{\Lambda}\right) \tag{69}$$

In terms of η^*, then, $f \sim \Lambda^{1/2}\eta^*$, and for η large and negative, the zero'th order equations (43) become

$$\begin{aligned} \frac{1}{S_c}\frac{d^2K^{(0)}}{d\eta^{*2}} + \frac{\eta^*}{2}\frac{dK^{(0)}}{d\eta^*} &= 0 \\ \frac{1}{P_r}\frac{d^2\mathcal{G}^{(0)}}{d\eta^{*2}} + \frac{\eta^*}{2}\frac{d\mathcal{G}^{(0)}}{d\eta^*} &= 0 \end{aligned} \tag{70}$$

so that the asymptotic solutions for $K^{(0)}$ and $\mathcal{G}^{(0)}$ for velocities different are exactly the solutions given in equations (46) with η^* replacing η. Therefore $\mathcal{R}(\eta) = K^{(0)} e^{-\mathcal{G}_0\left(\frac{1}{\mathcal{G}^{(0)}} - \frac{1}{\mathcal{G}_2}\right)}$ has the same functional form with η^* replacing η and can be written $\mathcal{R}(\eta^*)$.

Hence, the energy equation (44) can be written in terms of η^*, for η large and negative, in the following way;

$$\frac{d^2\theta^{(\omega)}}{d\eta^{*2}} + \frac{P_r}{2}\eta^* \frac{d\theta^{(\omega)}}{d\eta^*} - P_r\,\theta^{(\omega)} = -P_r(2\theta_1-1)(2\theta_2-1)\frac{2\theta_2}{\partial\theta_2^2}\,R(\eta^*) \tag{71}$$

since Λ cancels throughout the equation.

Again, it can be seen that equation (71) is exactly the equation for velocities equal with η^* replacing η. Therefore, the asymptotic solution before derived is valid with the notation $\theta^{(\omega)} = \theta^{(\omega)}(\eta^*)$. Moreover

$$\frac{\partial\theta}{\partial\eta} = \Lambda^{1/2}\frac{d\theta}{d\eta^*} = \Lambda^{1/2}\left(\frac{d\theta^{(\omega)}}{d\eta^*} + \xi\frac{d\theta^{(\omega)}}{d\eta^*}\right) = 0$$

and

$$\left.\frac{d\xi}{d\eta}\right|_{\eta_i} = \left.\frac{d\xi}{d\eta^*}\right|_{\eta_i}\Lambda^{1/2} = \frac{\Lambda^{1/2}}{\left(\frac{d\theta^{(\omega)}}{d\eta^*}\right)^2}\left(\frac{d^2\theta^{(\omega)}}{d\eta^{*2}}\frac{d\theta^{(\omega)}}{d\eta^*} - \frac{d^2\theta^{(\omega)}}{d\eta^{*2}}\frac{d\theta^{(\omega)}}{d\eta^*}\right) = 0$$

so that equations (58) and (59), defining η_i and ξ_i respectively remain unchanged in terms of η_i^* and the ξ_i associated with different velocities.

Thus, since $f' \neq \Lambda$, equation (58) may be written as follows:

$$\theta^{(\omega)}(\eta^*) = (2\theta_1-1)(2\theta_2-1)\frac{2\theta_2}{\partial\theta_2^2}\,R(\eta^*) \tag{72}$$

This relation defines η_i^*. Since the expansions for $\theta^{(\omega)}(\eta^*)$, and $R(\eta^*)$ are the same as those for $\theta^{(\omega)}(\eta)$, and $R(\eta)$ it is evident that

$$\eta_i^*(\Lambda) = \eta_i(\Lambda=1) \tag{73}$$

where $\eta_i(\Lambda=1)$ refers to that value derived for velocities equal. Substituting for η_i^*

$$\eta_i(\Lambda) = \frac{1}{\Lambda^{1/2}}\,\eta_i(\Lambda=1) - \frac{B}{\Lambda} \tag{74}$$

which can be used to calculate η_i for a given velocity ratio to check on the validity of the asymptotic solutions.

Finally, since

$$\xi_i(\Lambda) = -\left(\frac{d\vartheta^{(\omega)}}{d\eta^*}\Big/\frac{d\vartheta^{(\omega)}}{d\eta^*}\right)_{\eta_i^*(\Lambda)}$$

and since $\eta_i^*(\Lambda) = \eta_i(\Lambda=1)$, and $\vartheta^{(\omega)}(\eta^*)$ and $\vartheta^{(\omega)}(\eta^*)$ have the same functional form as $\vartheta^{(\omega)}(\eta)$ and $\vartheta^{(\omega)}(\eta)$, it is evident that

$$\xi_i(\Lambda) = \xi_i(\Lambda=1)$$

where, again, $\xi_i(\Lambda=1)$ refers to the ξ_i calculated for velocities equal.

Therefore, since $\xi_i(\Lambda)$ is independent of the velocity ratio, χ_i, the detachment distance, is proportional to u_{II}, the velocity of the lower stream, as indicated by the definition of ξ_i. Since the expansion used for f is not valid for $\Lambda=0$, this proportionality does not necessarily hold to the limit $u_{II}=0$. Moreover, since $\eta_i(\Lambda)$ depends on B and Λ, the constant B must be calculated for any given Λ to assure the fact that $\eta_i(\Lambda)$ is large enough to justify the asymptotic solutions. From Lock's computations B was found for the velocity ratio $\Lambda = 0.501$, to be -0.375, which then gives a value for $\eta_i(\Lambda)$ of approximately -10, a value which certainly justifies the solutions found. Moreover, since $B=0$ for

$\Lambda = 1$, it seems logical to suppose that χ_i is proportional to u_{II} for any velocity ratio from $\Lambda = 1$ to at least $\Lambda = 0.5$. While it is probable that the range of validity extends much closer to $\Lambda = 0$, no other values of B were calculated to prove this fact.

That χ_i's dependence on u_{II} is physically plausible is seen by a consideration of the physical processes taking place. Since the lower stream is the hotter stream, the first noticeable reaction takes place deep in it, the extent depending on the diffusion of combustible, so that the velocity at which this initially reacting material is being carried downstream is about u_{II}. Since the diffusion velocity and reaction rate remain constant if only u_{II} is changed, it follows that a given constant time interval exists, then, during which the combustible has been in a region of high temperature, producing a given quantity of heat, and therefore that as u_{II} decreases, the distance traveled in this constant time decreases. In particular, the given quantity of heat chosen is that amount necessary to produce the first bulge in the temperature profile.

VI. DEVELOPMENT OF THE LAMINAR FLAME

The perturbation scheme discussed in the previous section is, of course, inappropriate for following the transition to a laminar flame front. However, knowing what happens in the initial region allows one to use an approximate analysis to complete the solution through a laminar flame front. The technique which allows the best use of the information accumulated so far is the integral method introduced by von Kármán into the study of laminar and turbulent boundary layers. In this method, the differential equations are integrated across the streams utilizing a descriptive knowledge of the distribution of velocity, temperature, and fuel concentration. The resulting ordinary differential equations then describe the manner in which the geometric widths of assumed profiles vary along the direction of flow. Extension of the Kármán integral method to the present problem simply involves adding the integrated species conservation equation to the usual momentum and energy conservation relations.

Since the accuracy of the solution depends to a large extent on the profiles assumed for the unknown functions, it is necessary to choose profiles which exhibit the essential physical characteristics. While it is possible to choose many functions which would satisfy the boundary conditions, it was shown by Lock,[18] that for the case of pure incompressible mixing sinusoidal profiles gave good approximation to both the velocity and the velocity gradient at the centerline. Since in the present analysis, after the Howarth transformation, the momentum equation is exactly that for an incompressible pure mixing problem, the same

profiles and results may be used. Finally, since the sinusoidal profiles give such good results for the velocity profiles, it may be expected that this type of profile is adequate to describe the variation of both the temperature, and combustible concentration.

The momentum equation is the easiest equation to solve since it is independent of composition or temperature after the Howarth transformation. The two fluid streams are initially separate, and it is convenient to separate the integration into two separate parts. The streamline which separates the flows is not straight, but deflects slightly. This deflection is negligibly small, however, and it will be assumed that the zero streamline falls along the line $y=0$. The velocity u_c is constant along this streamline.

Supposing $y=\delta_1(x)$ to be the extent to which the velocity mixing region extends into the cool stream, and $y=-\delta_2(x)$ to be the extent into the "lower", hot stream, and integrating the momentum and continuity equation (34) in the usual manner,[19] one obtains, for $0 \le y \le \delta_1(x)$,

$$\frac{d}{dx}\int_0^{\delta_1(x)} U(1-U)\,dy = \frac{\nu}{u_1}\left.\frac{\partial U}{\partial y}\right|_{y=0} \tag{75}$$

and for $-\delta_2(x) \le y \le 0$,

$$\frac{d}{dx}\int_{-\delta_2(x)}^{0} U(1-U)\,dy = -\frac{\nu}{u_1}\left.\frac{\partial U}{\partial y}\right|_{y=0} \tag{76}$$

where

$$\left.\frac{\partial U}{\partial y}\right|_{y=\delta_1} = \left.\frac{\partial U}{\partial y}\right|_{y=-\delta_2} = 0 \quad ; \quad U(\delta_1)=1 \, , \; U(-\delta_2)=1$$

The results of these two relations must match at the dividing line so that the viscous shear be continuous. Since all fluid properties

are continuous at this point,

$$\left.\frac{\partial v}{\partial y}\right|_{y=0^+} = \left.\frac{\partial v}{\partial y}\right|_{y=0^-} \tag{77}$$

The energy relations may be handled in exactly the same way. However, as seen in the perturbation analyses, the temperature profiles have a different character accordingly as the value of X is less than or greater than X_i where a temperature maximum first occurs. It is necessary, then, to find the conditions necessary to compute X_i for this approximate integral method. The case discussed first is the only one which can be solved without recourse to information given by the perturbation computation, a point which will become apparent after the following discussion.

Denoting by $y = -\beta_2(x)$ and $y = -\Delta_2(x)$ the limits in the lower stream of the temperature and diffusion mixing regions respectively, one can see that for $P_r < S_c$, in the absence of reaction, $\beta_2(x) > \Delta_2(x)$; that is, the temperature mixing region is larger than the diffusion region. Moreover, as the reaction takes place only in the region $y > -\Delta_2(x)$ the result is to decrease the values of both $\beta_2(x)$ and $\Delta_2(x)$. This decrease takes place because as the reaction proceeds, heat is added, raising temperatures initially below T_{II}, and decreasing $\beta_2(x)$ along which $T = T_{II}$, and combustible is used up, decreasing $\Delta_2(x)$ along which $K = 0$.

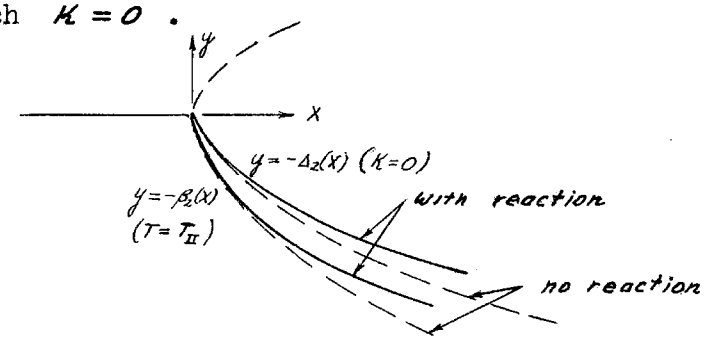

In order for a combustion wave to develop, the temperature of the combustible must reach and then exceed T_{II} until the adiabatic flame temperature is reached. Thus, the lower thermal boundary must decrease in value faster than that of the diffusion layer, and at some point then, $\beta_2(X) = \Delta_2(X)$. This point corresponds to $X = X_i$, since downstream of this point, T exceeds T_{II} in some region of the combustible so that a "bulge" in the temperature profile occurs, along with a bifurcation in $\beta_2(X)$. The lower branch is the more important line, marking the limit of the thermal layer.

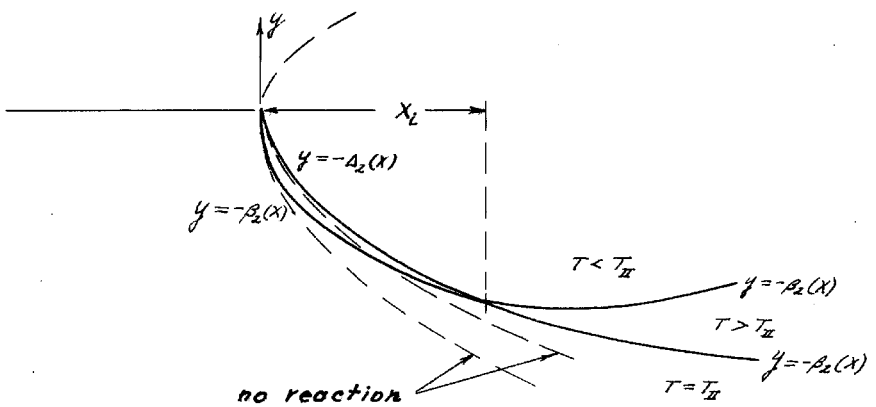

For $X > X_i$, a temperature profile with a maximum must be employed. While the line of maximum temperature does not coincide exactly with $y = -\Delta_2(X)$, the end of reaction, it must lie very close to it because of the overwhelming effect of the exponential on the reaction rate and hence the heat release. Thus, there should be little error in supposing the temperature maximum to occur at $y = -\Delta_2(X)$, so that $\frac{\partial \theta}{\partial y}\Big|_{y=-\Delta_2} = 0$. Although this does give some difficulty of solution for X slightly greater than X_i, where $|\beta_2 - \Delta_2|$ is small compared to $|\Delta_2|$, this difficulty can be resolved, as will be shown later.

It is convenient to make a division between the "upper" and "lower"

streams, when evaluating the energy and combustible concentration relations, along a line $y = \beta_o(x)$ above which the reaction is negligible due to the relatively low temperature. This may be taken as the isotherm with a temperature $\vartheta = \vartheta_o$ corresponding to that of the dividing streamline $y = 0$ in the absence of chemical reaction, if T_o, the temperature along this dividing streamline, is not so high that an appreciable addition to the integral of the reaction rate would be gained by continuing the integral into the upper stream. Since T_o depends on T_{II} and T_I, this means that the ϑ_o isotherm can be used only if T_{II} is not too great. In the "upper" region, one integration suffices, while in the "lower" region two integrations must be performed, for $x \gtrless x_i$.

Denoting by $y = \beta_1(x)$ the extent of the "upper" temperature region, and integrating the energy equation, (34), for $\beta_o(x) \leq y \leq \beta_1(x)$, one finds the following relation:

$$\frac{d}{dx}\int_{\beta_o(x)}^{\beta_1(x)} v(1-\vartheta)\,dy - (\vartheta_o - 1)\frac{d}{dx}\int_0^{\beta_o(x)} v\,dy = \frac{\nu}{\rho_r u_I}\left.\frac{\partial \vartheta}{\partial y}\right|_{\beta_o(x)} \tag{78}$$

while for $x \leq x_i$ and $-\beta_2(x) \leq y \leq \beta_o(x)$,

$$\frac{d}{dx}\int_{-\beta_2(x)}^{\beta_o(x)} v(\vartheta_2 - \vartheta)\,dy - (\vartheta_2 - \vartheta_o)\frac{d}{dx}\int_0^{\beta_o(x)} v\,dy = \frac{-\nu}{\rho_r u_I}\left.\frac{\partial \vartheta}{\partial y}\right|_{\beta_o(x)} - \frac{(\vartheta_f - 1)}{u_I \tau}\int_{-\beta_2(x)}^{\beta_o(x)} \kappa e^{-\vartheta_a/\vartheta}\,dy \tag{79}$$

since

$$\left.\frac{\partial \vartheta}{\partial y}\right|_{y=\beta_1} = \left.\frac{\partial \vartheta}{\partial y}\right|_{y=-\beta_2} = 0 \;;\; \vartheta(\beta_1) = 1,\ \vartheta(\beta_o) = \vartheta_o,\ \text{and}\ \vartheta(-\beta_2) = \vartheta_2.$$

Next, for $X \gg X_i$ and $-\Delta_2(x) \leq y \leq \beta_o(x)$,

$$\frac{d}{dx}\int_{-\Delta_2(x)}^{\beta_o(x)} v\vartheta\, dy + \vartheta_m(x)\frac{d}{dx}\int_{0}^{-\Delta_2(x)} v\, dy - \vartheta_0 \frac{d}{dx}\int_{0}^{\beta_o(x)} v\, dy = \frac{\nu}{P_r u_I}\frac{\partial \vartheta}{\partial y}\Big|_{\beta_o(x)} + \frac{(\vartheta_f - 1)}{u_I \tau}\int_{-\Delta_2(x)}^{\beta_o(x)} \kappa e^{-\vartheta_a/\vartheta}\, dy \tag{80}$$

where

$$\vartheta(-\Delta_2) = \vartheta_m(x), \text{ and } \frac{\partial \vartheta}{\partial y}\Big|_{y=-\Delta_2} = 0$$

while for $-\beta_2(x) \leq y \leq -\Delta_2(x)$,

$$\frac{d}{dx}\int_{-\beta_2(x)}^{-\Delta_2(x)} v(\vartheta_2 - \vartheta)\, dy + (\vartheta_m(x) - \vartheta_2)\frac{d}{dx}\int_{0}^{-\Delta_2(x)} v\, dy = 0 \tag{81}$$

since

$$\frac{\partial \vartheta}{\partial y}\Big|_{y=-\Delta_2} = \frac{\partial \vartheta}{\partial y}\Big|_{y=-\beta_2} = 0, \text{ and } \vartheta(-\beta_2) = \vartheta_2.$$

The matching condition at $\beta_o(x)$ expresses the physical fact that the heat conduction is continuous across $\beta_o(x)$, that is

$$\frac{\partial \vartheta}{\partial y}\Big|_{\beta_o^+} = \frac{\partial \vartheta}{\partial y}\Big|_{\beta_o^-} \tag{82}$$

Integration of the combustible concentration equation (34) presents the additional complication that the concentration $\kappa(\beta_o)$ along the line $\beta_o(x)$ is not constant. Integration above the line $\beta_o(x)$, with $\Delta_1(x)$ representing the extent of the diffusion region in the "upper" region, gives,

$$\frac{d}{dx}\int_{\beta_o(x)}^{\Delta_1(x)} u(1-\kappa)\,dy + (1-\kappa(\beta_o))\frac{d}{dx}\int_{0}^{\beta_o(x)} u\,dy = \frac{\nu}{S_c u_1}\left.\frac{\partial \kappa}{\partial y}\right|_{\beta_o(x)} \tag{83}$$

while integration below the line $\beta_o(x)$ gives,

$$\frac{d}{dx}\int_{-\Delta_2(x)}^{\beta_o(x)} u\kappa\,dy - \kappa(\beta_o)\frac{d}{dx}\int_{0}^{\beta_o(x)} u\,dy = \frac{\nu}{S_c u_1}\left.\frac{\partial \kappa}{\partial y}\right|_{\beta_o} - \frac{1}{u_1 \tau}\int_{-\Delta_2(x)}^{\beta_o(x)} \kappa\, e^{-\theta_o/\vartheta}\,dy \tag{84}$$

where

$$\left.\frac{\partial \kappa}{\partial y}\right|_{\beta_1} = \left.\frac{\partial \kappa}{\partial y}\right|_{-\Delta_2} = 0 \;;\quad \kappa(\Delta_1) = 1, \text{ and } \kappa(-\Delta_2) = 0.$$

The continuity of diffusive transport of combustible matter at $\beta_o(x)$ gives the matching relation

$$\left.\frac{\partial \kappa}{\partial y}\right|_{\beta_o^+} = \left.\frac{\partial \kappa}{\partial y}\right|_{\beta_o^-} \tag{85}$$

Equations (75) through (85), then, must be solved with assumed profiles for κ, ϑ, and u, to find the variation of β_1, β_o, β_2, Δ_1, Δ_2, $\kappa(\beta_o)$, ϑ_m, δ_1, δ_2 and u_c, the value of u along $y = 0$, in the two regions $x \gtrless x_i$. However, the energy equation has been integrated only when the Schmidt number exceeds the Prandtl number. Although this case is the one most usually encountered, it is conceivable that the other two cases, $P_r = S_c$ and $P_r > S_c$ could arise. It is evident that for either of the latter cases β_2 never crosses Δ_2 after the point $x = 0$ so that the method outlined cannot be used. Thus for $P_r > S_c$, $\Delta_2 > \beta_2$, in the absence of reaction. This implies that there is some combustible at a temperature T_{II} so that any heat addition will cause the temperature to rise above T_{II},

giving a "bulge", or maximum in the profile, and an immediate bifurcation in $\beta_2(X)$.

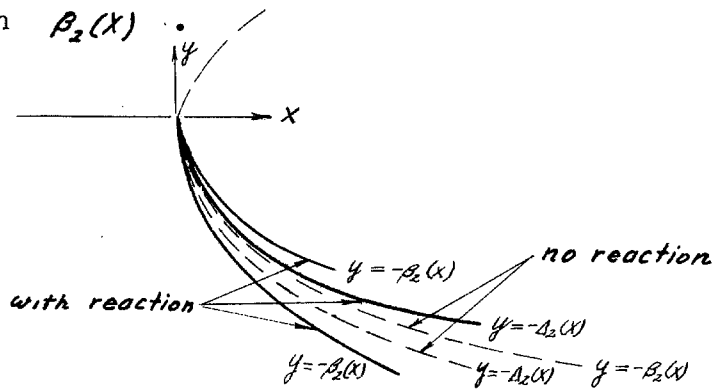

For the case $P_r = S_c$, $\Delta_2 = \beta_2$ in the absence of reaction so that some combustible is at a temperature as close as desired to T_{II} . Any reaction would make Δ_2 decrease and β_2 increase, then, with, again an immediate bifurcation of $\beta_2(X)$.

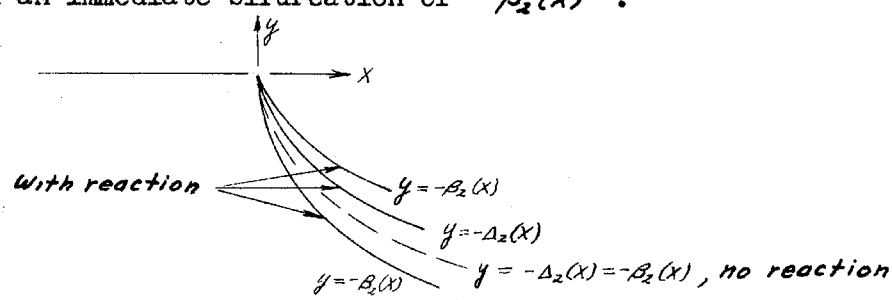

This can be seen by considering again the case of $P_r < S_c$ where, at some point $X = X_i$ and $\Delta_2 = \beta_2$. As P_r becomes closer and closer to S_c the initial difference between $\beta_2(X)$ and $\Delta_2(X)$ becomes smaller and smaller so that if T_{II} stays constant, X_i decreases. At the limit $P_r = S_c$, $X_i = 0$. This will be seen in the later analytic developments, also.

The preceding discussion then indicates that some other criteria must be used for $X = X_i$ when $P_r \geq S_c$. A possible substitute is as follows. In the absence of reaction, $\beta_2(X) \propto \sqrt{X}$ so that the value of η associated with $\beta_2(X)$ is also a constant, say η_2 . Also, it can be seen from a simple calculation that this η_2 is

approximately -3 for the case $\theta_2 = 3.5$ calculated in the perturbation analysis where $\eta_i = -6.5$. Thus, the first bulge in temperature profile actually occurs at such a large negative value of η that it is completely outside the range covered by the integral technique. Hence, what one is actually computing in the integral technique is the first point at which a "bulge", or maximum occurs, within the range of η covered by the integral technique. Therefore, it seems logical to suppose that one could define an X_i within the limits of accuracy of the integral technique by computing the η_2 associated with the simple mixing problem and calculate a f_i using η_2 instead of η_i. At this point then, one must also assume that $T = T_{II}$ and $\Delta_2(x_i) = \beta_2(x_i)$ where $\beta_2(x_i)$ is that value for the case of no reaction. While the values of β and Δ would be in error, being calculated from a simple mixing problem, the error would be insignificant in view of the fact that the heat addition up to the point $X = X_i$ is small, and that in the integral technique one is actually replacing infinite limits with finite limits to gain simplicity of solution. A comparison of the two methods of computing X_i when $P_r < S_c$ which will be given later in the numerical computations, showed very good results.

The profiles assumed for v, κ and ϕ are as follows:

$$v = v_c + (1 - v_c)\sin\left(\frac{\pi}{2}\frac{y}{\delta_1}\right) \qquad 0 \le y \le \delta_1(x)$$

$$= v_c + (1 - v_c)\sin\left(\frac{\pi}{2}\frac{y}{-\delta_2}\right) \qquad -\delta_2(x) \le y \le 0 \tag{86}$$

$$\begin{aligned} \kappa &= \kappa(\beta_0) + (1-\kappa(\beta_0))\sin\left(\frac{\pi}{2}\,\frac{y-\beta_0}{\Delta_1-\beta_0}\right), \quad \beta_0(x) \le y \le \Delta_1(x) \\ &= \kappa(\beta_0) - \kappa(\beta_0)\sin\left(\frac{\pi}{2}\,\frac{y-\beta_0}{-\Delta_2-\beta_0}\right), \quad -\Delta_2(x) \le y \le \beta_0(x) \end{aligned} \tag{87}$$

$$\left.\begin{aligned} \vartheta &= \vartheta_0 + (1-\vartheta_0)\sin\left(\frac{\pi}{2}\,\frac{y-\beta_0}{\beta_1-\beta_0}\right), \quad \beta_0(x) \le y \le \beta_1(x) \\ &= \vartheta_0 + (\vartheta_2-\vartheta_0)\sin\left(\frac{\pi}{2}\,\frac{y-\beta_0}{-\beta_2-\beta_0}\right), \quad -\beta_2(x) \le y \le \beta_0(x) \end{aligned}\right\} \; x \le x_i \tag{88}$$

$$\left.\begin{aligned} \vartheta &= \vartheta_0 + (1-\vartheta_0)\sin\left(\frac{\pi}{2}\,\frac{y-\beta_0}{\beta_1-\beta_0}\right), \quad \beta_0(x) \le y \le \beta_1(x) \\ &= \vartheta_0 + (\vartheta_m-\vartheta_0)\sin\left(\frac{\pi}{2}\,\frac{y-\beta_0}{-\Delta_2-\beta_0}\right), \quad -\Delta_2(x) \le y \le \beta_0(x) \\ &= \frac{\vartheta_m+\vartheta_2}{2} + \frac{\vartheta_m-\vartheta_2}{2}\cos\left(\pi\,\frac{y+\beta_2}{\beta_2-\Delta_2}\right), \quad -\beta_2(x) \le y \le -\Delta_2(x) \end{aligned}\right\} \; x \ge x_i \tag{89}$$

Substitution of these profiles into the preceding six integral equations for $x \le x_i$ and seven integral equations for $x \ge x_i$, yields the same number of ordinary differential equations for the functions $\delta_1(x)$, $\delta_2(x)$, $\beta_1(x)$, $\beta_0(x)$, $\beta_2(x)$, $\kappa(\beta_0)$, $\Delta_1(x)$, and $\Delta_2(x)$ for all x and for ϑ_m for $x \ge x_i$. The matching relations supply the remaining necessary equations. As an illustration it is instructive to use the same example employed in the perturbation analysis, that is, where $u_I = u_{II} = u$ or $\sigma = \sigma_c = \Lambda = 1$. This reduces by two the number of functions to be computed, $\delta_1(x)$ and $\delta_2(x)$ being absent since no shearing stresses are present. Upon evaluation of the integrals in equations (78), (79), (83), and (84), the following differential equations are obtained for the region $x \le x_i$.

$$\left(1-\frac{2}{\pi}\right)\frac{d}{dX}\left(\beta_1-\beta_0\right)+\frac{d\beta_0}{dX}=\frac{\nu}{P_r u}\frac{\pi}{2}\frac{1}{\left(\beta_1-\beta_0\right)}$$

$$\left(1-\frac{2}{\pi}\right)\frac{d}{dX}\left(\beta_0+\beta_2\right)-\frac{d\beta_0}{dX}=\frac{\nu}{P_r u}\frac{\pi}{2}\frac{1}{\left(\beta_0+\beta_2\right)}-\frac{2}{\pi}\left(\frac{\vartheta_1-1}{\vartheta_2-\vartheta_0}\right)\left(\frac{\beta_0+\Delta_2}{\vartheta_2-\vartheta_0}\right)\frac{K(\beta_0)I}{u\tau}\,e^{-\vartheta_a/\vartheta_2} \tag{90}$$

$$\left(1-\frac{2}{\pi}\right)\frac{d}{dX}\left(\left(1-K(\beta_0)\right)\left(\Delta_1-\beta_0\right)\right)+\left(1-K(\beta_0)\right)\frac{d\beta_0}{dX}=\frac{\nu}{S_c u}\frac{\pi}{2}\frac{\left(1-K(\beta_0)\right)}{\left(\Delta_1-\beta_0\right)}$$

$$\left(1-\frac{2}{\pi}\right)\frac{d}{dX}\left(K(\beta_0)\left(\beta_0+\Delta_2\right)\right)-K(\beta_0)\frac{d\beta_0}{dX}=\frac{\nu}{S_c u}\frac{\pi}{2}\frac{K(\beta_0)}{\left(\beta_0+\Delta_2\right)}-\frac{2}{\pi}\left(\frac{\beta_0+\Delta_2}{\vartheta_2-\vartheta_0}\right)\frac{K(\beta_0)I}{u\tau}\,e^{-\vartheta_a/\vartheta_2}$$

where I is a definite integral over the reaction zone given by,

$$I=\int_{\vartheta_0}^{\vartheta_2}\left(\frac{1-\frac{\vartheta-\vartheta_0}{\vartheta_2-\vartheta_0}}{1+\frac{\vartheta-\vartheta_0}{\vartheta_2-\vartheta_0}}\right)^{1/2}e^{-\vartheta_a\left(\frac{1}{\vartheta}-\frac{1}{\vartheta_2}\right)}d\vartheta \tag{91}$$

The integral I is obtained from the reaction rate integrals in the following way. Since $K=0$ for $y<-\Delta_2(x)$ the reaction rate integrals in equations (79) and (84) are really taken over the same interval, $-\Delta_2(x)$ to $\beta_0(x)$. Further, although for $y<\beta_0(x)$, K is a function of $\frac{y-\beta_0}{-\Delta_2-\beta_0}$ and ϑ a function of $\frac{y-\beta_0}{-\beta_2-\beta_0}$, $\frac{\beta_2}{\Delta_2}=\sqrt{\frac{S_c}{P_r}}$ when there is no reaction and $\frac{\beta_2}{\Delta_2}\to 1$ as reaction proceeds. Therefore, for S_c and P_r not too greatly different, little error is introduced in supposing both the K and ϑ profiles to be functions of $\frac{y-\beta_0}{-\Delta_2-\beta_0}$ (i.e.: $\beta_2\simeq\Delta_2$) only insofar as the integral is concerned. With this supposition, then

$$\int_{-\Delta_2(x)}^{\beta_0(x)}K\,e^{-\vartheta_a/\vartheta}dy=\int_{\vartheta=\vartheta_2}^{\vartheta=\vartheta_0}\frac{K}{\frac{d\vartheta}{dy}}\,e^{-\vartheta_a/\vartheta}d\vartheta$$

From the profile descriptions, however,

$$\vartheta = \vartheta_0 + (\vartheta_2 - \vartheta_0)\sin\left(\frac{\pi}{2}\frac{y-\beta_0}{-\beta_2-\beta_0}\right)$$

so that this approximation gives for ϑ ;

$$\vartheta \simeq \vartheta_0 + (\vartheta_2 - \vartheta_0)\sin\left(\frac{\pi}{2}\frac{y-\beta_0}{-\Delta_2-\beta_0}\right)$$

$$\frac{d\vartheta}{dy} = \frac{\vartheta_2-\vartheta_0}{-\Delta_2-\beta_0}\frac{\pi}{2}\cos\left(\frac{\pi}{2}\frac{y-\beta_1}{-\Delta_2-\beta_0}\right)$$

$$= -\frac{(\vartheta_2-\vartheta_0)}{\Delta_2+\beta_0}\frac{\pi}{2}\left(1-\left(\frac{\vartheta-\vartheta_0}{\vartheta_2-\vartheta_0}\right)^2\right)^{1/2}$$

while

$$\kappa = \kappa(\beta_0)\left(1-\sin\left(\frac{\pi}{2}\frac{y-\beta_0}{-\Delta_2-\beta_0}\right)\right)$$

$$\simeq \kappa(\beta_0)\left(1-\frac{\vartheta-\vartheta_0}{\vartheta_2-\vartheta_0}\right)$$

so that

$$\int_{-\Delta_2(x)}^{\beta_1(x)} \kappa e^{-\vartheta_2/\vartheta}dy \simeq \frac{2}{\pi}\frac{\kappa(\beta_0)(\Delta_2+\beta_0)}{(\vartheta_2-\vartheta_0)}\int_{\vartheta_0}^{\vartheta_2}\left(\frac{1-\frac{\vartheta-\vartheta_0}{\vartheta_2-\vartheta_0}}{1+\frac{\vartheta-\vartheta_0}{\vartheta_2-\vartheta_0}}\right)^{1/2} e^{-\vartheta_2/\vartheta}d\vartheta$$

$$= \frac{2}{\pi}\frac{\kappa(\beta_0)(\Delta_2+\beta_0)}{(\vartheta_2-\vartheta_0)} I\, e^{-\vartheta_2/\vartheta_2}$$

The equations (90) can be simplified since ϑ_0 , for this case of $\sigma \equiv 1$, is just the mean value $\frac{1+\vartheta_2}{2}$, being that value which would occur at the interface in the absence of combustion. Also from the trigonometric relations themselves and the matching conditions, it is easy to show that $\beta_0(x) = \frac{1}{2}(\beta_1(x) - \beta_2(x))$ while the concentration along $\beta_0(x)$ is $\kappa(\beta_0) = \frac{\beta_0+\Delta_2}{\Delta_1+\Delta_2}$. Substitution of these relations into

equations (90) and then solving the equations simultaneously for the derivatives of $\Delta_1+\Delta_2$, $\kappa(\beta_0)$, $\beta_1-\beta_0$, and β_0, yields, for $x \neq x_i$;

$$\frac{d}{dx}(\Delta_1+\Delta_2) = \frac{\pi^2}{2(\pi-2)}\frac{\nu}{S_c u}\frac{1}{(\kappa(\beta_0)(1-\kappa(\beta_0)))}\frac{1}{(\Delta_1+\Delta_2)} - \frac{4}{(\pi-2)}\frac{\kappa(\beta_0)(\Delta_1+\Delta_2) I e^{-\vartheta_0/\vartheta_2}}{(\vartheta_2-1) u \tau}$$

$$\frac{d\kappa(\beta_0)}{dx} = \frac{\pi^2}{4(\pi-2)}\frac{\nu}{S_c u}\frac{1-2\kappa(\beta_0)}{\kappa(\beta_0)(1-\kappa(\beta_0))}\frac{1}{(\Delta_1+\Delta_2)^2} + \frac{2\kappa(\beta_0)}{(\pi-2)}\left[\left(\frac{\vartheta_1-1}{\vartheta_2-1}-1\right)\kappa(\beta_0)-1\right]\frac{I e^{-\vartheta_0/\vartheta_2}}{(\vartheta_2-1) u \tau} \tag{92}$$

$$\frac{d}{dx}(\beta_1-\beta_0) = \frac{\pi^2}{2(\pi-2)}\frac{\nu}{P_r u}\frac{1}{(\beta_1-\beta_0)} - \frac{4}{(\pi-2)}\frac{(\vartheta_1-1)}{(\vartheta_2-1)}(\kappa(\beta_0))^2\frac{(\Delta_1+\Delta_2) I e^{-\vartheta_0/\vartheta_2}}{(\vartheta_2-1) u \tau}$$

$$\frac{d\beta_0}{dx} = \frac{4}{\pi}\frac{(\vartheta_1-1)}{(\vartheta_2-1)}(\kappa(\beta_0))^2(\Delta_1+\Delta_2)\frac{I e^{-\vartheta_0/\vartheta_2}}{(\vartheta_2-1) u \tau}$$

Now since a numerical integration is obviously called for, it is necessary to investigate the behavior of the solutions to equations (92) near the origin where integration must begin. The expansions are naturally in powers of x, following the usual boundary layer expansions. Thus: $\Delta_1+\Delta_2 = a_0 + a_1 x^{1/2} + a_2 x^{3/2} + \cdots$ with similar expansions for $\kappa(\beta_0)$, $(\beta_1-\beta_0)$, and β_0. Substituting the expansions in equations (92), and equating the coefficients of like powers of x gives the desired coefficients a_0, a_1, . . . etc. However, in order to show some comparison with the perturbation technique, they may be written very easily in terms of the dimensionless variables as,

$$\frac{\Delta_1+\Delta_2}{\sqrt{\frac{\nu x}{u}}} = \frac{2\pi}{\sqrt{S_c(\pi-2)}}\left(1 - \frac{\vartheta_0 I}{\pi-2}\xi + \cdots\right)$$

$$\kappa(\beta_0) = 1/2 + \left(\frac{\vartheta_1-1}{\vartheta_2-1}-1\right)\frac{\vartheta_0 I}{3(\pi-2)}\xi + \cdots \tag{93}$$

$$\frac{\beta_0}{\sqrt{\frac{\nu x}{u}}} = \frac{2\pi}{\sqrt{S_c(\pi-2)}} \frac{(\vartheta_2-1)}{(\vartheta_2-1)} \frac{2}{3\pi} \vartheta_2 I \left\{ + \cdots \right.$$

$$\frac{\beta_1-\beta_0}{\sqrt{\frac{\nu x}{u}}} = \frac{\beta_0+\beta_2}{\sqrt{\frac{\nu x}{u}}} = \frac{\pi}{\sqrt{P_r(\pi-2)}} \left(1 - \sqrt{\frac{P_r}{S_c}} \frac{(\vartheta_2-1)}{(\vartheta_2-1)} \frac{\vartheta_2 I}{(\pi-2)} \left\{ + \cdots \right. \right) \tag{93}$$

Actually, these expressions give a fairly accurate idea of the behavior of the mixing and reaction zones for $X \leq X_i$. For example, the value of X_i itself, determined by the condition $\Delta_2(X_i) = \beta_2(X_i)$, may be calculated from these results by noting that since $\Delta_2 + \beta_0 = K(\beta_0)(\Delta_1 + \Delta_2)$ and $\beta_2 + \beta_0 = \beta_1 - \beta_0$, the value of X_i satisfies the relation, $\beta_1(X_i) - \beta_0(X_i) = K(\beta_0)[\Delta_1(X_i) + \Delta_2(X_i)]$. Then, from equations(93), it follows directly that

$$\left\{_i = \frac{\left(\sqrt{\frac{S_c}{P_r}} - 1\right)}{\vartheta_2 \left(\frac{\vartheta_2-1}{\vartheta_2-1} - 1 \right)} \frac{3(\pi-2)}{5I} \right. \tag{94}$$

which agrees with the perturbation computation in the sense that this approximate $\left\{_i$ varies little with T_{II} , so that the main variation of X_i with T_{II} is exponential.

The calculations carried out for the region $X \leq X_i$ are shown in Figure 6 for the numerical values corresponding to azomethane which have been employed earlier, with $\vartheta_2 = 3.50$ as before. The dotted line indicates the point at which the integration of I could be stopped with negligible error. The Runge Kutta method was employed for the numerical solution of the differential equations. This method allowed one to change the increment in the stepwise solution without setting up the equations again, and seemed the most efficient method to use in view of the number

of equations to be solved simultaneously. While the solution of equations (92) required only the solution of the equations for $\frac{d}{dx}(\Delta_1+\Delta_2)$ and $\frac{dK(\beta_0)}{dx}$ simultaneously, the solution for $x \geq x_i$ required the solution of three equations simultaneously as will be seen later. The calculations show x_i to be 0.190 centimeters as compared to the 0.071 calculated by the perturbation scheme. However, as was mentioned earlier, the ξ_i calculated in the perturbation solution was for a temperature maximum occurring far outside the limits of applicability of the integral technique. Thus, one should really compare the perturbation and integral methods in the manner described earlier where the first interaction of the temperature maximum with the lower pure mixing boundary is computed. For the present case, the η corresponding to the mixing boundary can be computed from the expansion for $\frac{\beta_0+\beta_2}{\sqrt{\frac{\nu x}{u}}}$, equations (93), with $\beta_0 = I = 0$. Then $\eta_2 = -\frac{\beta_2}{\sqrt{\frac{\nu x}{u}}} = -\frac{\pi}{\sqrt{P_r(\pi-2)}} = -3.08$. The ξ_i corresponding to this η_2 was calculated (Appendix C) to be $\left[\xi_i\right]_{\eta_i=-3.08} \simeq 0.223$ so that $x_i = 0.20$ cm. which shows good agreement, and indicates that this method of calculating an approximate x_i for use in the integral method, would give good results.

For $x \geq x_i$, the differential equations are more involved than those for the region $x \leq x_i$ due to the more complicated temperature profiles and the addition of an unknown $\vartheta_m(x)$, the maximum temperature. Performing the indicated integrations in equations (78), (80), (81), (83), and (84) yields the following differential equations:

$$\left(1-\frac{2}{\pi}\right)\frac{d}{dx}(\beta_1-\beta_0) + \frac{d\beta_0}{dx} = \frac{\nu}{P_r u}\,\frac{\pi}{2}\,\frac{1}{(\beta_1-\beta_0)}$$

$$\vartheta_0\left(1-\frac{2}{\pi}\right)\frac{d}{dx}(\beta_0+\Delta_2) + \frac{2}{\pi}\frac{d}{dx}\left(\vartheta_m(\beta_0+\Delta_2)\right) - \vartheta_0\frac{d\beta_0}{dx} - \vartheta_m\frac{d\Delta_2}{dx} = -\frac{\nu}{P_r u}\,\frac{\pi}{2}\,\frac{(\vartheta_m-\vartheta_0)}{(\beta_0+\Delta_2)} + \tag{95}$$

$$+\frac{2}{\pi}(\vartheta_f-1)\left(\frac{\beta_0+\Delta_2}{\vartheta_m-\vartheta_0}\right)\frac{K(\beta_0)\,I(\vartheta_m)}{u\tau}\,e^{-\vartheta_0/\vartheta_2}$$

$$\frac{1}{2}\frac{d}{dx}\left((\beta_2-\Delta_2)(\vartheta_2-\vartheta_m)\right)-(\vartheta_m-\vartheta_2)\frac{d\Delta_2}{dx}=0$$

$$\left(1-\frac{2}{\pi}\right)\frac{d}{dx}\left((1-K(\beta_0))(\Delta_1-\beta_0)\right)+(1-K(\beta_0))\frac{d\beta_0}{dx}=\frac{\nu}{s_c u}\frac{\pi}{2}\left(\frac{1-K(\beta_0)}{\Delta_1-\beta_0}\right) \qquad (95)$$

$$\left(1-\frac{2}{\pi}\right)\frac{d}{dx}\left(K(\beta_0)(\beta_0+\Delta_2)\right)-K(\beta_0)\frac{d\beta_0}{dx}=\frac{\nu}{s_c u}\frac{\pi}{2}\frac{K(\beta_0)}{(\beta_0+\Delta_2)}-\frac{2}{\pi}\frac{(\beta_0+\Delta_2)}{(\vartheta_m-\vartheta_0)}\frac{K(\beta_0)I(\vartheta_m)e^{-\vartheta_0/\vartheta_2}}{u\tau}$$

where, now

$$I(\vartheta_m)=\int_{\vartheta_0}^{\vartheta_m}\left(\frac{1-\frac{\vartheta-\vartheta_0}{\vartheta_m-\vartheta_0}}{1+\frac{\vartheta-\vartheta_0}{\vartheta_m-\vartheta_0}}\right)^{1/2}e^{-\vartheta_0\left(\frac{1}{\vartheta}-\frac{1}{\vartheta_2}\right)}d\vartheta \qquad (96)$$

is a function of $\vartheta_m(x)$. $I(\vartheta_m)$ is computed in the same manner as I , except that no approximation is used, both K and ϑ being functions of $\frac{y-\beta_0}{\beta_0+\Delta_2}$ in this region.

From the matching conditions and the profiles themselves, it can be shown that

$$\vartheta_m=(\vartheta_0-1)\left(\frac{\beta_0+\Delta_2}{\beta_1-\beta_0}\right)+\vartheta_0 \qquad (97)$$

and also, the previously derived relation for $K(\beta_0)$ still holds,

$\beta_0+\Delta_2=K(\beta_0)(\Delta_1+\Delta_2)$.

Substitution of these relations into the equations (95) and solution of the resulting equations for the sought after derivatives yields;

$$\frac{d}{dx}(\Delta_1+\Delta_2)=\frac{\pi^2}{2(\pi-2)}\frac{\nu}{S_c u}\frac{1}{K(\beta_0)(1-K(\beta_0))}\frac{1}{(\Delta_1+\Delta_2)}-\frac{4}{(\pi-2)}\frac{(\beta_1-\beta_0)\,I(\vartheta_m)\,e^{-\vartheta_0/\vartheta_2}}{(\vartheta_2-1)\,u\,\tau}$$

$$\frac{d}{dx}(\beta_1-\beta_0)=\frac{(4-\pi)}{4K(\beta_0)\frac{(\Delta_1+\Delta_2)}{(\beta_1-\beta_0)}+\pi}\left\{\frac{\pi^2}{2(\pi-2)}\frac{\nu}{S_c u}\frac{1}{K(\beta_0)(1-K(\beta_0))}\frac{1}{(\Delta_1+\Delta_2)}\left[1+\right.\right.$$

$$\left.+2\frac{S_c}{P_r}\frac{\pi-2}{4-\pi}(1-K(\beta_0))\right]+\frac{\pi^3}{2(\pi-2)(4-\pi)}\frac{\nu}{P_r u}\frac{1}{(\beta_1-\beta_0)}-$$

$$\left.-\frac{4}{(\pi-2)}\frac{I(\vartheta_m)\,e^{-\vartheta_0/\vartheta_2}}{(\vartheta_2-1)\,u\,\tau}(\beta_1-\beta_0)\left[1+K(\beta_0)+\frac{4(\pi-2)}{(4-\pi)}\frac{(\vartheta_1-1)}{(\vartheta_2-1)}\frac{(\beta_1-\beta_0)}{(\Delta_1+\Delta_2)}\right]\right\}$$

$$\frac{dK(\beta_0)}{dX}=\frac{1}{2(\Delta_1+\Delta_2)}\left\{(1-K(\beta_0))\frac{d}{dX}(\Delta_1+\Delta_2)-\frac{d}{dX}(\beta_1-\beta_0)\right. \tag{98}$$

$$\left.+\frac{\pi^2}{2(\pi-2)}\frac{\nu}{S_c u}\frac{1}{(\Delta_1+\Delta_2)(1-K(\beta_0))}\left[\frac{S_c}{P_r}\frac{(\Delta_1+\Delta_2)(1-K(\beta_0))}{\beta_1-\beta_0}-1\right]\right\}$$

$$\frac{d\beta_0}{dX}=\frac{\pi}{2}\frac{\nu}{P_r u}\frac{1}{(\beta_1-\beta_0)}-\frac{\pi-2}{\pi}\frac{d}{dX}(\beta_1-\beta_0)$$

$$\frac{d}{dX}\left((\beta_2-\Delta_2)\frac{K(\beta_0)(\Delta_1+\Delta_2)}{(\beta_1-\beta_0)}\right)+2\left(\frac{K(\beta_0)(\Delta_1+\Delta_2)}{(\beta_1-\beta_0)}-1\right)\left(\frac{d}{dX}\left(K(\beta_0)(\Delta_1+\Delta_2)\right)-\frac{d}{dX}(\beta_0)\right)=0$$

The solution of these equations was obtained numerically employing, as before, the Runge Kutta method, using as initial values for $\beta_1(X)$, $\beta_0(X)$, $\beta_2(X)$, $\Delta_1(X)$ and $\Delta_2(X)$, those values which were obtained at $X=X_c$.

in the preceding calculations. The calculations were carried out to the point at which a laminar flame developed, at which time $\frac{d}{dx}(\Delta_1+\Delta_2) = \frac{d}{dx}(\beta_1-\beta_0) = \frac{d}{dx}(\beta_0+\Delta_2) = 0$ since then the thicknesses of the zones remain constant. Thus, the values for $\Delta_1+\Delta_2$, $K(\beta_0)$, and $\beta_1-\beta_0$ were obtained by solving the first three equations of (98) simultaneously. Knowing these values, the other two equations were solved separately, and also $\vartheta_m(x)$ was computed (Appendix D).

Figure 7 shows the downstream variation of ϑ_m from ϑ_2 at $x=x_i$ to ϑ_f at the x distance at which a laminar flame developed. The exponential increase of the maximum temperature is shown as the gas moves away from the point of initial mixing. Also of interest is the comparison with ϑ_m obtained from the first order perturbation. This shows that at least for ϑ the first order solution is good for the major part of the mixing zone.

The detailed progress of the various regions and zones are traced in figure 8, in which the vertical scale is exaggerated for clarity. While $\Delta_1(x)$ and $\beta_1(x)$ are really separate lines, the scale of the plot is such that the difference cannot be noted. Figure 8 demonstrates well the relatively sudden appearance of the laminar flame propagating into the combustible. This is indicated by the rapid convergence of the lines representing different temperatures and hence the appearance of strong temperature gradients. This plot also illustrates the total distance traversed before a laminar flame is developed, and indicates that for $u_I = u_{II} = 200$ cm/sec, and $T_{II}/T_I = 3.50$, a combustible with the physical properties of azomethane travels approximately .75 cm downstream before the flame front is developed. Since for $\vartheta_2 = 3.50$, $\mathcal{L} = 0.874$, this

means that $\zeta \sim 1$ at the end of the mixing region.

It should be mentioned that all plots showing a vertical y or η scale are drawn for the corresponding incompressible flow. It seemed unnecessary to transform back into the compressible plane since only the vertical scale would be affected and the axial or X direction and variations of functions in the X direction are of most interest. Furthermore, the thicknesses represented in the integral technique are approximations so that transformation would serve little value.

It is evident that knowing all thicknesses, and θ_m, the detailed temperature profiles can be computed, and this is shown in figure 9 using $\beta_1(X)$ as a base. Figure 9 again illustrates well the rapid change in the profiles from almost mixing profiles to those with the steep gradients noted at the end of the mixing zone. It is interesting to note that the major steepening of the profiles occurs in the last ten per cent of the mixing zone.

The calculations for $\beta_2(X)$ for $X \geq X_i$ should be discussed at this point. Because of the assumption that maximum temperature occurs at $y = -\Delta_2(X)$ no conduction terms are found in the equation for $\beta_2 - \Delta_2$, (98). While this assumption is justified throughout most of the region $X \geq X_i$, for $X - X_i$ small, the heat conducted, though small, is of the same order as that convected. Hence, some measure of the heat conducted from the combustion region, must be made. Denoting by ε the y distance from $y = -\Delta_2(X)$ to the line along which a maximum actually occurs, one can compute the derivative $\frac{\partial \theta}{\partial y}$ as follows:

$$\left.\frac{\partial \vartheta}{\partial y}\right|_{y=-\Delta_2} = \left.\frac{\partial \vartheta}{\partial y}\right|_{\vartheta=\vartheta_m} - \varepsilon \left.\frac{\partial^2 \vartheta}{\partial y^2}\right|_{\vartheta=\vartheta_m} + \cdots$$

However,

$$\left.\frac{\partial \vartheta}{\partial y}\right|_{\vartheta=\vartheta_m} = 0$$

so,

$$\left.\frac{\partial \vartheta}{\partial y}\right|_{y=-\Delta_2} \simeq -\varepsilon \left.\frac{\partial^2 \vartheta}{\partial y^2}\right|_{\vartheta=\vartheta_m}$$

Next, from equation (34), one can write the energy equation along the line where $\vartheta = \vartheta_m$ as

$$\left.\frac{\partial \vartheta}{\partial x}\right|_{\vartheta_m} = \frac{\nu}{P_r u} \left.\frac{\partial^2 \vartheta}{\partial y^2}\right|_{\vartheta_m} + \frac{\vartheta_f - 1}{u\tau} K(\vartheta_m) e^{-\vartheta_a/\vartheta_m}$$

From the values of ϑ_m for χ close to χ_i, computed from the first three of equations (98), it is apparent that $\frac{\partial \vartheta}{\partial x}$ is very small, (Appendix D)

$$\left.\frac{\partial \vartheta}{\partial x}\right|_{\vartheta_m} \simeq \frac{0.088}{0.040} = 0.22$$

while the heat release term is of order

$$\frac{(\vartheta_f - 1)}{u\tau} K(\vartheta_m) e^{-\vartheta_a/\vartheta_m} \simeq \frac{4.5\,(3.917 \times 10^3)}{200} K(\vartheta_m)$$

$$\simeq 88\, K(\vartheta_m)$$

so that even if $K(\vartheta_m)$ is supposed as small as 2×10^{-2}, the reaction term is an order of magnitude larger than the convection term. Therefore, for $\chi - \chi_i \ll 1$, this convection term is neglected so that

$$\left.\frac{\partial^2 \vartheta}{\partial y^2}\right|_{\vartheta_m} \simeq -\frac{P_r u}{\nu}\,\frac{(\vartheta_f-1)}{u\tau}\,\kappa(\vartheta_m)\,e^{-\vartheta_a/\vartheta_m}$$

and

$$\frac{\nu}{P_r u}\left.\frac{\partial \vartheta}{\partial y}\right|_{y=-\Delta_2} \simeq \varepsilon\,\frac{(\vartheta_f-1)}{u\tau}\,\kappa(\vartheta_m)\,e^{-\vartheta_a/\vartheta_m}$$

$$\simeq \varepsilon\,\frac{(\vartheta_f-1)}{u\tau}\,\bar{\kappa}\,e^{-\vartheta_a/\vartheta_2}$$

since $\vartheta_m \simeq \vartheta_2$ at $x \simeq x_i$ and $\kappa(\vartheta_m)$ can be replaced by a constant, $\bar{\kappa}$, as a first approximation. ε may be defined as a characteristic length associated with the conduction process and may be interpreted as

$$\varepsilon = C_2(\beta_2 - \Delta_2)$$

with C_2 as a constant of proportionality. Finally, then, the conduction term may be written as

$$\frac{\nu}{P_r u}\left.\frac{\partial \vartheta}{\partial y}\right|_{y=-\Delta_2} = C_2\bar{\kappa}\,\frac{(\vartheta_f-1)}{u\tau}\,e^{-\vartheta_a/\vartheta_2}\,(\beta_2-\Delta_2) \qquad (99)$$

with the constants $C_2\bar{\kappa}$ still to be determined.

When the slope at $y = -\Delta_2(x)$ is not considered to be zero, the third of equations (95) becomes;

$$\frac{d}{dx}\left[(\beta_2-\Delta_2)(\vartheta_m-\vartheta_2)\right] = -2(\vartheta_m-\vartheta_2)\frac{d\Delta_2}{dx} + \frac{2\nu}{u P_r}\left.\frac{\partial \vartheta}{\partial y}\right|_{y=-\Delta_2(x)} \qquad (100)$$

Now, observation of the values calculated for $\vartheta_m - \vartheta_2$ and $\Delta_2(x)$ as $x - x_i$ increases (see Appendix D) showed that these two functions are initially linear in $x - x_i$. Thus, expanding each function in a series, one finds the first term adequate for $x - x_i$ small enough. If $\vartheta_m - \vartheta_2 = C_3(x - x_i)$, $\Delta_2 - \Delta_2(x_i) = C_4(x - x_i)$, and one uses equation (99) for the conduction term, equation (100) becomes;

$$\frac{d}{d\bar{x}}\left[(\beta_2-\Delta_2)\bar{x}C_3\right] = -2C_3C_4\bar{x} + 2C_2\bar{\kappa}\frac{(\vartheta_f-1)}{u\tau}e^{-\vartheta_a/\vartheta_2}(\beta_2-\Delta_2)$$

if

$$\bar{x} = x - x_i$$

It is evident that a linear expression for $\beta_2-\Delta_2$ satisfies this equation as well as the condition $\beta_2-\Delta_2=0$ at $\bar{x}=0$, so that

$$\beta_2-\Delta_2 = \frac{C_4}{\frac{C_2\bar{\kappa}}{C_3}\frac{(\vartheta_f-1)}{u\tau}e^{-\vartheta_a/\vartheta_2}-1}(x-x_i) \qquad (101)$$

if

$$x - x_i << 1$$

From equation (101), one can see that $\beta_2-\Delta_2$ becomes sensitive to the choice of $C_2\bar{\kappa}$ only when $\frac{C_2}{C_3}\bar{\kappa}\frac{(\vartheta_f-1)}{u\tau}e^{-\vartheta_a/\vartheta}$ becomes of order 1. For the conditions used in the numerical example, $\left(\vartheta_2 = 3.5,\ u = 200\ cm/sec,\ C_3 = 0.21\right)$, $C_2\bar{\kappa}$ would have to be of order 3×10^{-3} before $\beta_2-\Delta_2$ became very sensitive to the choice of $C_2\bar{\kappa}$. Thus, for C_2 of the order of 1, a lower bound on $\bar{\kappa}$ would be about 3×10^{-3}, since below that value, $\beta_2-\Delta_2$ would become negative, that is, the conduction term would be insufficient, a fact one knows to be physically untrue.

As an upper bound on $\bar{\kappa}$, one can use the value of κ calculated at the maximum reaction rate (equation (39)) as $\frac{1}{\vartheta_2-1}\frac{\vartheta_2^2}{\vartheta_a} \simeq 6\times10^{-2}$. Since the maximum temperature occurs close to, but at a slightly lower concentration value than that for maximum reaction rate, due to conduction, the value of $\bar{\kappa}$ must be less than 6×10^{-2}. Hence for $C_2 \sim 1$, $3\times10^{-3} < \bar{\kappa} < 6\times10^{-2}$. The value finally chosen was $\bar{\kappa} = 2\times10^{-2}$, which is close to that value occurring at the maximum rate. With $C_2 = 1/2$,

then, $C_2 \bar{\kappa} = 10^{-2}$ a value which is well above the minimum. This choice of constants, then, puts each constant in the proper order of magnitude range.

Since the preceding analysis is good only for $x - x_i << 1$, and serves only as a start for the computations for $\beta_2 - \Delta_2$, another, more general calculation of the conduction term must be made. After the breakdown of the linear variation of the various functions with $x - x_i$, the simple boundary layer approximation may be used. Thus $\frac{\partial^2 \vartheta}{\partial y} = C_1 \frac{\vartheta_\infty - \vartheta_2}{\beta_2 - \Delta_2}$ was used for the conduction term at the end of the region of applicability of the linear conduction term. At this point, then, the two conduction terms were equated to give C_1. For the case calculated, this point occurred at $x - x_i \approx 0.08$ cm, which gave a value of C_1 of about 1/5. Since C_1 is generally of the order of 1, the calculated value was in the correct range. As $\beta_2 - \Delta_2$ increased the conduction term became smaller, and finally was negligible, whereupon equation (100) reverted to the third of equations (95).

While the above approximations are very crude, it is believed that they give the correct relative order of magnitude of the variable β_2 as compared to Δ_2. Since the integral approach in itself is an approximate method, however, these calculations must be interpreted as a qualitative picture of the depth to which the higher temperatures penetrate.

While, in general, the lines $\beta_1(x)$, $\beta_0(x)$, $\beta_2(x)$, etc., show what one would expect to occur physically, the decreases in $\beta_1(x)$ and $\Delta_1(x)$ which occur just before a laminar flame develops, shown in figure 8, are physically impossible, since they indicate that the fluid heats up slightly, is cooled, and then is heated up to the flame temperature as

it flows downstream. One probable cause of this situation is the fact that since profiles with finite boundaries are used, and since the slope of the profile at the matching line controls the thickness of the upper zone, the extreme rapidity with which the slope grows just before a laminar flame develops, caused inaccuracies in the thicknesses.

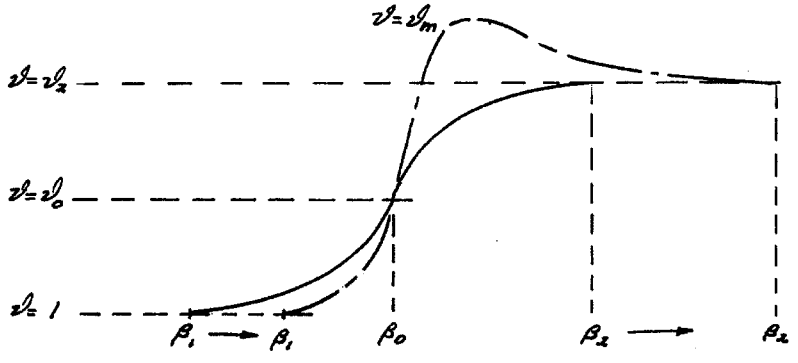

Thus, as is illustrated in the sketch, $\left.\frac{\partial\vartheta}{\partial y}\right|_{\beta_0} \sim \frac{\vartheta_0-1}{\beta_1-\beta_0}$, so that as $\frac{\partial\vartheta}{\partial y}$ increases, $\beta_1-\beta_0$ must decrease. Hence a slight inaccuracy in the rate of growth of the slope could lead to the result noted in figure 8, where $\beta_1-\beta_0$ attains values which should occur just slightly farther downstream.

It is interesting, next, to calculate a flame speed existent with the present conditions, and using the integral technique. It is evident that after a laminar flame develops, all lines $\beta_1(x)$, $\beta_0(x)$, $\Delta_1(x)$, $\Delta_2(x)$, etc. will lie parallel to one another. Hence one may define a normal flame speed as that velocity perpendicular to β_1 in the compressible plane. Hence, denoting by the subscript c the aforementioned thicknesses in the compressible plane, one finds that

$$u_{on} = \left[u_0 \sin\alpha - v_0 \cos\alpha\right]_{\beta_{1c}} \qquad (102)$$

where $[u_o, v_o]_{\beta_{1c}}$, u_{on} and α are defined in the sketch.

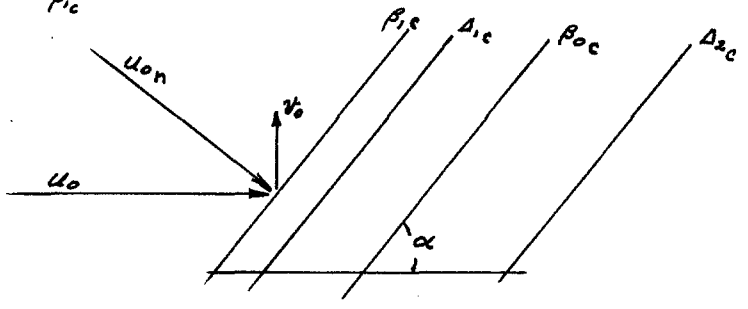

One can assume that the flame has propagated far enough into the upper stream that it is outside the regular velocity boundary layer in the incompressible plane. Thus, since u is unchanged in going from the incompressible to the compressible plane, this means that $u_o = u_I$ in the compressible plane also.

Next, from equation (30)

$$v_o(\beta_{1c}) = -\left\{ -v(\beta_1) + u_I \left.\frac{\partial y}{\partial x_o}\right|_{\beta_{1c}, x_o} \right\}$$

since $\rho(\beta_1) = \rho_I$, $u_o = u_I$. However,

$$\left.\frac{\partial y}{\partial x_o}\right|_{\beta_{1c}, x_o} = \left.\frac{dy}{dx_o}\right|_{\beta_{1c}, x_o} - \frac{\partial y}{\partial y_o}\left.\frac{dy_o}{dx_o}\right|_{\beta_{1c}, x_o}$$

$$= \left.\frac{dy}{dx_o}\right|_{\beta_{1c}, x_o} - \frac{\rho}{\rho_I}\left.\frac{dy_o}{dx_o}\right|_{(\beta_{1c}), x_o}$$

$$= \frac{d\beta_1}{dx} - \frac{d\beta_{1c}}{dx_o}$$

since at $y_o = \beta_{1c}$, $y = \beta_1$, etc. Also $\tan\alpha = \frac{d\beta_{1c}}{dx_o}$ while $x = x_o$, and $\frac{d\beta_1}{dx} = \frac{d\beta_o}{dx}$ so that, substituting in equation (102), one obtains the equation

$$u_{o_n} = u_n = u_I \cos\alpha \left[\frac{d\beta_o}{dx} - \frac{v(\beta_1)}{u_I} \right]$$

If the boundary layer assumptions are satisfied, $\cos\alpha \simeq 1$, so that

$$u_n = u_I \left[\frac{d\beta_o}{dx} - \frac{v(\beta_1)}{u_I} \right] \tag{103}$$

which is recognized as the incompressible flame speed derived in the section describing the reduction of the equations of change into an equivalent one dimensional system. Since in the present case $v \equiv 0$ and $u_I = u_{II} = u$ equation (103) reduces to

$$u_n = u \frac{d\beta_o}{dx} \tag{104}$$

The $\frac{d\beta_o}{dx}$ which exists at the fully developed flame may be computed by noting that since all lines are parallel, $\frac{d}{dx}(\beta_1 - \beta_o) = 0$, $\frac{d}{dx}(\Delta_1 + \Delta_2) = 0$, and $\frac{d}{dx}(\Delta_1 - \beta_o) = 0$ so that $\frac{dK(\beta_o)}{dx} = 0$. From equations (98), then, one can get the conditions on the thicknesses and temperatures, themselves. Thus,

$$\frac{\pi^2}{2(\pi-2)} \frac{\nu}{S_c u} \frac{1}{K(\beta_o)(1-K(\beta_o))(\Delta_1+\Delta_2)} = \frac{4}{(\pi-2)} (\beta_1 - \beta_o) \frac{I(\lambda\beta_m) e^{-\lambda\beta_o/\lambda\beta_2}}{u\tau(\lambda\beta_2 - 1)}$$

$$\frac{\pi^2}{2(\pi-2)} \frac{\nu}{S_c u} \frac{1}{K(\beta_o)(1-K(\beta_o))(\Delta_1+\Delta_2)} \left[1 + 2\frac{S_c}{P_r} \left(\frac{\pi-2}{4-\pi} \right) (1-K(\beta_o)) \right] +$$

(105)

$$+ \frac{\pi^3}{2(\pi-2)(4-\pi)} \frac{1}{P_r} \frac{\nu}{u(\beta_1-\beta_o)} \frac{1}{} = \frac{4}{(\pi-2)} \frac{I(\lambda\beta_m) e^{-\lambda\beta_o/\lambda\beta_2}}{u\tau(\lambda\beta_2-1)} (\beta_1-\beta_o) \left[1 + K(\beta_o) + \frac{4(\pi-2)}{(4-\pi)} \frac{(\lambda\beta_1-1)(\beta_1-\beta_o)}{(\lambda\beta_2-1)(\Delta_1+\Delta_2)} \right]$$

$$\frac{S_c}{P_r} \left(\frac{\Delta_1+\Delta_2}{\beta_1-\beta_o} \right) (1-K(\beta_o)) = 1$$

$$\frac{d\beta_0}{dx} = \frac{\pi}{2}\frac{\nu}{P_r u}\frac{1}{(\beta_1-\beta_0)}$$

Simultaneous solution of the first three equations yields the following results

$$\frac{\beta_1-\beta_0}{\Delta_1+\Delta_2} = \frac{1}{2\frac{(\vartheta_f-1)}{(\vartheta_2-1)} - 1 + \frac{P_r}{S_c}}$$

$$K(\beta_0) = 1 - \left(\frac{\beta_1-\beta_0}{\Delta_1+\Delta_2}\right)\frac{P_r}{S_c} \qquad (106)$$

$$\beta_1-\beta_0 = \frac{\pi}{2}\left(\frac{\nu}{2P_r}\frac{\gamma}{I(\vartheta_m)}\frac{(\vartheta_2-1)}{K(\beta_0)}e^{\vartheta_0/\vartheta_2}\right)^{1/2}$$

Also from equation (97) and the matching relation for $K(\beta_0)$

$$\vartheta_m = K(\beta_0)\left(\frac{\Delta_1+\Delta_2}{\beta_1-\beta_0}\right)(\vartheta_0-1) + \vartheta_0$$

so that with substitution of the above relations for $K(\beta_0)$ and $\frac{\Delta_1+\Delta_2}{\beta_1-\beta_0}$

$$\vartheta_m = \left[2\left(\frac{\vartheta_f-1}{\vartheta_2-1}\right)-1\right](\vartheta_0-1)+\vartheta_0$$

However, $\vartheta_f-1 = 2(\vartheta_0-1)$, so that

$$\vartheta_m = \vartheta_f \qquad (107)$$

i.e.; the maximum temperature is, in fact, the adiabatic flame temperature, at the fully developed flame.

Finally, after substitution for $\frac{d\beta_0}{dx}$, $\beta_1-\beta_0$, and $K(\beta_0)$, the normal flame speed may be written as

$$u_n = \left[\frac{2\nu S_c}{P_r^2} \frac{I(\vartheta_f)}{\tau(\vartheta_2 - 1)} e^{-\vartheta_2/\vartheta_2} \left\{ \frac{2\left(\frac{\vartheta_f - 1}{\vartheta_2 - 1}\right) - 1}{1 + \frac{S_c}{P_r}\left(2\,\frac{\vartheta_f - 1}{\vartheta_2 - 1} - 1\right)} \right\} \right]^{1/2} \qquad (108)$$

which indicates that the flame speed varies with S_c and P_r essentially as $\frac{\sqrt{S_c}}{P_r}$. While this variation with transport properties agrees with other derivations of the flame speed, the numerical values for u_n is almost twice that calculated for azomethane by Hirschfelder, for example. This is due in part to the simplifying assumptions made for the transport properties; however, even more, this discrepancy is due to the fact that by neglecting the combustion effects in the upper stream, ϑ_0 then assumes the character of an ignition temperature found in one dimensional thermal theory, and the usual difficulty of defining the proper ignition temperature is incurred.

VII. CONCLUDING REMARKS

Through the application of a boundary layer type of analysis to the problem of ignition and combustion in the mixing zone between parallel streams of combustible and combustion products some of the essential features have been deduced with relative ease. Thus, there is illustrated the basic change in temperature profile from a smooth mixing profile to that associated with combustion where a "bulge" exists due to a temperature maximum within the thermal mixing region. Also, although the stream of combustible eventually ignites, it is shown that when the temperature of the hot stream is too low, the distance (or time) required is excessive. Then the flame develops so far downstream that it is essentially "blown off" any finite apparatus. A general qualitative picture of the character of the mixing and reacting zone is given to the point at which a laminar flame develops, showing the relative thicknesses of the temperature and combustible concentration "boundary layers" and the downstream growth of the maximum temperature. Finally, in the Appendix A the equations are developed whereby the preceding methods may be used for a ternary system in which the local concentrations of two of the constituents are small compared to the third.

In a broader sense the analysis shows that a new class of combustion problems is open to investigation through extension of the usual boundary layer concepts. In addition to the present one, this class includes such important problems as the theory of thermal quenching near a cool wall, the ignition and flame stabilization on a heated surface from which the boundary layer is unseparated, the erosive burning of solid

propellant grains, and a great many others. There is no essential difficulty in proceeding to problems with axial symmetry and it seems quite possible that the process may be extended to include cases of turbulent mixing. Thus the theory of the plane laminar flame together with the description of such boundary layer regions as may be treated by the methods just described, would seem to disclose the essential features of a relatively wide class of problems which involve steady, constant pressure deflagration.

REFERENCES

1. Hirschfelder, J. O., Curtiss, C. F., Hummel, H., Adams II, E., Henkel, M. J., and Spaulding, W., "Theory of Propagation of Flames, Parts I, II, III", Third Symposium on Combustion, Flame, and Explosion Phenomena, Williams and Wilkins Company, (1949), pp. 121-140.

2. Mallard, E., and Le Chatelier, H., "Recherches Experimentelles et Theoretiques sur la Combustion des Melanges Gazeuses Explosifs", Annales des Mines (1883), Series 8, Vol. 4, pp. 274-295.

3. Boys, S. F., and Corner, J., "The Structure of the Reaction Zone in a Flame", Proc. Roy. Soc. (London), (1949), Series A, Vol. 197, pp. 90-106.

4. von Kármán, T., and Millan, G., "The Thermal Theory of Constant Pressure Deflagration", Biezeno Anniversary Volume on Applied Mechanics, N. V. De Technische Uitgeverij H. Stam, Haarlem, Antwerpen, Djakarta, (1953), pp. 59-69.

5. Scurlock, A. C., "Flame Stabilization and Propagation in High Velocity Gas Streams", Meteor Report No. 19, Massachusetts Institute of Technology, (1948), pp. 150.

6. Gross, R. A., "Aerodynamics of a Two Dimensional Flame", Combustion Tunnel Laboratory Interim Technical Report No. 2, Harvard University, (1952), pp. 76.

7. von Kármán, T., and Millan, G., "Thermal Theory of a Laminar Flame Front near a Cold Wall", Fourth (International) Symposium on Combustion, Williams and Wilkins, Baltimore, (1953). pp. 173-177.

8. Hirschfelder, J. O., Curtiss, C. F., Bird, R. B., and Spatz, E. L., "The Properties of Gases" (Mark II), Chapter 7, Kinetic Theory of Gases, University of Wisconsin, CF 1500-A, February, (1952), pp. 88-97.

9. Chapman, S., and Cowling, T. G., "The Mathematical Theory of Non-Uniform Gases," Cambridge, at the University Press, (2nd Ed.), (1952), pp. 134-136.

10. Hirschfelder, J. O., Curtiss, C. F., Bird, R. B., and Spatz, E. L., Op. cit., pp. 61-69, 72.

11. Chapman, S., and Cowling, T. G., Op. cit., p. 248.

12. Howarth, L., "Concerning the Effect of Compressibility on Laminar Boundary Layers and Their Separation", Proc. Roy. Soc. (London) (1948), Series A., Vol. 194, No. A1036, pp. 16-42.

13. Dorodnitzyn, A., "Laminar Boundary Layers in Compressible Fluids", C. R. Academy of Sciences, U. R. S. S., (1942), Vol. 34, No. 8, pp. 213-219.

14. Lock, R. C., "The Velocity Distribution in the Laminar Boundary Layer Between Parallel Streams", Quart. Journ. Mech. and Applied Math., (1951), Vol IV, Pt. 1, pp. 42-63.

15. Adams, E. P., "Smithsonian Mathematical Formulae and Tables of Elliptic Functions", Publication 267, Smithsonian Institution, Washington, (1947), p. 180.

16. Hirschfelder, J. O., Curtiss, C. F., Hammel, H., Adams II, E., Henkel, M. J., and Spaulding, W., Op. cit., p. 136.

17. Lock, R. C., Op. cit., p. 53

18. Lock, R. C., Op. cit., p. 50.

19. Goldstein, S., "Modern Development in Fluid Mechanics", Clarendon Press, Oxford, 1st Edition, (1938), pp. 131-134.

20. Hirschfelder, J. O., Curtiss, C. F., Hammel, H., Adams II, E., Henkel, M. J., and Spaulding, W., Op. cit., p. 129.

21. Bromley, L. A., and Wilke, C. R., "Viscosity Behavior of Gases", Industrial and Engineering Chemistry, July, (1951), Vol. 43, pp. 1641-1648.

22. Hirschfelder, J. O., Curtiss, C. F., Hammel, H., Adams II, E., Henkel, M. J., and Spaulding, W., Op. cit., p. 124.

APPENDIX A

COMBUSTION IN A LAMINAR MIXING ZONE INVOLVING THREE COMPONENTS

The general conservation equations (2), (10), (3), (15), (6), (7), and (8) written for an arbitrary number of components, can be modified through the use of the boundary layer assumptions to the following:

$$\frac{\partial}{\partial x_o}(\rho u_o) + \frac{\partial}{\partial y_o}(\rho v_o) = 0 \tag{A-1}$$

$$\rho u_o \frac{\partial K_i}{\partial x_o} + \rho v_o \frac{\partial K_i}{\partial y_o} = -\frac{\partial}{\partial y_o}(\rho_i v_i) + m_i \dot{K}_i \qquad i = 1, 2, 3, 4, \ldots \tag{A-2}$$

$$\rho u_o \frac{\partial u_o}{\partial x_o} + \rho v_o \frac{\partial u_o}{\partial y_o} = \frac{\partial}{\partial y_o}\left(\mu \frac{\partial u_o}{\partial y_o}\right) \tag{A-3}$$

$$\rho u_o \frac{\partial T}{\partial x_o} + \rho v_o \frac{\partial T}{\partial y_o} = \frac{1}{\bar{c}_p}\frac{\partial}{\partial y_o}\left(\lambda \frac{\partial T}{\partial y_o}\right) - \frac{1}{\bar{c}_p}\sum_i m_i \hat{h}_i \dot{K}_i - \sum_i \frac{c_{p_i}}{\bar{c}_p} \rho_i v_i \frac{\partial T}{\partial y_o} \tag{A-4}$$

$$P = nkT = \text{constant} \tag{A-5}$$

$$v_i = \frac{n^2}{n_i \rho} \sum_{j \neq i} m_j D_{ij} \frac{\partial}{\partial y_o}\left(\frac{n_i}{n}\right) \tag{A-6}$$

where D_{ij} is the multi component diffusion coefficient and thermal diffusion and viscous dissipation have been neglected.

The coefficient of viscosity for the mixture is defined as[21]

$$\mu = \sum_i \frac{\mu_i}{1 + \frac{1}{N_i} \sum_{j \neq i} N_j \phi_{ij}} \tag{A-7}$$

with

$$\phi_{ij} = \frac{\left[1 + \left(\frac{\mu_i}{\mu_j}\right)^{1/2} \left(\frac{M_j}{M_i}\right)^{1/4}\right]^2}{\frac{4}{\sqrt{2}} \left[1 + \frac{M_i}{M_j}\right]^{1/2}} \tag{A-8}$$

where N_i = mole fraction , and M_i = molecular weight.

The multi component diffusion coefficients have been studied by Curtiss and Hirschfelder. In particular, the ternary diffusion coefficient may be written as follows;[22]

$$D_{12} = \mathcal{D}_{12} \left[1 + \frac{n_3 \left(\frac{m_3}{m_2} \mathcal{D}_{13} - \mathcal{D}_{12}\right)}{n_1 \mathcal{D}_{23} + n_2 \mathcal{D}_{31} + n_3 \mathcal{D}_{12}}\right] \tag{A-9}$$

with the others obtained by cyclical permutation of the indicies. Again, $\mathcal{D}_{ij}$ indicates a binary diffusion coefficient.

The problem which is to be considered now is the ignition and combustion in a laminar mixing zone consisting of a ternary mixture in which the relative concentrations of two of the constituents are small compared to the third. Also, the two small concentration components consist of the combustible and product of combustion of a simple first order reaction while the large concentration component is an inert gas. In this case, then, the upper stream is supposed to consist, initially, of a cool mixture of the inert gas and combustible, with the lower stream consisting, initially, of a hot mixture of the inert gas and the products of combustion.

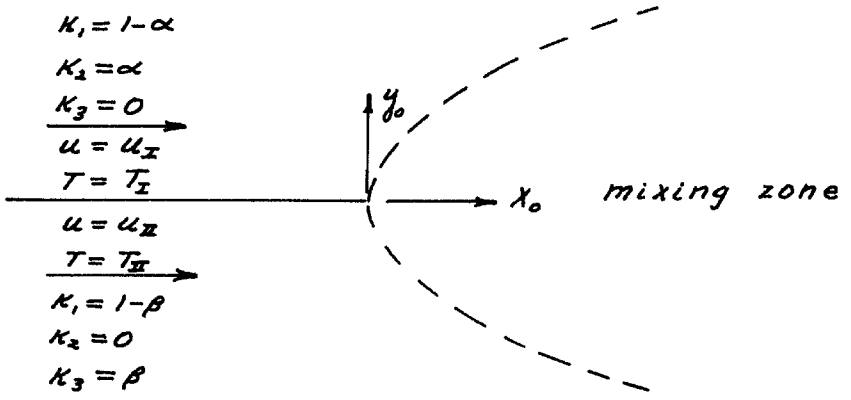

Again it is supposed that $C_{p_i} = C_{p_j} = \bar{C}_p = C_p$.

Thus if one denotes κ_1 as the mass concentration of the inert gas, κ_2 as the concentration of the combustible, and κ_3 as the concentration of the product of combustion, then $\kappa_2 << 1$, $\kappa_3 << 1$, and $\kappa_2 \rightarrow b\,\kappa_3$ in the reaction.

Since $\kappa_i = \frac{m_i}{m}\frac{M_i}{\bar{M}} = \frac{n_i}{n}\frac{m_i}{\bar{m}}$, it is apparent that for $\frac{m_i}{m}\frac{M_i}{\bar{M}} << 1$ something must be said about the ratios $\frac{m_i}{m}$ and $\frac{M_i}{\bar{M}}$. (Here n_i and m_i refer to molecular quantities and m_i and M_i refer to molar quantities. They are connected by Avogadro's number, $m_i = \frac{n_i}{(Av.\ No.)}$, $M_i = m_i\,(Av.\ No.)$) It is assumed that the mole fractions $\frac{m_i}{m} = N_i << 1$ for the components $i = 2, 3$, while all the molecular weights are of the same order, i.e. $\frac{M_i}{\bar{M}} \sim 1$.

With the foregoing assumptions, then, that $\frac{m_2}{m}$, $\frac{m_3}{m}$ and thus κ_2 , and κ_3 are negligible compared to unity, one may investigate the density and transport coefficients for the mixture. Thus:

$$\rho = m_1 M_1 + m_2 M_2 + m_3 M_3$$

$$= m\,(N_1 M_1 + N_2 M_2 + N_3 M_3) \qquad \text{(A-10)}$$

$$= m\,\bar{M}$$

However $N_1 \sim 1$ and $M_1 \sim M_2 \sim M_3$, while $N_2 << 1$ and $N_3 << 1$. Therefore, it will be supposed that the variation of the average molecular weight, $\overline{M}$, is negligible, with $\overline{M}$ being calculated either as the initial average molecular weight, or as $\overline{M} \simeq M_1$.

Supposing the molecules to be Maxwellian with the same force constants, implies that

$$\mu_i \propto \sqrt{M_i}\, T$$

so that

$$\frac{\mu_i}{\mu_j} = \sqrt{\frac{M_i}{M_j}}$$

and

$$\phi_{ij} = \frac{\sqrt{2}}{\left[1 + M_i/M_j\right]^{1/2}} \sim 1$$

while

$$\mu = \frac{N_1 \mu_1}{N_1 + N_2 \phi_{12} + N_3 \phi_{13}} + \frac{N_2 \mu_2}{N_2 + N_1 \phi_{21} + N_3 \phi_{23}} + \frac{N_3 \mu_3}{N_3 + N_1 \phi_{31} + N_2 \phi_{32}}$$

so that to the same order of approximation,

$$\mu \simeq \mu_1 \tag{A-11}$$

From the Eucken correction, for a mixture

$$\lambda = \mu \left(\bar{C}_p + \frac{5}{4} \frac{R}{\overline{M}} \right) \tag{A-12}$$

Hence, with the knowledge of μ, C_p, and M, λ is known.

Finally, one can write the ternary diffusion coefficients as

$$D_{ij} = \mathcal{D}_{ij}\, \Delta_{ij} \tag{A-13}$$

where, for example, Δ_{12} is, from equation (A-9),

$$\Delta_{12} = 1 + \frac{n_3\left(\frac{m_3}{m_2}\mathcal{D}_{13} - \mathcal{D}_{12}\right)}{n_1\mathcal{D}_{23} + n_2\mathcal{D}_{31} + n_3\mathcal{D}_{12}} \tag{A-14}$$

with the others being obtained by cyclical permutation of the indices. In terms of N_i , Δ_{21} becomes

$$\Delta_{21} = 1 + \frac{N_3\left(\frac{M_3}{M_1}\mathcal{D}_{23} - \mathcal{D}_{21}\right)}{N_1\mathcal{D}_{23} + N_2\mathcal{D}_{31} + N_3\mathcal{D}_{12}}$$

Taking account of the fact that the $\mathcal{D}_{ij}$'s do not differ by an order of magnitude since the molecular weights are of the same order, then to the given order of approximation,

$$\Delta_{21} \simeq 1 \tag{A-15}$$

The remaining Δ_{ij}'s and their approximations are listed below

$$\Delta_{23} = 1 + \frac{N_1\left(\frac{M_1}{M_3}\mathcal{D}_{21} - \mathcal{D}_{23}\right)}{N_1\mathcal{D}_{23} + N_2\mathcal{D}_{31} + N_3\mathcal{D}_{12}} \tag{A-16}$$

$$\simeq \frac{M_1}{M_3}\frac{\mathcal{D}_{21}}{\mathcal{D}_{23}}$$

$$\Delta_{31} = 1 + \frac{N_2\left(\frac{M_2}{M_1}\mathcal{D}_{32} - \mathcal{D}_{31}\right)}{N_1\mathcal{D}_{23} + N_2\mathcal{D}_{31} + N_3\mathcal{D}_{12}} \tag{A-17}$$

$$\simeq 1$$

$$\Delta_{32} = 1 + \frac{N_1\left(\frac{M_1}{M_2}\mathcal{D}_{31} - \mathcal{D}_{32}\right)}{N_1\mathcal{D}_{23} + N_2\mathcal{D}_{31} + N_3\mathcal{D}_{12}} \tag{A-18}$$

$$\simeq \frac{M_1}{M_2}\frac{\mathcal{D}_{31}}{\mathcal{D}_{32}}$$

It is apparent, that with the foregoing assumptions, $\rho\mu$ = constant,

and $P_r = \frac{c_p \mu}{\lambda}$ = constant, and a Schmidt number, defined as

$$S_{ij} = \frac{\mu}{\rho D_{ij}} = \frac{\rho \mu}{\rho^2 D_{ij}} = \frac{\rho \mu}{n^2 \bar{m}^2 \frac{T}{n}} = \text{constant}$$

since $D_{ij} \propto \frac{T^s}{n}$ and $P = nkT$. Thus, the Howarth transformation may again be applied, uncoupling the momentum from the species and energy conservation equations. Performing again the transformations in equations (24) to (31), with $m_2 K_2 = -\frac{\rho K_2}{\tau} e^{-A/RT} = -m_3 K_3$ from a simple Arrhenius rate law, one can derive the following equations,

$$\frac{\partial u}{\partial x} + \frac{\partial v}{\partial y} = 0$$

$$u \frac{\partial K_2}{\partial x} + v \frac{\partial K_2}{\partial y} = -\frac{\partial}{\partial y}\left(\frac{\rho_2 v_2}{\rho_2}\right) - \frac{K_2}{\tau} e^{-A/RT}$$

$$u \frac{\partial K_3}{\partial x} + v \frac{\partial K_3}{\partial y} = -\frac{\partial}{\partial y}\left(\frac{\rho_3 v_3}{\rho_3}\right) + \frac{K_2}{\tau} e^{-A/RT} \qquad \text{(A-19)}$$

$$u \frac{\partial u}{\partial x} + v \frac{\partial u}{\partial y} = \nu \frac{\partial^2 u}{\partial y^2}$$

$$u \frac{\partial T}{\partial x} + v \frac{\partial T}{\partial y} = \frac{\nu}{P_r} \frac{\partial^2 T}{\partial y^2} + \frac{\overline{\Delta H}_{23}}{c_p} \frac{K_2}{\tau} e^{-A/RT}$$

$$v_i = \frac{n^2}{n_i \rho_2} \sum_{j \neq i} m_j D_{ij} \frac{\partial}{\partial y}\left(\frac{n_j}{n}\right)$$

where $\sum_i m_i \hat{h}_i K_i = m_2 K_2 (\hat{h}_2 - \hat{h}_3)$ since $K_1 = 0$ and $\sum_i m_i K_i = 0$, from continuity considerations. $\Delta H_{23} = \hat{h}_2 - \hat{h}_3$ is again interpreted as an average heat release per unit gram of the reactant over the temperature range.

Next, v_2 must be computed.

$$v_2 = \frac{n^2}{n_2 \rho_I}\left\{ m_1 \mathcal{D}_{21} \Delta_{21} \frac{\partial}{\partial y}\left(\frac{n_1}{n}\right) + m_3 \mathcal{D}_{23} \Delta_{23} \frac{\partial}{\partial y}\left(\frac{n_3}{n}\right)\right\}$$

$$= \frac{n^2}{n_2 \rho_I}\left\{ - m_1 \mathcal{D}_{21} \Delta_{21} \frac{\partial N_2}{\partial y} + \left(m_3 \mathcal{D}_{23} \Delta_{23} - m_1 \mathcal{D}_{21} \Delta_{21}\right)\frac{\partial N_3}{\partial y}\right\}$$

since $n = n_1 + n_2 + n_3$. Further,

$$v_2 = \frac{n^2}{n_2 \rho_I}\left\{ - \frac{m_1}{m_2} \mathcal{D}_{12} \Delta_{21} \frac{\partial K_2 \bar{m}}{\partial y} + \left(\mathcal{D}_{23} \Delta_{23} - \frac{m_1}{m_3} \mathcal{D}_{12} \Delta_{21}\right)\frac{\partial K_3 \bar{m}}{\partial y}\right\}$$

However, since $\bar{m} \simeq$ constant, and with the approximations for Δ_{ij} ,

$$v_2 = - \frac{\rho}{\rho_2} \frac{m_2}{\bar{m}} \frac{\rho}{\rho_I}\left\{ \frac{m_1}{m_2} \mathcal{D}_{12} \frac{\partial K_2}{\partial y}\right\}$$

since $\mathcal{D}_{ij} = \mathcal{D}_{ji}$. Thus,

$$\frac{\rho_2 v_2}{\rho_I} = - \frac{\rho \mu}{\rho_I^2 S_{12}} \frac{m_1}{\bar{m}} \frac{\partial K_2}{\partial y}$$

or since $\rho \mu = \rho_I \mu_I$, and $\bar{m} \simeq m_1$.

$$\frac{\rho_2 v_2}{\rho_I} = - \frac{\nu}{S_{12}} \frac{\partial K_2}{\partial y} \qquad \text{(A-20)}$$

Likewise, the same type of analysis gives for the third component,

$$\frac{\rho_3 v_3}{\rho_I} = - \frac{\nu}{S_{13}} \frac{\partial K_3}{\partial y} \qquad \text{(A-21)}$$

It is evident that if the expressions just derived for $\frac{\rho_2 v_2}{\rho_I}$ and $\frac{\rho_3 v_3}{\rho_I}$ are substituted in the species conservation equations (A-19), a set of equations exactly similar to those for the binary system (equation (32) of text) are obtained and hence the transformation to the η and x variables can be carried out in the same manner. The equations (A-19) then become,

$$f''' + \frac{f}{2} f'' = 0$$

$$\frac{1}{S_{12}} \frac{\partial^2 \bar{K}_2}{\partial \eta^2} + \frac{f}{2} \frac{\partial \bar{K}_2}{\partial \eta} - f' x \frac{\partial \bar{K}_2}{\partial x} = \frac{x}{u_1 \tau} \bar{K}_2 e^{-\vartheta_a/\vartheta}$$

$$\frac{1}{S_{13}} \frac{\partial^2 \bar{K}_3}{\partial \eta^2} + \frac{f}{2} \frac{\partial \bar{K}_3}{\partial \eta} - f' x \frac{\partial \bar{K}_3}{\partial x} = -\frac{\alpha}{\beta} \frac{x}{u_1 \tau} \bar{K}_2 e^{-\vartheta_a/\vartheta} \qquad \text{(A-22)}$$

$$\frac{1}{P_r} \frac{\partial^2 \vartheta}{\partial \eta^2} + \frac{f}{2} \frac{\partial \vartheta}{\partial \eta} - f' x \frac{\partial \vartheta}{\partial x} = -\alpha \frac{\Delta \bar{H}_{23}}{c_p T_1} \frac{x}{u_1 \tau} \bar{K}_2 e^{-\vartheta_a/\vartheta}$$

Here, ϑ and f have the same definition as in the text, and α and β are the initial concentrations of K_2 and K_3 respectively, so that

$$K_2 = \alpha \bar{K}_2$$

$$K_3 = \beta \bar{K}_3 \qquad \text{(A-23)}$$

The boundary conditions are as follows,

$$f' = 1 \ , \ f'' = 0 \ , \ \text{at} \ \eta = \infty$$

$$f' = \Lambda \ , \ f'' = 0 \ , \ \text{at} \ \eta = -\infty \qquad \text{(A-24)}$$

$$\bar{K}_2 = 1 \ , \ \bar{K}_3 = 0, \ \vartheta = 1 \ , \ \frac{\partial \bar{K}_2}{\partial \eta} = \frac{\partial \bar{K}_3}{\partial \eta} = \frac{\partial \vartheta}{\partial \eta} = 0 \quad \text{at} \ \eta = \infty \ (\text{all } x)$$

$$\bar{K}_2 = 0, \ \bar{K}_3 = 1 \ , \ \vartheta = \vartheta_2, \ \frac{\partial \bar{K}_2}{\partial \eta} = \frac{\partial \bar{K}_3}{\partial \eta} = \frac{\partial \vartheta}{\partial \eta} = 0 \ \text{at} \ \eta = -\infty \ (\text{all } x)$$

with initial conditions $\bar{K}_2 = 1$, $\bar{K}_3 = 0$, and $\vartheta = 1$ in the upper stream and $\bar{K}_2 = 0$, $\bar{K}_3 = 1$, and $\vartheta = \vartheta_2$, in the lower stream.

Since, in terms of $\bar{K}_2$, the problem is exactly similar to the binary problem in that the limits of $\bar{K}_2$ are 1 and 0 , while ϑ goes from 1 to ϑ_2 in the same interval if $S_c = P_r$, the definition of

ℓ , the characteristic chemical length is the same. Hence, defining $\xi = \frac{x}{\ell}$ again, one can write the species and energy conservation equations in terms of ξ as,

$$\frac{1}{S_{12}}\frac{\partial^2 \bar{K}_2}{\partial \eta^2} + \frac{f}{2}\frac{\partial \bar{K}_2}{\partial \eta} - f'\xi\frac{\partial \bar{K}_2}{\partial \xi} = \Lambda(\vartheta_2-1)\frac{\vartheta_2}{\vartheta_2^2}\xi \bar{K}_2 e^{-\vartheta_a\left(\frac{1}{\vartheta}-\frac{1}{\vartheta_2}\right)}$$

$$\frac{1}{S_{13}}\frac{\partial^2 \bar{K}_3}{\partial \eta^2} + \frac{f}{2}\frac{\partial \bar{K}_3}{\partial \eta} - f'\xi\frac{\partial \bar{K}_3}{\partial \xi} = -\frac{\alpha}{\beta}\Lambda(\vartheta_2-1)\frac{\vartheta_2}{\vartheta_2^2}\xi \bar{K}_2 e^{-\vartheta_a\left(\frac{1}{\vartheta}-\frac{1}{\vartheta_2}\right)} \qquad \text{(A-25)}$$

$$\frac{1}{P_r}\frac{\partial^2 \vartheta}{\partial \eta^2} + \frac{f}{2}\frac{\partial \vartheta}{\partial \eta} - f'\xi\frac{\partial \vartheta}{\partial \xi} = -\alpha\Lambda\frac{\overline{\Delta H}_{23}}{c_p T_2}(\vartheta_2-1)\frac{\vartheta_2}{\vartheta_2^2}\xi \bar{K}_2 e^{-\vartheta_a\left(\frac{1}{\vartheta}-\frac{1}{\vartheta_2}\right)}$$

with the proper expansions for $\xi << 1$ being

$$\bar{K}_2 = \bar{K}_2^{(0)}(\eta) + \xi \bar{K}_2^{(1)}(\eta) + \xi^2 \bar{K}_2^{(2)}(\eta) + \cdots$$

$$\bar{K}_3 = \bar{K}_3^{(0)}(\eta) + \xi \bar{K}_3^{(1)}(\eta) + \xi^2 \bar{K}_3^{(2)}(\eta) + \cdots \qquad \text{(A-26)}$$

$$\vartheta = \vartheta^{(0)}(\eta) + \xi \vartheta^{(1)}(\eta) + \xi^2 \vartheta^{(2)}(\eta) + \cdots$$

The zero'th and first order equations are then

$$\frac{1}{S_{12}}\frac{d^2 \bar{K}_2^{(0)}}{d\eta^2} + \frac{f}{2}\frac{d\bar{K}_2^{(0)}}{d\eta} = 0$$

$$\frac{1}{S_{13}}\frac{d^2 \bar{K}_3^{(0)}}{d\eta^2} + \frac{f}{2}\frac{d\bar{K}_3^{(0)}}{d\eta} = 0 \qquad \text{(A-27)}$$

$$\frac{1}{P_r}\frac{d^2 \vartheta^{(0)}}{d\eta^2} + \frac{f}{2}\frac{d\vartheta^{(0)}}{d\eta} = 0$$

and

$$\frac{1}{S_{12}}\frac{d^2\bar{K}_2^{(1)}}{d\eta^2}+\frac{f}{2}\frac{d\bar{K}_2^{(1)}}{d\eta}-f'\bar{K}_2^{(1)}=\Lambda(\vartheta_2-1)\frac{\vartheta_a}{\vartheta_2^2}\bar{K}_2^{(0)}e^{-2\vartheta_a\left(\frac{1}{\vartheta^{(0)}}-\frac{1}{\vartheta_2}\right)}$$

$$\frac{1}{S_{13}}\frac{d^2\bar{K}_3^{(1)}}{d\eta^2}+\frac{f}{2}\frac{d\bar{K}_3^{(1)}}{d\eta}-f'\bar{K}_3^{(1)}=-\frac{\alpha}{\beta}\Lambda(\vartheta_2-1)\frac{\vartheta_a}{\vartheta_2^2}\bar{K}_2^{(0)}e^{-2\vartheta_a\left(\frac{1}{\vartheta^{(0)}}-\frac{1}{\vartheta_2}\right)} \qquad \text{(A-28)}$$

$$\frac{1}{P_r}\frac{d^2\vartheta^{(1)}}{d\eta^2}+\frac{f}{2}\frac{d\vartheta^{(1)}}{d\eta}-f'\vartheta^{(1)}=-\alpha\Lambda\frac{\overline{\Delta H}_{23}}{c_p T_1}(\vartheta_2-1)\frac{\vartheta_a}{\vartheta_2^2}\bar{K}_2^{(0)}e^{-2\vartheta_a\left(\frac{1}{\vartheta^{(0)}}-\frac{1}{\vartheta_2}\right)}$$

From equations (A-27) and (A-28) it is seen that for $\alpha=0$, the problem reduces to a pure mixing problem of two components, K_1 and K_3, while for α finite, the zero'th order solution in f, covers the pure mixing problem with all three components. The first order problem, then, consists of the three components with small heat release. It can be seen that for α and f small the heat addition is very small.

In view of the fact that the equations and boundary conditions are the same as those encountered in the binary problem, the solutions for the case of velocities equal can be written immediately.

$$\vartheta^{(0)}=\frac{\vartheta_2+1}{2}-\frac{(\vartheta_2-1)}{2}\,erf\left(\sqrt{\frac{P_r}{4}}\,\eta\right)$$

$$K_2^{(0)}=\frac{\alpha}{2}\left\{1+erf\left(\sqrt{\frac{S_{12}}{4}}\,\eta\right)\right\} \qquad \text{(A-29)}$$

$$K_3^{(0)}=\frac{\beta}{2}\left\{1-erf\left(\sqrt{\frac{S_{13}}{4}}\,\eta\right)\right\}$$

$$\vartheta^{(1)}(\eta) = \alpha P_r \frac{\overline{\Delta H_{23}}}{c_p T_I} (\vartheta_2 - 1) \frac{\vartheta_a}{\vartheta_2^2} \int_{-\infty}^{\infty} G(\eta, \bar{\eta}; P_r) R(\bar{\eta}) d\bar{\eta}$$

$$K_2^{(1)}(\eta) = -\alpha S_{12} (\vartheta_2 - 1) \frac{\vartheta_a}{\vartheta_2^2} \int_{-\infty}^{\infty} G(\eta, \bar{\eta}; S_{12}) R(\bar{\eta}) d\bar{\eta} \qquad \text{(A-30)}$$

$$K_3^{(1)}(\eta) = \alpha S_{13} (\vartheta_2 - 1) \frac{\vartheta_a}{\vartheta_2^2} \int_{-\infty}^{\infty} G(\eta, \bar{\eta}; S_{13}) R(\bar{\eta}) d\bar{\eta}$$

where

$$R(\eta) = \bar{K}_2^{(0)} e^{-\vartheta_a \left(\frac{1}{\vartheta^{(0)}} - \frac{1}{\vartheta_2}\right)} , \quad \frac{\overline{\Delta H_{23}}}{c_p T_I} = \vartheta_f - 1 ,$$

and G is the same Green's function computed in the text.

APPENDIX B

CALCULATION OF PHYSICAL PARAMETERS

1) Reaction

The reaction considered was the decomposition of azomethane, $C_2H_6N_2 \rightarrow C_2H_6 + N_2$, which follows a first order reaction. While the products are a mixture of ethane and nitrogen, it is assumed that this mixture is one component, with the average properties of the actual mixture. For example, the molecular weight of the product of reaction is $M_2 = \frac{M_{C_2H_6} + M_{N_2}}{2} = 29. \frac{gms}{mole}$.

2) $\overline{\Delta H_{12}}$, C_p

From data presented in reference 1,

$$\Delta H_{12} = 862 + \int_{300\,^\circ K}^{T} (C_{p_1} - C_{p_2})\, dT \qquad (B\text{-}1)$$

$$= 862 + \int_{300\,^\circ K}^{T} \left(0.035 - \frac{1.55 \times 10^{2}}{T} + \frac{3.31 \times 10^{4}}{T^2}\right) dT$$

where subscripts 1 and 2 refer to azomethane and a mixture of hydrogen and ethane respectively. Thus, at $T = 300\,^\circ K$, $\Delta H_{12} = 862\ cal/gm$ while at $T = T_f = 1650\,^\circ K$, $\Delta H_{12} = 736\ cal/gm$. The average ΔH_{12} is used for the calculations,

$$\overline{\Delta H_{12}} = 800\ cal/gm \qquad (B\text{-}2)$$

However, $\overline{\Delta H_{12}} = C_p (T_f - T_I)$, where $T_f = 1650\,^\circ K$, and $T_I = 300\,^\circ K$ Therefore,

$$C_p = \frac{\overline{\Delta H_{12}}}{T_f - T_I} = 0.593\ cal/gm \qquad (B\text{-}3)$$

3) P_r

From the Eucken correction,

$$\lambda = \mu\left(\bar{C}_p + 1.25\frac{R}{\bar{M}}\right) = \mu C_p\left(1 + \frac{1.25R}{C_p\bar{M}}\right) \qquad (B\text{-}4)$$

where $\bar{M}$ is the average molecular weight.

Since, $R = 1.987$ cal/mole/°K , $\bar{M} = \frac{1}{2}(58+29) = 43.5 \frac{gm}{mole}$,

with C_p as calculated,

$$P_r = \frac{C_p\mu}{\lambda} = \frac{1}{\left(1 + \frac{1.25R}{C_p\bar{M}}\right)} = 0.91 \qquad (B\text{-}5)$$

4) S_c

From reference 1 again, Eucken's form for λ is written as

$$\lambda = \left(C_{p_{mole}} + 1.25R\right)\frac{\rho\vartheta_{12}P}{RT}$$

where $C_{p_{mole}}$ is the molar specific heat. In terms of C_p , then

$$\lambda = \left(C_p + \frac{1.25R}{\bar{M}}\right)\frac{\bar{M}P\rho\vartheta_{12}}{RT}$$

However, since the usual form for λ is listed above, it is obvious that the assumption was $\mu = \frac{\bar{M}P}{RT}\rho\vartheta_{12}$, or, since $P = \rho\frac{R}{\bar{M}}T$, and $\mu = \rho\vartheta_{12}$ so that

$$S_c = \frac{\mu}{\rho\vartheta_{12}} = 1 \qquad (B\text{-}6)$$

The same assumption is used in the present paper.

5) ϑ_a

Since $A = 50$ kcal , (reference 1),

$$\vartheta_a = \frac{A}{RT_I} = 83.870 \qquad (B\text{-}7)$$

6) ν

Since $\nu = \nu_I = \frac{\mu_I}{\rho_I}$, and ρ_I can be calculated with the given data, $\rho_I = \frac{P/\bar{M}}{R T_I} = 1.767 \times 10^{-3}$ gms/cc , it is necessary to calculate μ_I. However, $\mu_I = \frac{P_r}{c_p} \lambda_I = S_c \rho_I (\mathcal{D}_{12})_I$ so that λ_I or $(\mathcal{D}_{12})_I$ must be calculated. In reference 1 it was assumed that $\lambda \sim T^{1/2} C_p(T)$ while in the present analysis $\lambda \sim T$. Hence a λ_I was chosen such that λ then agreed closely over the temperature range T_I to T_f with the values given in reference 1, in order to keep a comparatively consistent set of physical parameters. The following graph shows a plot of both the laminar variation and the variation chosen by Hirschfelder et al.

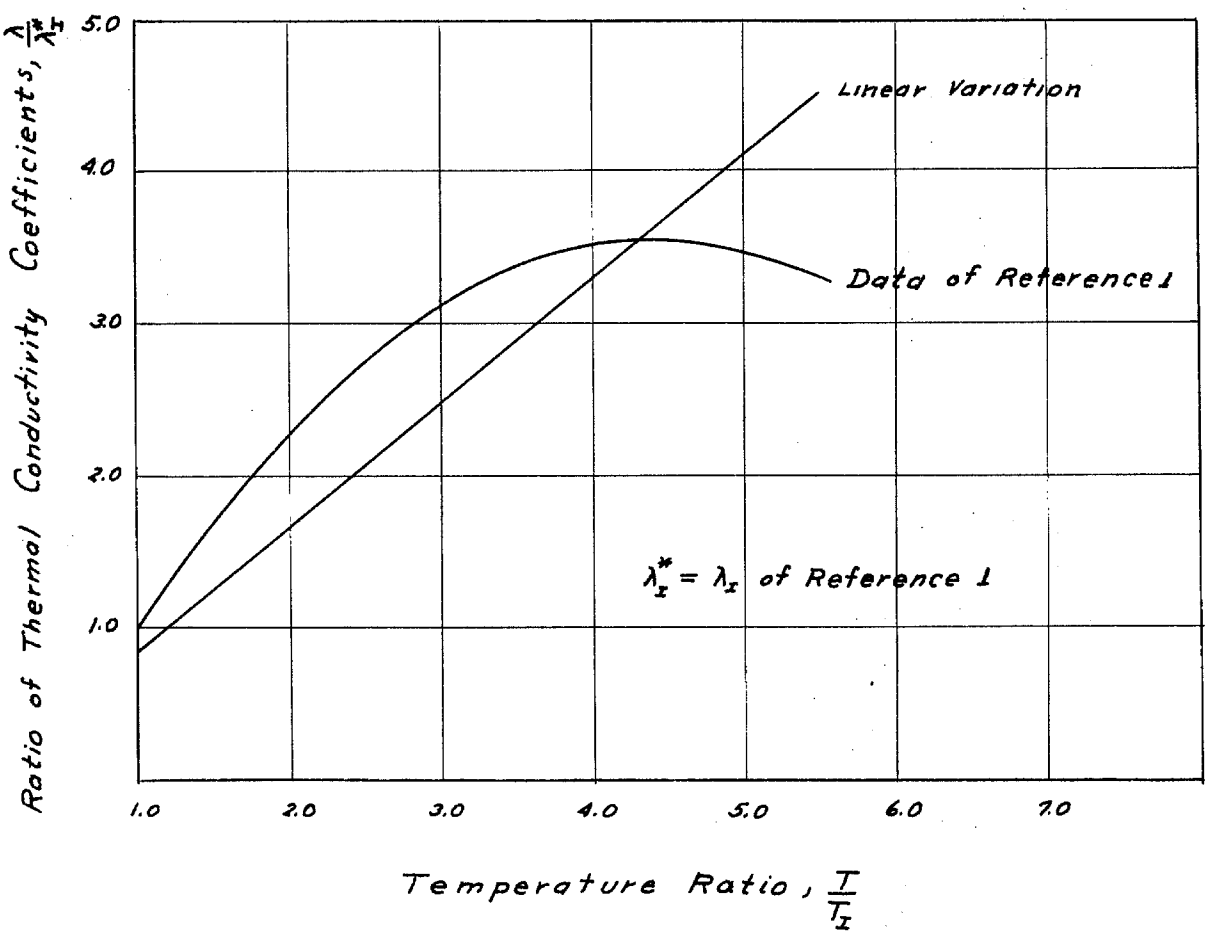

It was found that a fairly good representation was obtained with λ_I equal to eight tenths of the λ_I calculated from the equation given in reference 1. Thus,

$$\lambda_I = 0.8 \left[C_p(T_I) + 2.484 \right] \left[1.694 \times 10^{-7} \right] (T_I)^{1/2}$$

$$C_p(T_I) = M_1 \left[0.988 - \frac{4.90 \times 10^{2}}{T_I} + \frac{8.10 \times 10^{4}}{T_I^{2}} \right]$$

so that

$$\lambda_I = 4.06 \times 10^{-5} \text{ cal/cm/°K/sec} \qquad \text{(B-9)}$$

Then

$$\nu_I = 3.53 \times 10^{-2} \text{ cm}^2\text{/sec} \qquad \text{(B-10)}$$

A summary of all values used follows

Reaction $C_2H_6N_2 \longrightarrow C_2H_6 + N_2$

$A = 50$ kcal

$\tau = 10^{-14}$ sec

$R = 1.987$ cal/mole/°K

$\bar{M} = 43.5$ gms/mole

$C_p = 0.593$ cal/gm/°K

$P_r = 0.91$

$S_c = 1$

$\nu_I = \nu = 3.53 \times 10^{-2}$ cm²/sec

$T_I = 300$ °K

$\vartheta_a = 83.870$

$T_f = 1650$ °K

APPENDIX C

CALCULATIONS FOR PERTURBATION METHOD

From equation (55) of the text,

$$\vartheta^{(1)}(\eta) = -\sqrt{\frac{P_r}{\pi}}\,\frac{(\vartheta_2-1)}{4}(\vartheta_2-1)\,\frac{\vartheta_2}{\vartheta_2^2}\left\{\mathcal{H}_1(\eta)\int_{-\infty}^{\eta}\mathcal{H}_2(\bar\eta)\,e^{\frac{P_r}{4}\bar\eta^2}R(\bar\eta)\,d\bar\eta\right.$$

$$\left. + \mathcal{H}_2(\eta)\int_{\eta}^{\infty}\mathcal{H}_1(\bar\eta)\,e^{\frac{P_r}{4}\bar\eta^2}R(\bar\eta)\,d\bar\eta\right\}$$

Since, from equation (49), it is evident that $\mathcal{H}_2(\eta) = -\mathcal{H}_1(-\eta)$ it was necessary to compute only one. $\kappa^{(0)}(\eta)$ and $\vartheta^{(0)}(\eta)$ were calculated using the tabulated error function, and after tabulating $e^{-\vartheta_2/\vartheta^{(0)}}$ and $e^{\frac{P_r}{4}\bar\eta^2}$, the kernel of each of the integrals was calculated for a range $-8 \le \eta \le 8$ at increments of $\Delta\eta = 0.25$. Using Simpson's rule for numerical integration, then, this gave values for the integrals at increments of $\Delta\eta = 0.50$ over the same range. Table I gives the values of $\vartheta^{(0)}(\eta)$, $\kappa^{(0)}(\eta)$, $\mathcal{H}_2(\eta)$, $I_1(\eta)$, $I_2(\eta)$ and $\vartheta^{(1)}(\eta)$ over the range $-6.5 \le \eta \le 5.5$. Where

$$I_1(\eta) = \int_{-\infty}^{\eta}\mathcal{H}_2(\bar\eta)\,e^{\frac{P_r}{4}\bar\eta^2}R(\bar\eta)\,d\bar\eta$$

$$I_2(\eta) = \int_{\eta}^{\infty}\mathcal{H}_1(\bar\eta)\,e^{\frac{P_r}{4}\bar\eta^2}R(\bar\eta)\,d\bar\eta \qquad \text{(C-1)}$$

for $\vartheta_2 = 3.50$.

In order to calculate η_i from equation (64) of the text, it was necessary to compute $\mathcal{C}$, where

$$\mathcal{C} = -\int_{-\infty}^{\infty} \mathcal{H}_1(\bar{\eta})\, e^{\frac{P_r}{4}\bar{\eta}^2} R(\bar{\eta})\, d\bar{\eta}$$

This was calculated from the numerical work using the definition of $\mathcal{C}$ Thus,

$$\int_{\eta}^{\infty} \mathcal{H}_1(\bar{\eta})\, e^{\frac{P_r}{4}\bar{\eta}^2} R(\bar{\eta})\, d\bar{\eta} \sim -\mathcal{C} + \frac{2P_r\, e^{-\frac{\eta^2}{4}(S_c - P_r)}}{\sqrt{S_c}\,(S_c - P_r)}$$

Values of the integral are given in Table I. By letting $\eta = -6$, -7, and -8, $\mathcal{C}$ was calculated to be 17.408, 17.397, 17.395; the value used then, was $\mathcal{C} = 17.40$. With this value of $\mathcal{C}$, η_i was calculated by trial and error from Equation (64) to be $\eta_i = -6.57$.

From equation (66),

$$\zeta_i = \frac{\sqrt{P_r}}{2}\,\frac{\vartheta_2^2}{\vartheta_a(\vartheta_f - 1)}\,\eta_i^2 \left\{\left(1 - \frac{6}{P_r \eta_i^2}\right)\left(\mathcal{C} - \frac{2P_r\, e^{-\frac{\eta_i^2}{4}(S_c - P_r)}}{\sqrt{S_c}\,(S_c - P_r)}\right) - \frac{8}{S_c^{3/2}}\,\frac{e^{-\frac{\eta_i^2}{4}(S_c - P_r)}}{\eta_i^2}\left[1 - \frac{12}{\eta_i^2}\left(\frac{1}{S_c} + \frac{1}{P_r}\right)\right]\right\}^{-1}$$

Substituting values of $\eta_i = -6.57$, $S_c = 1$, $P_r = 0.91$, $\vartheta_f = 5.50$, gives

$$\zeta_i = 0.556\,\frac{\vartheta_2^2}{\vartheta_a} \qquad \text{(C-2)}$$

Therefore

$$x_i = 0.556\,\frac{\vartheta_2^2}{\vartheta_a}\,\ell$$

$$= 0.556\, u_{II}\, \tau(\vartheta_2 - 1)\, e^{\vartheta_2/\vartheta_2}$$

so that for $u_{II} = u_I = 200$ cm/sec. and $\tau = 10^{-14}$,

$$x_i = 1.112 \times 10^{-12} (\vartheta_2 - 1) e^{\vartheta_2/\vartheta_2} \quad (cm) \tag{C-3}$$

Some representative values, then, for x_i as a function of ϑ_2 are

ϑ_2	x_i (cm)
3.5	0.071
3.25	0.404
3.00	3.082
2.75	34.24

It was necessary, also to compute an equivalent x_i for an η_i of -3.08 so as to compare with the Kármán integral method, according to the method described in the text. From equations (59), (46), and (65),

$$\xi_i = -2 \frac{\vartheta_2^2}{\vartheta_2} \frac{e^{-\frac{P_r}{4}\eta_i^2}}{(\vartheta_f - 1)\left\{ \frac{d\chi_1}{d\eta} I_1(\eta) + \frac{d\chi_2}{d\eta} I_2(\eta) \right\}_{\eta_i}}$$

so that

$$x_i = -2 \frac{(\vartheta_2 - 1)}{(\vartheta_f - 1)} u_{II} \tau e^{\vartheta_2/\vartheta_2} \frac{e^{-\frac{P_r}{4}\eta_i^2}}{\left\{ \frac{d\chi_1}{d\eta} I_1(\eta) + \frac{d\chi_2}{d\eta} I_2(\eta) \right\}_{\eta_i}} \tag{C-4}$$

where $I_1(\eta)$ and $I_2(\eta)$ are given in Table I for integer and half integer values of η. From the development preceding equation (54) in the text,

$$\frac{d\chi_1}{d\eta} = \frac{2}{\eta}\left[\chi_1 - \sqrt{\pi}\left(erf\left(\sqrt{\frac{P_r}{4}}\eta\right) - 1\right)\right]$$

$$\frac{d\chi_2}{d\eta} = \frac{2}{\eta}\left[\chi_2 - \sqrt{\pi}\left(erf\left(\sqrt{\frac{P_r}{4}}\eta\right) + 1\right)\right]$$

After substitution of $\eta_2 = 3.5$ and the given values for P_t, S_t, etc., X_i was calculated for values of $\eta_i = -2.5$, -3.0, and -3.5 giving the following values for X_i

η_i	X_i (cm)
- 2.5	0.584
- 3.0	0.215
- 3.5	0.129

Plotting the given values of X_i vs η_i and reading the value for $\eta_i = \eta_2 = -3.08$, gave $X_i = 0.20$ cm.

APPENDIX D

NUMERICAL VALUES OF THICKNESSES, $K(\beta_0)$, AND MAXIMUM TEMPERATURE

The differential equations obtained using the integral technique were solved numerically using the Runge Kutta method. The equations did not contain X explicitly, making calculations easier. The physical parameters used were those calculated in Appendix B.

For $\vartheta_2 = 3.5$, the initial conditions calculated from the expansions (equations (93), text) were, for $X = 10^{-3}$ cm.

$$\Delta_1 + \Delta_2 = 2.469 \times 10^{-3} \text{ cm}$$

$$K(\beta_0) = 0.5001$$

$$\beta_1 - \beta_0 = \beta_0 + \beta_2 = 1.294 \times 10^{-3} \text{ cm}$$

$$\beta_0 = 0.000$$

The results of integrating equations (92) of the text are presented in Table II. The values existing at $X = X_i$ were then used as initial values for integrating equations (98) of the text, the results of which are presented in Table II. The accuracy of the values in Table II is approximately 2 per cent since the values of $I(\vartheta_m)$ were read from a graph of $I(\vartheta_m)$ vs ϑ_m similar to that shown in the following sketch. Separate graphs of $I(\vartheta_m)$ vs ϑ_m were drawn for various ranges of ϑ_m , but the accuracy was no better than 2 per cent. The predicted final values were computed from equations (106).

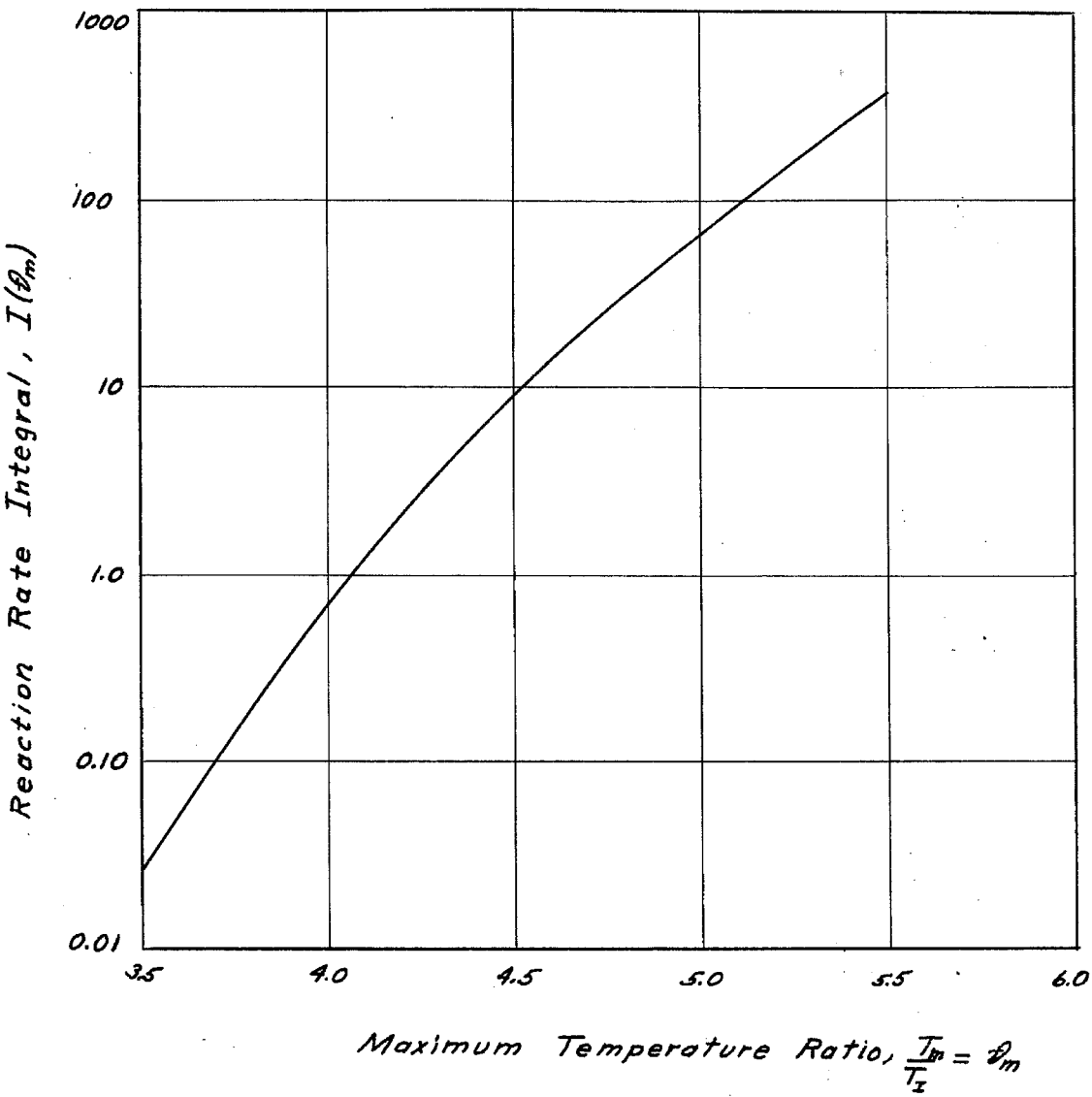
1000
100
10
1.0
0.10
0.01
3.5
4.0
4.5
5.0
5.5
6.0
Reaction Rate Integral, $I(\phi_m)$
Maximum Temperature Ratio, $\frac{T_m}{T_I} = \phi_m$

TABLE I

PERTURBATION FUNCTIONS

η	$\vartheta^{(0)}(\eta)$	$K^{(0)}(\eta)$	$\mathcal{H}_2(\eta)$	$I_1(\eta)\times10^3$	$I_2(\eta)$	$\vartheta^{(1)}(\eta)$
5.5	1.0003	0.9999	52.3362	7.3790	0.0000	0.0000
5.0	1.0009	0.9998	43.8672	7.3790	0.0000	0.0000
4.5	1.0030	0.9992	36.1563	7.3790	0.0000	0.0001
4.0	1.0087	0.9977	29.3496	7.3790	0.0000	0.0002
3.5	1.0228	0.9933	23.2966	7.3790	0.0000	0.0005
3.0	1.0538	0.9831	18.0421	7.3790	0.0000	0.0015
2.5	1.1147	0.9615	13.5767	7.3790	0.0000	0.0038
2.0	1.2217	0.9214	9.8782	7.3790	0.0000	0.0091
1.5	1.3895	0.8556	6.9140	7.3790	0.0000	0.0199
1.0	1.6249	0.7603	4.6283	7.3790	0.0000	0.0405
0.5	1.9199	0.6382	2.9461	7.3790	0.0000	0.0766
0.0	2.2500	0.5000	1.7725	7.3789	0.0000	0.1355
-0.5	2.5801	0.3618	1.0022	7.3682	0.0000	0.2252
-1.0	2.8751	0.2398	0.5295	7.1889	-0.0012	0.3513
-1.5	3.1105	0.1444	0.2602	6.2313	-0.0182	0.4956
-2.0	3.2783	0.0787	0.1184	4.2056	-0.1218	0.5801
-2.5	3.3853	0.0386	0.0497	2.1004	-0.4490	0.5267
-3.0	3.4462	0.0170	0.0192	0.8023	-1.0997	0.3683
-3.5	3.4772	0.0067	0.0068	0.2498	-2.0544	0.2055
-4.0	3.4913	0.0023	0.0022	0.0650	-3.2180	0.0915
-4.5	3.4970	0.0007	0.0006	0.0153	-4.4912	0.0350
-5.0	3.4991	0.0002	0.0002	0.0031	-5.8008	0.0112
-5.5	3.4997	0.0001	0.0001	0.0006	-7.1023	0.0035
-6.0	3.49994	0.00001	0.0000	0.0001	-8.3618	0.0008
-6.5	3.49999	0.0000	0.0000	0.0000	-9.5533	0.0001

TABLE II

THICKNESSES AND $K(\beta_o)$ FOR $X \leq X_i$

X (mm)	$(\Delta_1+\Delta_2)$ (mm)	$K(\beta_o)$	$(\beta_o+\Delta_2)$ (mm)	$(\beta_1-\beta_o)$ (mm)	
0.01	0.0247	0.5001	0.0123	0.0129	
0.02	0.0349	0.5001	0.0175	0.0183	
0.03	0.0427	0.5002	0.0214	0.0224	
0.13	0.0893	0.5007	0.0447	0.0467	
0.23	0.118	0.5012	0.0593	0.0618	
0.33	0.141	0.5017	0.0709	0.0737	
0.43	0.161	0.5022	0.0808	0.0838	
0.53	0.178	0.5027	0.0896	0.0927	
0.63	0.194	0.5032	0.0976	0.1007	
0.73	0.208	0.5037	0.105	0.108	
0.83	0.222	0.5042	0.112	0.115	
0.93	0.234	0.5047	0.118	0.121	
1.03	0.246	0.5052	0.124	0.127	
1.23	0.268	0.5063	0.136	0.138	
1.43	0.288	0.5074	0.146	0.148	
1.63	0.306	0.5085	0.155	0.157	
1.83	0.323	0.5096	0.164	0.165	
1.90	0.339	0.5100	0.168	0.168	$x=x_i$

TABLE II (Continued)

THICKNESSES, $K(\beta_o)$, AND MAXIMUM TEMPERATURE FOR $X \geq X_i$

X (mm)	$(\Delta_1+\Delta_2)$ (mm)	$K(\beta_o)$	$(\beta_o+\Delta_2)$ (mm)	$(\beta_i-\beta_o)$ (mm)	β_o (mm)	$(\beta_2-\Delta_2)$ (mm)	$(\delta_m-\delta_i)$
1.90	0.329	0.510	0.168	0.168	0.0054	0	0.00
2.10	0.344	0.511	0.178	0.175	0.0062	0.002	0.004
2.30	0.359	0.512	0.183	0.182	0.0070	0.005	0.009
2.50	0.372	0.513	0.191	0.189	0.0080	0.007	0.015
2.70	0.385	0.514	0.198	0.195	0.0090	0.009	0.020
2.90	0.397	0.515	0.204	0.200	0.0100	0.011	0.026
3.10	0.408	0.516	0.211	0.205	0.0112	0.012	0.034
3.30	0.419	0.517	0.217	0.210	0.0125	0.013	0.041
3.50	0.429	0.518	0.222	0.214	0.0138	0.014	0.049
3.70	0.438	0.520	0.228	0.218	0.0153	0.015	0.058
4.10	0.455	0.523	0.238	0.224	0.0185	0.017	0.076
4.50	0.468	0.526	0.246	0.228	0.0223	0.020	0.099
4.70	0.474	0.528	0.250	0.230	0.0245	0.021	0.111
4.90	0.479	0.530	0.254	0.230	0.0268	0.023	0.125
5.10	0.482	0.532	0.257	0.231	0.0294	0.026	0.140
5.30	0.485	0.534	0.259	0.230	0.0322	0.029	0.156
5.50	0.487	0.537	0.261	0.229	0.0353	0.033	0.176
5.70	0.487	0.539	0.262	0.227	0.0387	0.037	0.196
5.90	0.485	0.542	0.263	0.224	0.0426	0.043	0.220
6.10	0.481	0.546	0.263	0.219	0.0470	0.051	0.249
6.30	0.474	0.550	0.261	0.213	0.0520	0.060	0.280
6.50	0.464	0.554	0.257	0.205	0.0579	0.073	0.319
6.70	0,448	0.560	0.251	0.194	0.0650	0.090	0.369
6.90	0.424	0.567	0.240	0.178	0.0739	0.114	0.435
7.00	0.406	0.571	0.232	0.168	0.0795	0.131	0.479
7.10	0.383	0.576	0.220	0.155	0.0862	0.153	0.533
7.20	0.352	0.582	0.205	0.138	0.0942	0.180	0.603
7.22	0.345	0.583	0.201	0.134	0.0960	0.186	0.619
7.24	0.337	0.584	0.197	0.130	0.0979	0.193	0.636
7.26	0.328	0.586	0.192	0.126	0.100	0.200	0.656
7.28	0.319	0.587	0.187	0.122	0.102	0.208	0.678
7.30	0.309	0.589	0.182	0.117	0.104	0.217	0.700
7.32	0.298	0.591	0.176	0.111	0.107	0.226	0.725
7.34	0.286	0.592	0.169	0.106	0.110	0.235	0.754
7.36	0.272	0.594	0.162	0.0994	0.112	0.247	0.784
7.38	0.258	0.596	0.153	0.0927	0.115	0.259	0.818
7.40	0.241	0.598	0.144	0.0853	0.119	0.272	0.859
7.42	0.222	0.600	0.133	0.0772	0.122	0.287	0.904
7.44	0.200	0.602	0.120	0.0682	0.127	0.304	0.956
7.46	0.175	0.604	0.106	0.0583	0.131	0.322	1.019
7.48	0.147	0.605	0.0892	0.0476	0.136	0.343	1.091
7.50	0.117	0.606	0.0707	0.0365	0.142	0.365	1.174

TABLE II (Continued)

THICKNESSES, $K(\beta_o)$, AND MAXIMUM TEMPERATURE FOR $X \geq X_i$

X (mm)	$(\Delta_1+\Delta_2)$ (mm)	$K(\beta_o)$	$(\beta_o+\Delta_2)$ (mm)	$(\beta_1-\beta_o)$ (mm)	β_o (mm)	$(\beta_2-\Delta_2)$ (mm)	$(\vartheta_m-\vartheta_2)$
7.52	0.0856	0.605	0.0518	0.0258	0.148	0.388	1.259
7.54	0.0586	0.608	0.0356	0.0173	0.154	0.412	1.326
7.56	0.0412	0.626	0.0258	0.0124	0.160	0.433	1.359
7.58	0.0329	0.661	0.0218	0.0102	0.166	0.439	1.405
7.59	0.0294	0.679	0.0200	0.00919	0.169	0.430	1.470
7.60	0.0253	0.697	0.0177	0.00784	0.173	0.417	1.565
7.61	0.0203	0.715	0.0145	0.00616	0.178	0.399	1.699
7.62	0.0150	0.730	0.0110	0.00442	0.185	0.386	1.851
7.6225	0.0142	0.733	0.0104	0.00416	0.187	0.384	1.884
7.6275	0.0129	0.737	0.00953	0.00374	0.191	0.383	1.939
7.6325	0.0121	0.739	0.00897	0.00348	0.195	0.387	1.969
7.6375	0.0117	0.740	0.00866	0.00334	0.200	0.392	1.988
7.6400	0.0116	0.740	0.00862	0.00332	0.202	0.396	1.993
7.6425	0.0116	0.741	0.00857	0.00330	0.204	0.400	1.995
			Predicted Values				
	0.0115	0.7407	0.00850	0.00327			2.00

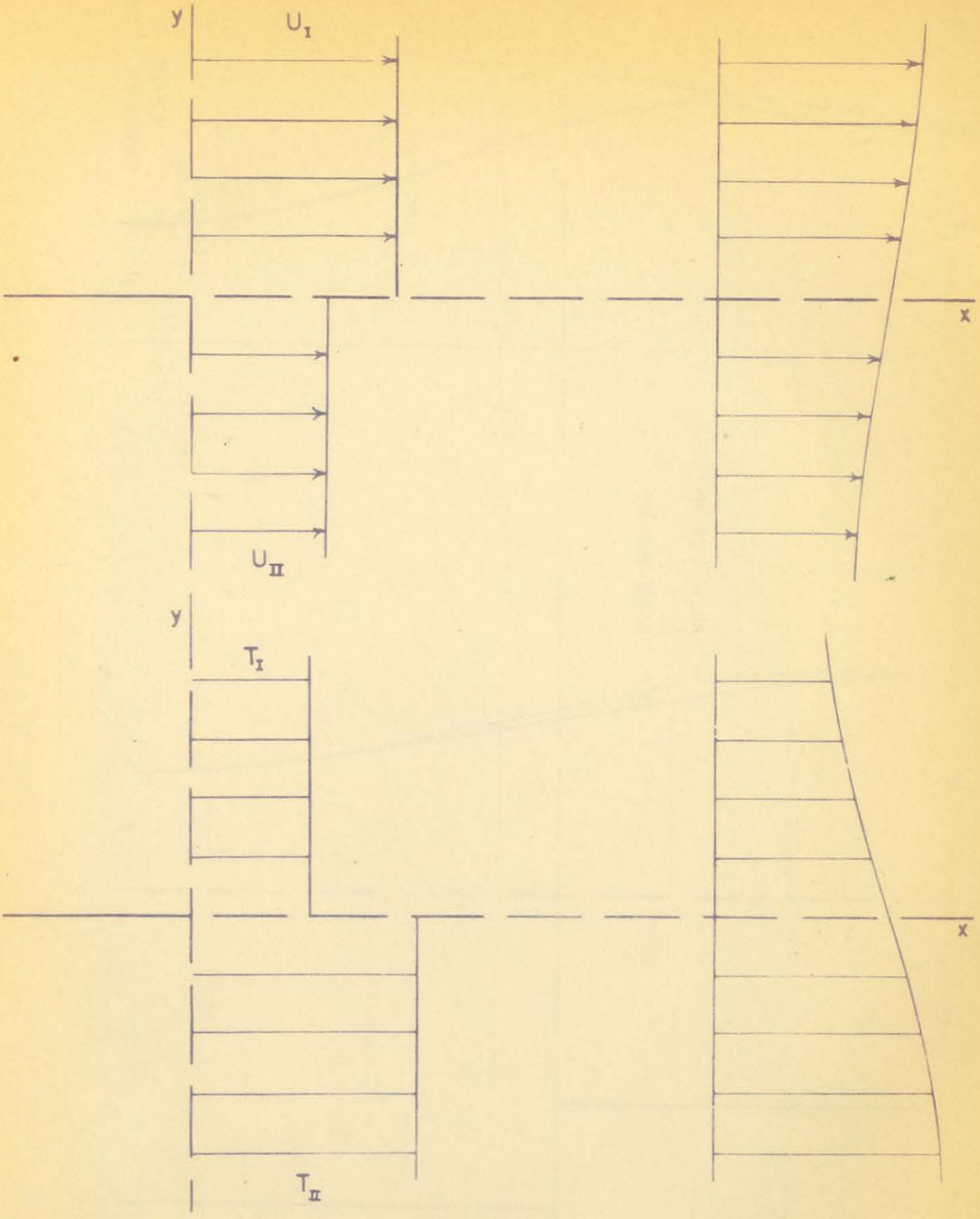

FIGURE I — VELOCITY AND TEMPERATURE PROFILES FOR A MIXING REGION WITHOUT CHEMICAL REACTION

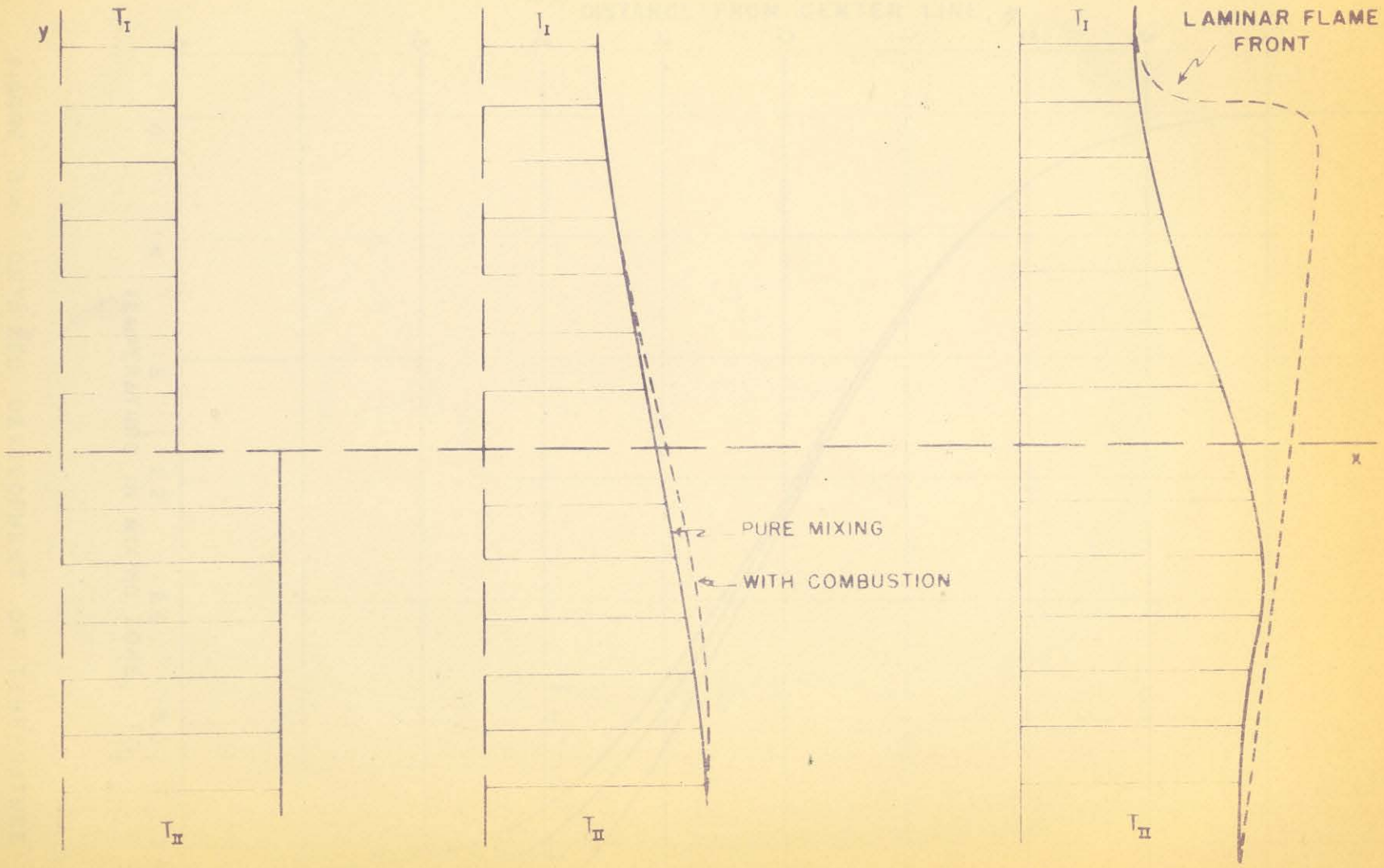

FIGURE 2 — TEMPERATURE PROFILES AND DEVELOPMENT OF LAMINAR FLAME IN MIXING REGION WITH CHEMICAL REACTION

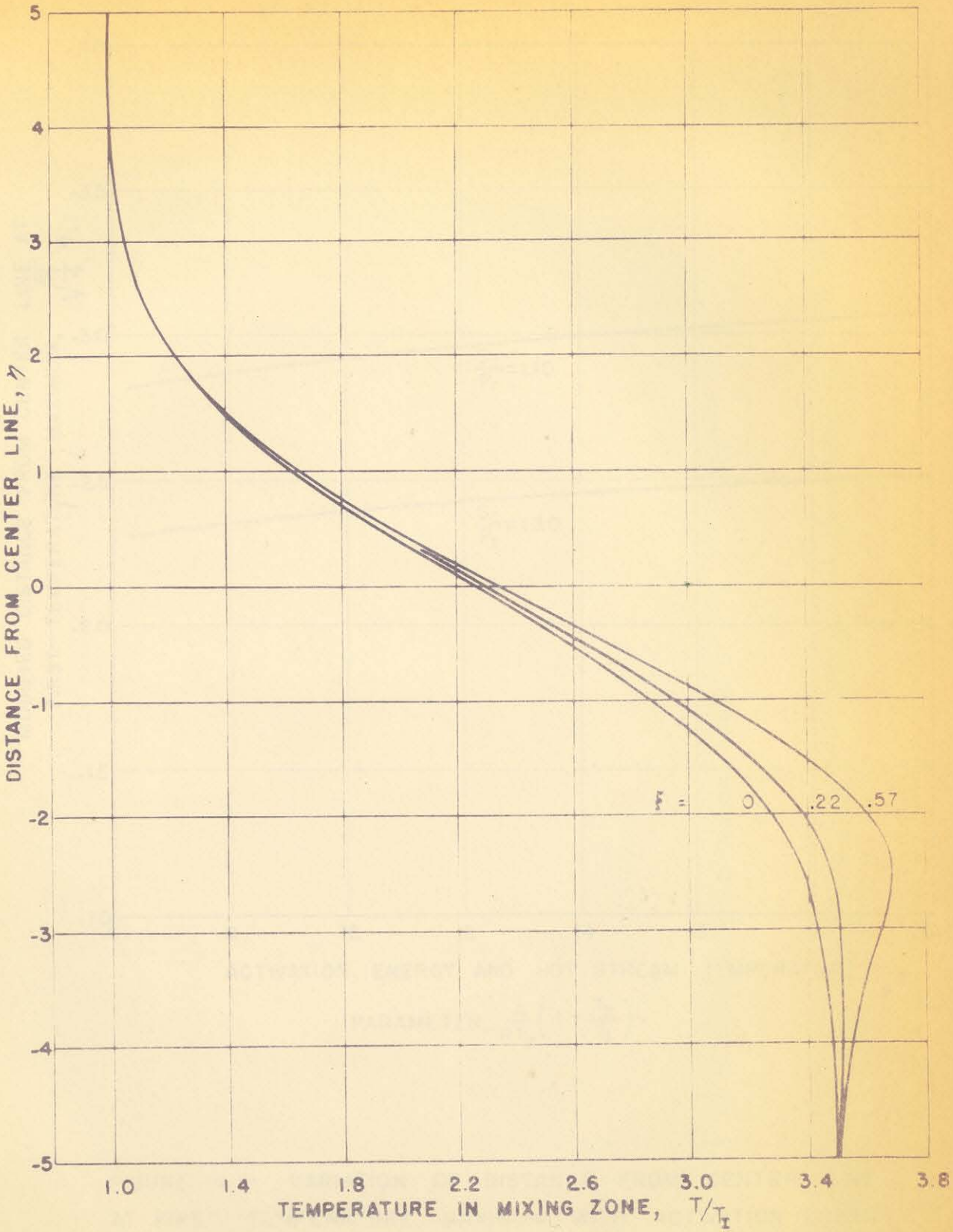

FIGURE 3 — DETAILED DEVELOPMENT OF TEMPERATURE PROFILES DURING THE EARLY STAGES OF REACTION

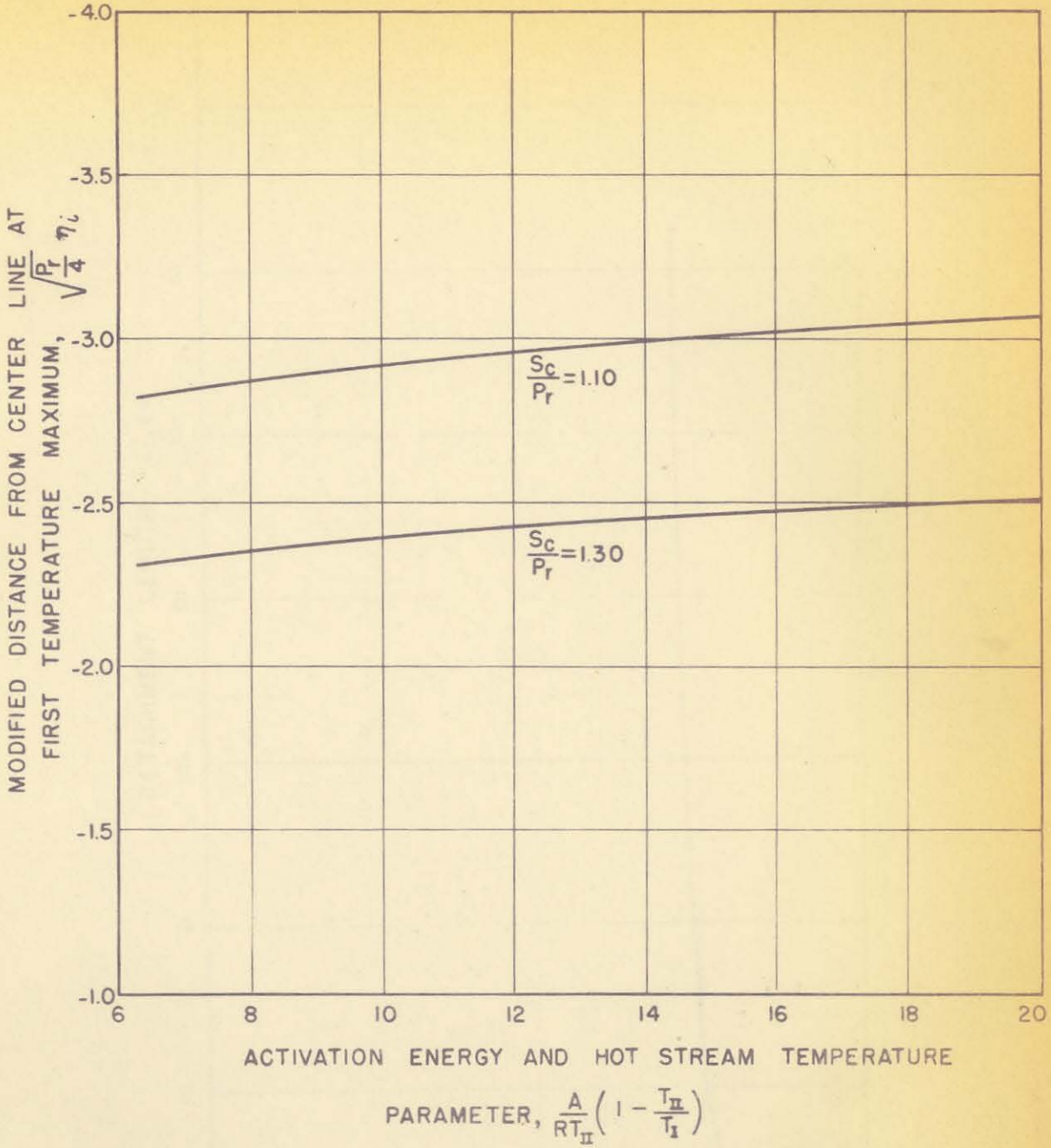

FIGURE 4 — VARIATION OF DISTANCE FROM CENTER LINE AT FIRST TEMPERATURE MAXIMUM WITH ACTIVATION ENERGY, HOT STREAM TEMPERATURE, AND SCHMIDT AND PRANDTL NUMBERS

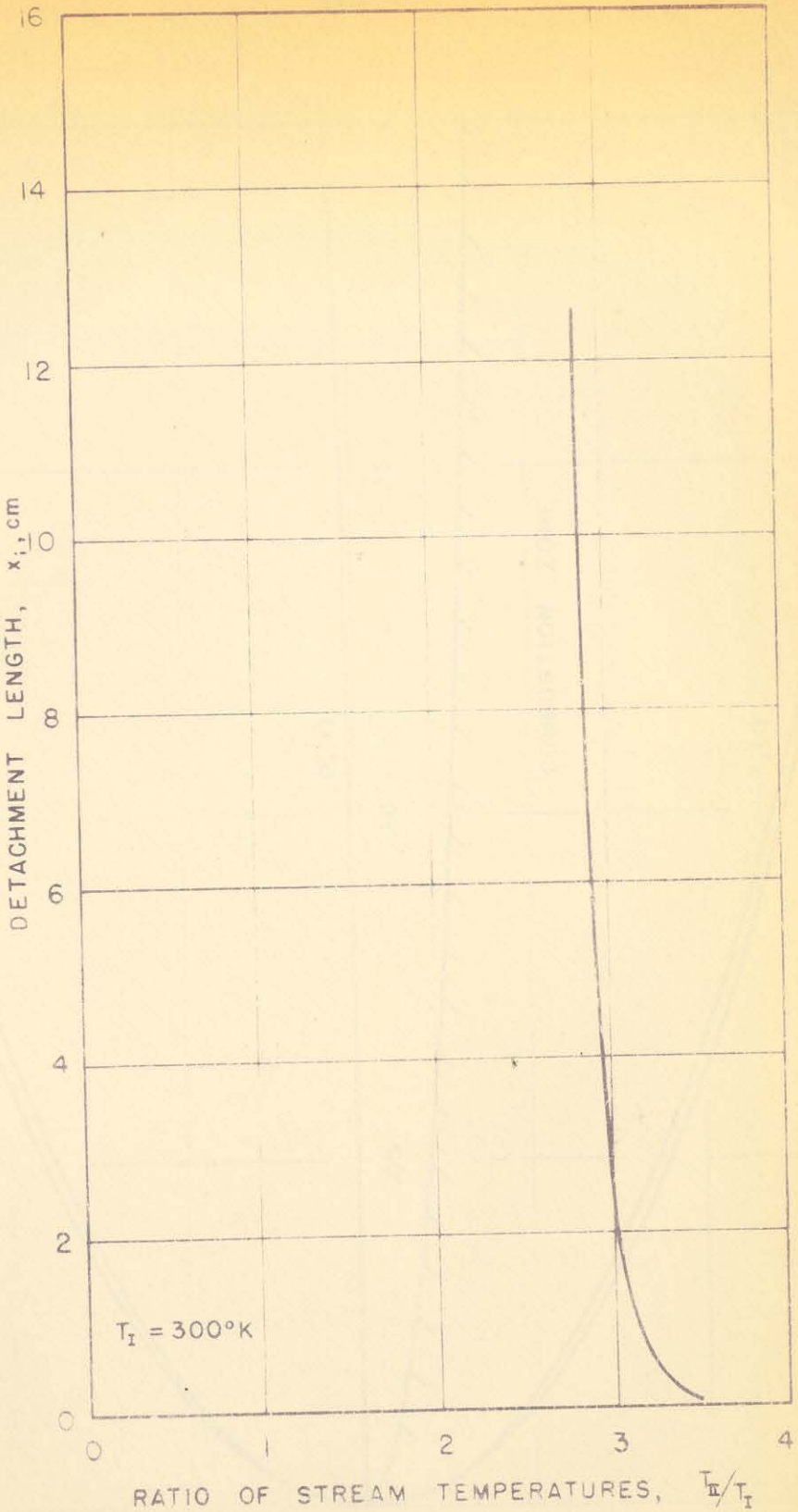

FIGURE 5 — VARIATION OF DETACHMENT LENGTH WITH TEMPERATURE OF THE HOT GAS STREAM

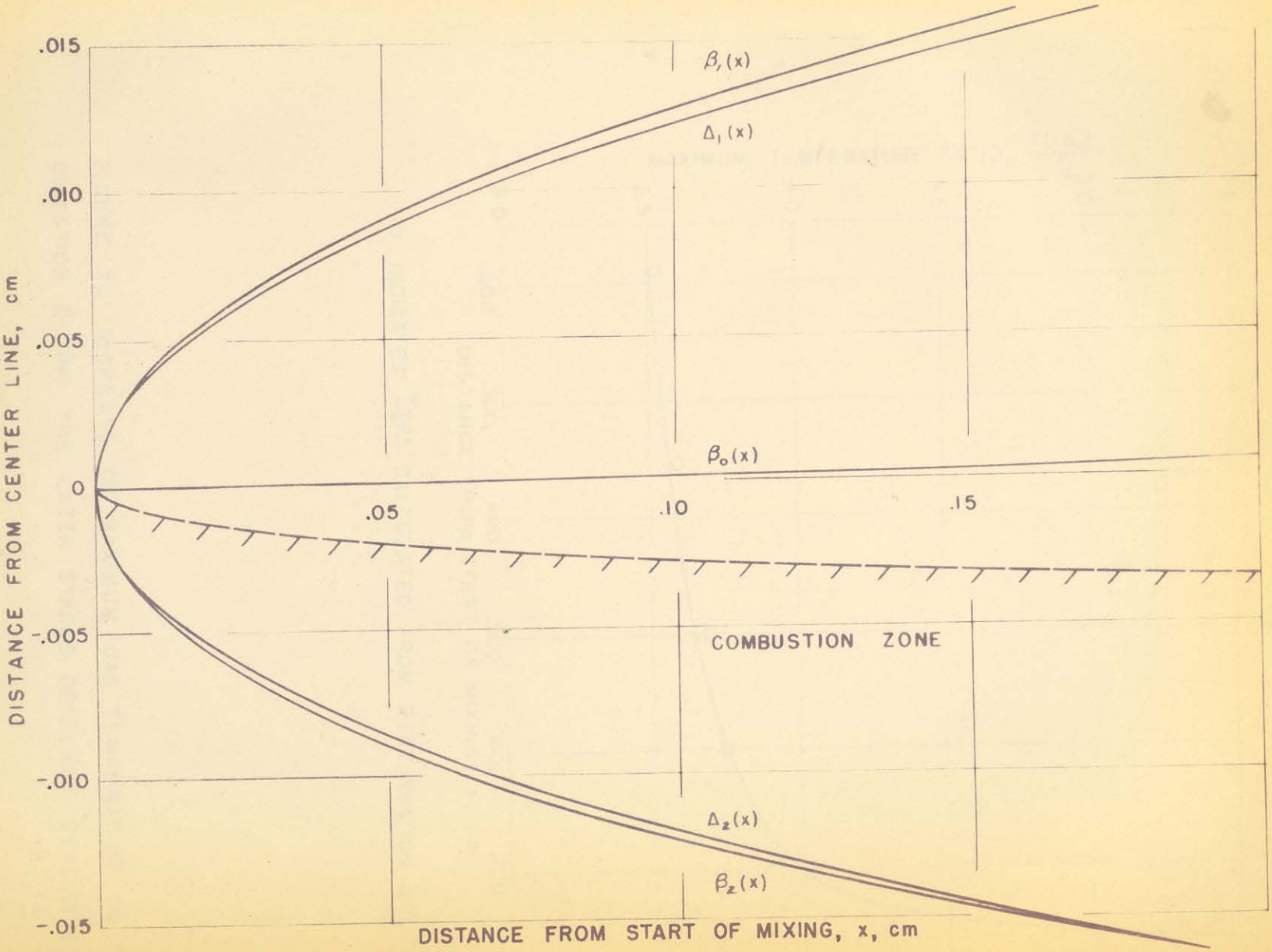

FIGURE 6 — GROWTH OF THICKNESS OF TEMPERATURE AND COMPOSITION LAYERS IN INITIAL REACTION ZONE

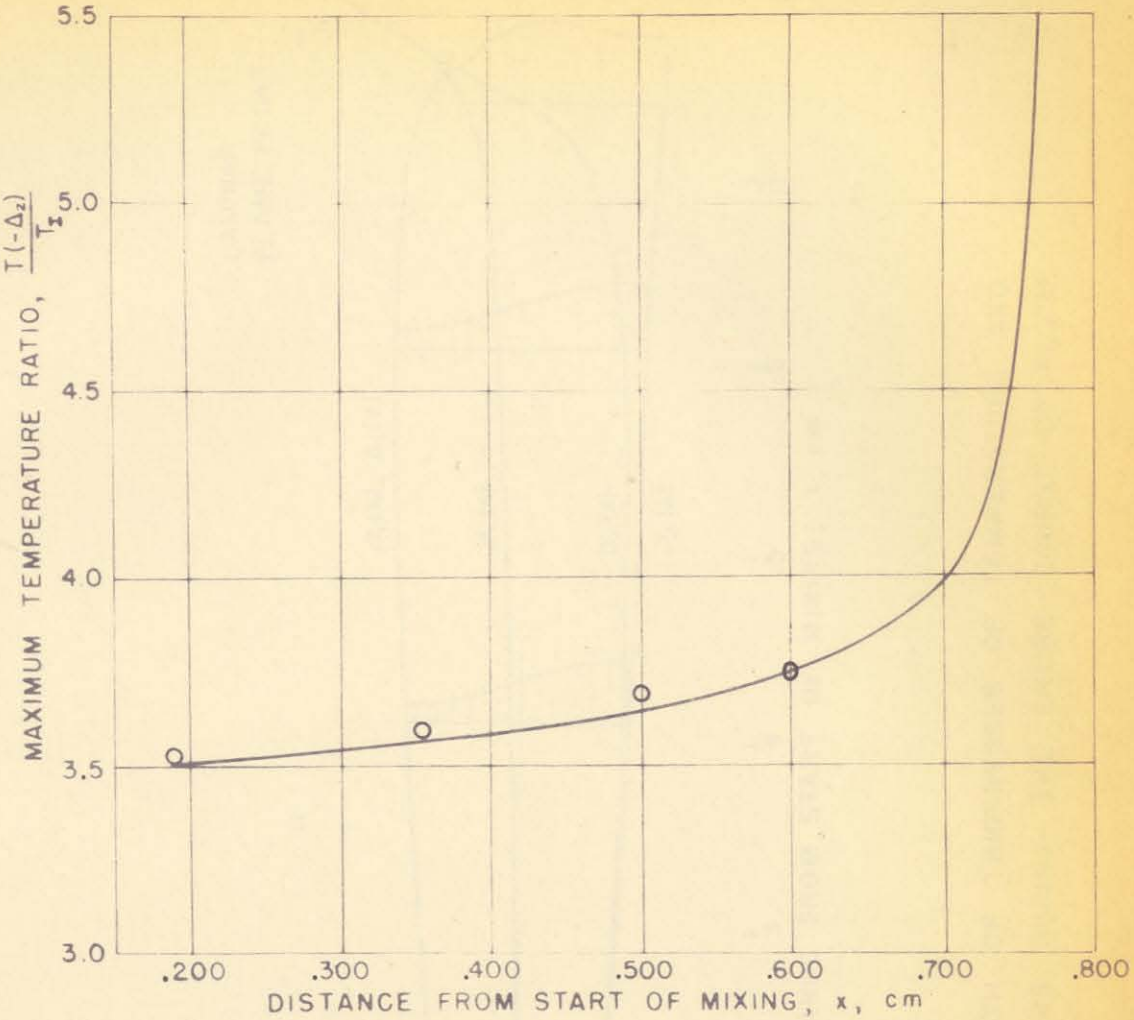

FIGURE 7— INCREASE OF MAXIMUM GAS TEMPERATURE IN FLOW DIRECTION DURING THE LATER STAGES OF FLAME DEVELOPMENT

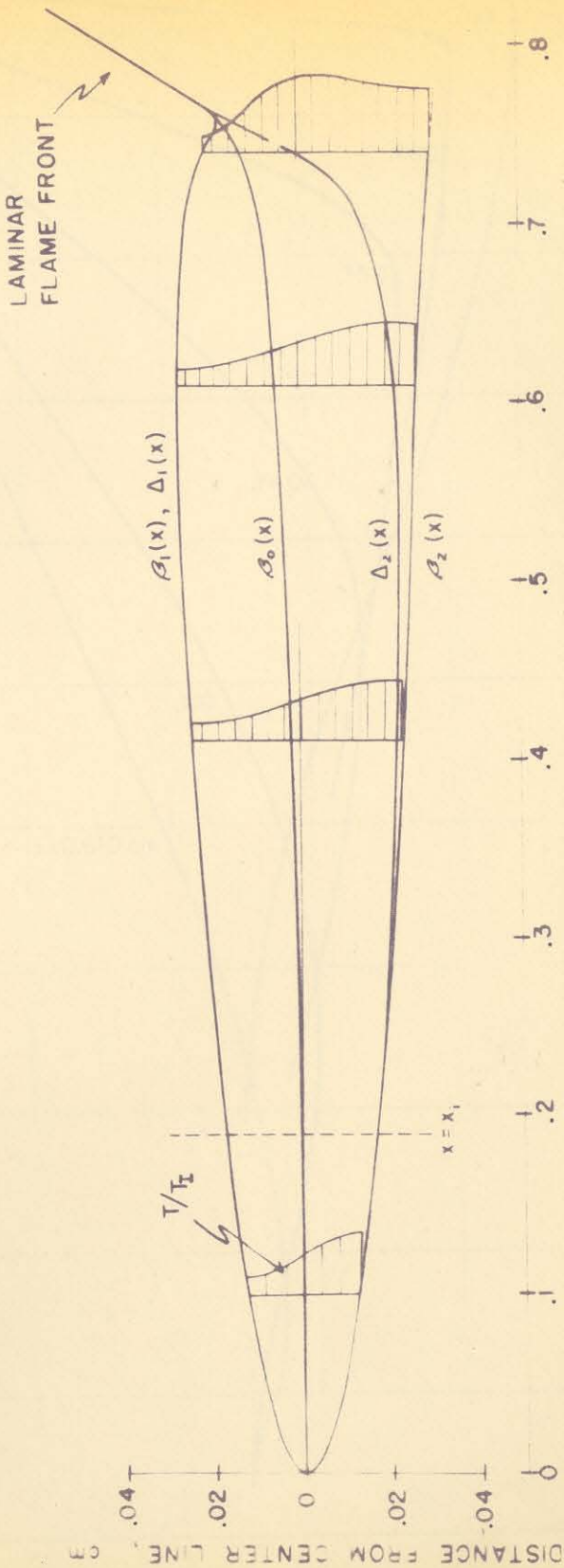

FIGURE 8 – GROWTH OF THICKNESSES OF TEMPERATURE AND COMPOSITION LAYERS DURING THE ENTIRE COURSE OF FLAME DEVELOPMENT

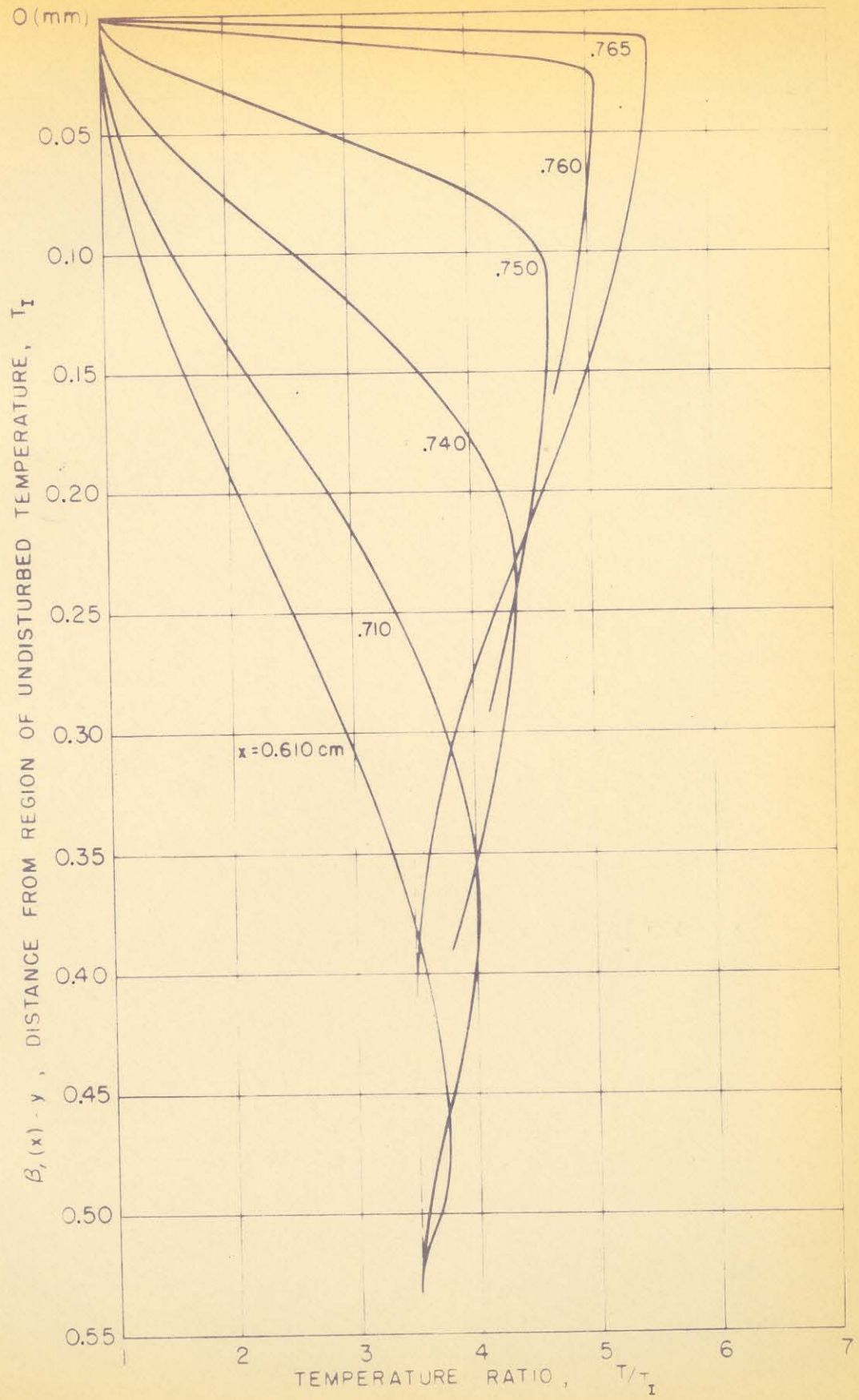

FIGURE 9 – TEMPERATURE PROFILES LEADING TO LAMINAR FLAME